ARTHROPOD SYSTEMATICS & PHYLOGENY

78 (2): 321 – 360
2020

SENCKENBERG

Systematics of the *Mecocephala* group (Hemiptera: Heteroptera: Pentatomidae) based on a phylogenetic perspective: Inclusion of *Hypanthracos*, description of three new genera, and redescription of *Ogmocoris*

Lurdiana D. Barros*[1,2], Kim R. Barão[3] & Jocélia Grazia[1,2]

[1] Departamento de Zoologia, Instituto de Biociências, Universidade Federal do Rio Grande do Sul, Av. Bento Gonçalves, 9500, 91501-970, Porto Alegre, RS, Brazil; — [2] Programa de Pós-Graduação em Biologia Animal, Universidade Federal do Rio Grande do Sul, Porto Alegre, RS, Brazil; Lurdiana Dayse de Barros* [lurdiana.barros@gmail.com]; Jocélia Grazia [jocelia@ufrgs.br] — [3] Laboratório de Sistemática e Diversidade de Artrópodes, Unidade Educacional Penedo, Campus Arapiraca, Universidade Federal de Alagoas, Penedo, AL, Brazil; Kim Ribeiro Barão [kim.barao@penedo.ufal.br] — * Corresponding author

Accepted on September 9, 2020.
Published online at www.senckenberg.de/arthropod-systematics on October 8, 2020.

Editor in charge: Christian Schmidt

Abstract. As a result of the first phylogenetic analysis of the *Mecocephala* group, *Hypanthracos* Grazia & Campos, 1996 is included to the *Mecocephala* group; *H. meridionalis* is redescribed, and four new species in three new genera are described: the genus *Chimerocoris* **gen.n.** is proposed to accommodate *C. luridus* **sp.n.**, the genus *Liscocephala* **gen.n.** is proposed to accommodate *L. fumosa* **sp.n.** and the genus *Triunfus* **gen.n.** is proposed to accommodate two new species: *T. carvalhoi* **sp.n.** and *T. incarnatus* **sp.n.** The new taxa are distributed in Brazil and Uruguay. In addition, *Ogmocoris* Mayr, 1864 is redescribed, a lectotype is designated, and the genitalia of both sexes for *O. hypomelas* (Burmeister) are described for the first time. The standard terminology for the male genitalia of members of the *Mecocephala* group is proposed. Photographs, illustrations, and a distribution map are also provided for all the species.

Key words. Stink bug, Morphological phylogeny, Taxonomy, South America.

1. Introduction

The Pentatomidae, commonly known as stink bugs, comprise about 5,000 species. The family is divided into nine subfamilies (Grazia et al. 2008). The Pentatominae is the most diverse subfamily, and it is currently divided into 42 tribes (Rider et al. 2018). The tribe Carpocorini is also a very diverse and heterogeneous group presently containing 107 extant genera (ca. 500 species). The Carpocorini, as well as most tribes within the Pentatominae, has never been the subject of phylogenetic analyses. Traditionally, the genera assigned to the Carpocorini have been organized into groups of genera – *Carpocoris* group (Mulsant & Rey 1866), *Mormidea* group (Rider & Eger 2008), *Oebalus* group (Barcellos & Grazia 2008), *Euschistus* group (Rolston 1974, Barão et al. 2020) and *Mecocephala* group (Schwertner et al. 2002) –, based especially in morphological similarity and taxonomic history.

The *Mecocephala* group is one of the most diverse groups of genera including 44 species, assigned to 13 genera, all with similar morphology, and all are distributed in the Neotropical Region (Schwertner et al. 2002, Frey-da-Silva 2005, Barros et al. in press.), as follows: *Amauromelpia* Fernandes & Grazia, 1998, *Glyphepomis* Berg, 1891, *Hypatropis* Bergroth, 1891, *Luridocimex* Grazia, Fernandes & Schwertner, 1998, *Mecocephala* Dallas, 1851, *Ogmocoris* Mayr, 1864, *Parahypatropis* Grazia & Fernandes, 1996, *Paramecocephala* Benvegnú, 1968, *Paratibraca* Campos & Grazia, 1995, *Pedinonotus* Fernandes & Grazia, 2002, *Prolatucoris* Barros, Brugn-

era & Grazia, in press., *Tibraca* Stål, 1860, and *Stysiana* Grazia, Fernandes & Schwertner, 1999. Several species (e.g. *Tibraca limbativentris* Stål, 1860, *Glyphepomis adroguensis* Berg, 1891 and *Hypatropis inermis* (Stål, 1872) are considered economically important because they feed on cultivated plants, mainly rice (Pantoja et al. 2005, Farias et al. 2012, Krinski et al. 2015).

Historically, the genera have been grouped based on characters of head and genital morphology. The head is usually long, with the anteocular portion longer than the head width across the eyes; antennomere 2 is reduced; and the male genitalia has reduced parameres and the tenth segment frequently covers the genital cup. In an effort to better delimit this group, we are revising all included genera and species. Moreover, even though there is no formal proposal in the literature, the genus *Hypanthracos* Grazia & Campos, 1996 has been added to the *Mecocephala* group, mainly due to similarities in its head and genitalic morphology. According to Grazia & Campos (1996), *Hypanthracos* is related to *Tibraca* by the shape of the head, the disposition of the clypeus and mandibular plates, the shape and length of the labium, the shape of the mesosternal carina, the presence of two layers in the ventral rim of the pygophore, and the presence of processes in the phallotheca. In contrast, Barão et al. (2017) in a study of the morphological variation of external thoracic scent efferent system (ESES) in Carpocorini, sampling ten genera belonging to the *Mecocephala* group as well as *Hypanthracos*, demonstrated that even though *Hypanthracos* shares many morphological characters with the other genera of this group, its ESES morphology is very different from the others: "the evaporatorium is poorly developed on meso- and metapleuron and anterolateral margin of metapleural evaporatorium is tapered" (Barão et al. 2017).

Furthermore, measurement ratios of some structures, especially the head (e.g., width vs. length, eye width, length of antennomeres, total labial length, and the lengths of individual labiomeres) are usually considered important characters for differentiating genera belonging to this group. Some of these measurements are used as diagnostic characters, but they have never been used or tested in a phylogenetic analysis for the group.

During our effort to revise and update the systematics and taxonomy of this group, several new taxa have been discovered through the analysis of type material and literature. In this paper, we gathered representatives of eight genera of the *Mecocephala* group as well as three outgroup genera to test, through a phylogenetic analysis (using continuous and discrete characters), the hypothesis that the four undescribed taxa represent three new genera (and four new species) tentatively placed in the *Mecocephala* group. Also, we tested the inclusion of *Hypanthracos* in this group. Additionally, we redescribe *Hypanthracos meridionalis* Grazia & Campos, and *Ogmocoris*, including a designation of lectotype, and the internal male and female genitalia described for the first time for *O. hypomelas* (Burmeister), and we propose a standard terminology for the male genitalia of members of the *Mecocephala* group.

2. Material and methods

2.1. Material

We have selected 31 species belonging to three groupings within Carpocorini of the Neotropics (*Euschistus*, *Mormidea*, and *Mecocephala* groups), listed in Table 1, Fig. S1. Outgroup selection was based on taxonomic history and morphological diversity of characters here studied, obtained from several collections, and from the literature (Table 1). The ingroup taxa comprises 17 (about 39%) of the species currently assigned to the *Mecocephala* group + *Hypanthracos meridionalis*. Four other undescribed taxa were included to test their phylogenetic relationship with the other genera of *Mecocephala* group. Trees were rooted on *Carpocoris purpureipennis* (De Geer), a species belonging in the type genus of the Carpocorini. The additional material examined is listed in Electronic Supplement 1.

2.2. Methods

2.2.1. Phylogenetic analysis

A total of 144 characters were used, 12 continuous and 132 discrete. The terminals were coded based on the examination of the specimens or from the literature (Table 1). The matrix of discrete characters was constructed using Mesquite 3.51 (Maddison & Maddison 2018) and the matrix of continuous characters using a spreadsheet. Continuous characters comprise the range of one standard deviation around the mean, rescaled to vary between 0 and 1, in order to weight the same as a hierarchically perfect character. The character declarations follow Sereno (2007). Some characters were provided by Grazia (1997), Weiler et al. (2016), Barão et al. (2017) and Barão et al. (2020). The following notations for characters are used in the Results and Discussion sections: '(X:Y)', in which X represents the character and Y represents the state.

A combined matrix was used and imported to the TNT 1.5 (Goloboff et al. 2016) and analyzed under equal weights (EW) and implied weights (IW). Strict consensus was calculated for the two weighting schemes as well as for Jackknife frequencies. The phylogenetic analysis was conducted with traditional search (*rseed* 1; *mult* = 1000; *tbr hold* = 150). The concavity value (*k*) for the IW analyses was estimated through the Mirande's protocol (Mirande 2009) using the default parameters. The 11 runs resulted in 1 tree each; trees were compared with Subtree Pruning Regrafting distances (SPRdiff). Six values of K (k0–k5, values shown in Table 3) were equally optimal and we performed another analysis using the average of these values, (*k*-value = 4.274) for phylogenetic discussion. Topology stability was calculated for each weighting scheme by Jackknife with symmetric resampling, recording absolute-group frequencies (AF)

Table 1. List of terminals included in the analysis, with information on the genitalia studied per species and sex, number of specimens measured per species, and literature used for species determination when available.— ***Symbols***: "*" only data on external genitalia was available; "L", data on internal genitalia was retrieved from literature.— ***Abbreviation***: N – sample number.

		Genitalia			
Group of Carpocorini	**Species**	♂	♀	**N**	**Literature for determination**
Euschistus (Rolston 1974)	*Agroecus griseus* Dallas, 1851	X	X	20	Rider & Rolston (1987)
	Agroecus scabricornis (Herrich-Schäffer, 1844)	X	X	20	Rider & Rolston (1987)
	Berecynthus hastator (Fabricius, 1798)	X	X	20	Grazia & Hildebrand (1982)
	Carpocoris purpureipennis (De Geer, 1773)	X[L]	X[L]	6	
	Diceraeus melacanthus Dallas, 1851	X	X	10	Barão et al. (2020)
	Dichelops (*Dichelops*) *leucostigmus* (Dallas, 1851)	X	X	20	Grazia (1978), Klein et al. (2012)
	Euschistus (*Euschistus*) *heros* (Fabricius, 1794)	X	X	20	Rolston (1974)
Mormidea (Rider & Eger 2008)	*Lattinellica decora* (Walker, 1867)	X*[L]	X*[L]	2	Rider & Eger (2008)
	Mormidea cornicollis Stål, 1860	X	X	20	Rolston (1978b)
Mecocephala (Schwertner et al. 2002)	*Chimerocoris luridus* sp.n.	X*	—	1	
	Glyphepomis adroguensis Berg, 1891	X	X	18	Campos & Grazia (1998)
	Glyphepomis setigera Kormilev & Pirán, 1952	X	X	14	Campos & Grazia (1998)
	Hypatropis inermis (Stål, 1872)	X	X	14	Fernandes & Grazia (1996)
	Hypatropis sternalis (Stål, 1869)	X	X	2	Fernandes & Grazia (1996)
	Hypanthracos meridionalis Grazia & Campos, 1996	X*[L]	X	2	Grazia & Campos (1996)
	Liscocepala fumosa sp.n.	—	X*	1	
	Mecocephala acuminata Dallas, 1851	X	X	3	Schwertner et al. (2002)
	Mecocephala bonariensis Schwertner, Grazia & Fernandes, 2002	X	X	10	Schwertner et al. (2002)
	Mecocephala magna Schwertner, Grazia & Fernandes, 2002	X	X	10	Schwertner et al. (2002)
	Ogmocoris hypomelas (Burmeister, 1835)	X	X	4	Frey-da-Silva et al. (2002)
	Ogmocoris paranaensis Frey-da-Silva, Grazia & Fernandes, 2002	X*		1	Frey-da-Silva et al. (2002)
	Paramecocephala australis Frey-da-Silva & Grazia, 2002	X	X	38	Frey-da-Silva et al. (2002)
	Paramecocephala foveata Benvegnú, 1968	X*[L]	X*[L]	2	Benvegnú (1968), Frey-da-Silva et al. (2002)
	Paramecocephala fusca (Haglund, 1868)	X*	X*	5	Frey-da-Silva et al. (2002)
	Paratibraca infuscata Campos & Grazia, 1995	X	X	10	Campos & Grazia (1995)
	Pedinonotus catarinensis Fernandes & Grazia, 2002	X	X	14	Fernandes & Grazia (2002)
	Tibraca limbativentris Stål, 1860	X	X	20	Fernandes & Grazia (1998)
	Tibraca similima Barber, 1941	X	X	20	Fernandes & Grazia (1998)
	Tibraca exigua Fernandes & Grazia, 1998	X	X	20	Fernandes & Grazia (1998)
	Triunfus carvalhoi sp.n.	—	X	2	
	Triunfus incarnatus sp.n.	—	X	1	

and Group present/Contradicted (GC) frequency differences, using 1000 pseudo-replicates, removal probability of 36%, and collapsing nodes with values less than 50% – search parameters were the same as described above.

2.2.2. Morphology and its documentation

Twenty morphometric parameters were obtained and are presented in Table 4. Measurements [mean (minimum−maximum)] are given in millimetres, followed by sample number. The standard deviation is presented when the sample number is ≥ 3. The measurements for a single specimen correspond to the absolute value of the holotype. The male genitalia and measurements of *Paramecocephala foveata* Benvegnú were based on the study of the prepared plate of the holotype and from the literature (Benvegnú 1968, Frey-da-silva et al. 2002); and for the study of the female genitalia, we used the photographic examination made available by Frey-da-silva (pers. comm.).

2.2.3. Specimen preparation

The genitalia were macerated with aqueous supersaturated potassium hydroxide solution (KOH) and stained with Congo red, when necessary. For those specimens in which the pygophore remained dark, a solution of sodium hypochlorite (NaClO) diluted in water was used for depigmentation. For *O. paranaensis* Frey-da-Silva, Grazia & Fernandes, *Liscocephala fumosa* **sp.n.** and *Chimerocoris luridus* **sp.n.**, the internal genitalia were not dissected because those species were represented by a single specimen each.

For Scanning Electron Microscopy (SEM) of external scent efferent system, the left meso- and metapleuron of dried preserved specimens were removed, cleaned manually with forceps and fine tipped brush and isopropyl alcohol, kept submerged in Renu® contact lens solution for 48 h, and then agitated in an ultrasonic bath (5.400 kHz) with water and detergent solution for 45 s. Afterward, meso- and metapleuron were dehydrated at 50° C for 48 h, sputter coated with carbon and gold and

Table 2. Character matrix for taxa included in phylogenetic analysis.— ***Symbols***: "–" inapplicable data (for continuous characters: "?"); "?" missing data.

Character:	0	0	0	0
	0	0	0	0
Taxon:	**1**	**2**	**3**	**4**
Carpocoris purpureipennis	?	0.418-0.471	0.265-0.287	0.599-0.664
Agroecus griseus	0.362-0.458	0.385-0.488	0.186-0.268	0.539-0.611
Agroecus scabricornis	0.397-0.451	0.343-0.398	0.207-0.255	0.532-0.566
Berecynthus hastator	0.027-0.044	0.282-0.377	0.239-0.285	0.543-0.596
Chimerocoris luridus sp.n.	0.543	0.404	0.431	0.617
Diceraeus melacanthus	0.042-0.057	0.225-0.296	0.165-0.219	0.531-0.592
Dichelops (*Dichelops*) *leucostigmus*	0.053	0.247-0.293	0.132-0.198	0.487-0.526
Euschistus (*Euschistus*) *heros*	0.057-0.072	0.327-0.407	0.294-0.352	0.565-0.639
Glyphepomis adroguensis	0.005-0.028	0.052-0.124	0.000-0.160	0.341-0.408
Glyphepomis setigera	0.000-0.017	0.000-0.030	0.045-0.070	0.297-0.329
Hypanthracos meridionalis	0.517-0.784	0.330-0.569	0.304-0.471	0.499-0.705
Hypatropis inermis	0.098-0.133	0.185-0.260	0.066-0.113	0.475-0.548
Hypatropis sternalis	0.103	0.208-0.244	0.079-0.098	0.483-0.544
Lattinellica decora	0.336	0.268-0.304	0.155	0.494-0.535
Liscocephala fumosa sp.n.	0.357	0.091	0.155	0.398
Mecocephala acuminata	0.267	0.388-0.443	0.444-0.527	0.617-0.684
Mecocephala bonariensis	0.719-0.868	0.630-0.755	0.635-0.721	0.782-0.856
Mecocephala magna	0.853-0.999	0.850-1.000	0.832-1.000	0.859-1.000
Mormidea cornicollis	0.091-0.117	0.273-0.329	0.161-0.205	0.506-0.577
Ogmocoris hypomelas	0.638	0.586-0.678	0.500-0.511	0.666-0.728
Ogmocoris paranaensis	0.826	0.821	0.588	0.938
Pedinonotus catarinensis	0.116-0.130	0.195-0.264	0.125-0.171	0.465-0.506
Paratibraca infuscata	0.351-0.496	0.190-0.268	0.188-0.234	0.432-0.487
Tibraca exigua	0.461-0.540	0.316-0.390	0.266-0.328	0.520-0.595
Tibraca limbativentris	0.581-0.732	0.455-0.528	0.423-0.493	0.641-0.721
Tibraca similima	0.581-0.682	0.461-0.550	0.411-0.461	0.668-0.718
Paramecocephala australis	0.614-0.687	0.470-0.548	0.438-0.502	0.621-0.690
Paramecocephala foveata	0.578-0.598	0.504-0.560	0.415-0.452	0.668-0.847
Paramecocephala fusca	0.506-0.546	0.300-0.372	0.348-0.384	0.527-0.590
Triunfus carvalhoi sp.n.	0.420	0.151-0.188	0.207-0.229	0.483-0.503
Triunfus incarnatus sp.n.	0.428	0.182	0.250	0.486

Character:	0	0	0	0
	0	0	0	0
Taxon:	**5**	**6**	**7**	**8**
Carpocoris purpureipennis	0.282-0.358	0.776-1.000	0.311-0.356	0.549
Agroecus griseus	0.318-0.357	0.496-0.592	0.370-0.495	0.437-0.538
Agroecus scabricornis	0.295-0.345	0.463-0.575	0.345-0.442	0.349
Berecynthus hastator	0.234-0.318	0.382-0.477	0.308-0.444	0.246-0.338
Chimerocoris luridus sp.n.	0.342	0.236	0.496	0.345
Diceraeus melacanthus	0.342	0.517-0.610	0.308-0.396	0.300-0.389
Dichelops (*Dichelops*) *leucostigmus*	0.263-0.355	0.413-0.553	0.258-0.327	0.464
Euschistus (*Euschistus*) *heros*	0.353-0.506	0.601-0.687	0.485-0.625	0.507-0.570
Glyphepomis adroguensis	0.037-0.116	0.085-0.111	0.015-0.079	0.026-0.126
Glyphepomis setigera	0.005-0.080	0.075-0.121	0.000-0.050	0.000-0.136
Hypanthracos meridionalis	0.308-0.541	0.272-0.300	0.560-0.789	?
Hypatropis inermis	0.351-0.490	0.341-0.432	0.401-0.585	0.379-0.482
Hypatropis sternalis	0.507	0.335	0.539	?
Lattinellica decora	0.000-0.092	0.469-0.497	0.067-0.113	0.208
Liscocephala fumosa sp.n.	0.111	0.000	0.204	0.055
Mecocephala acuminata	0.891	0.500	1000	?
Mecocephala bonariensis	0.476-0.594	0.255-0.343	0.492-0.663	0.559-0.620
Mecocephala magna	0.636-0.728	0.373-0.427	0.621-0.696	0.634
Mormidea cornicollis	0.182-1.000	0.667-0.946	0.443-0.527	0.564-1.000
Ogmocoris hypomelas	0.507	0.236	0.805	?
Ogmocoris paranaensis	0.605	0.375	0.918	?
Pedinonotus catarinensis	0.627-0.770	0.380-0.471	0.624-0.773	0.676-0.847
Paratibraca infuscata	0.215-0.291	0.201-0.257	0.234-0.351	0.203-0.234

Table 2 continued.

Tibraca exigua	0.239–0.338	0.171–0.223	0.328–0.404	0.208–0.286
Tibraca limbativentris	0.462–0.552	0.334–0.393	0.585–0.686	0.354–0.458
Tibraca similima	0.453–0.517	0.294–0.351	0.491–0.610	0.372–0.430
Paramecocephala australis	0.416–0.508	0.301–0.350	0.440–0.501	0.376–0.418
Paramecocephala foveata	0.363–0.596	0.191–0.275	0.636–0.713	0.305
Paramecocephala fusca	0.318–0.406	0.212–0.261	0.323–0.422	0.293
Triunfus carvalhoi sp.n.	0.177	?	0.431	0.242
Triunfus incarnatus sp.n.	0.243	?	0.480	0.293
Character:	**0**	**0**	**0**	**0**
	0	**1**	**1**	**1**
Taxon:	**9**	**0**	**1**	**2**
Carpocoris purpureipennis	0.287–0.380	0.147–0.200	0.046–0.080	0.039–0.098
Agroecus griseus	0.196–0.270	0.141–0.187	0.033–0.052	0.043–0.058
Agroecus scabricornis	0.211–0.286	0.130–0.168	0.027–0.036	0.039–0.047
Berecynthus hastator	0.240–0.328	0.140–0.193	0.046–0.062	0.042–0.060
Chimerocoris luridus sp.n.	0.450	0.452	0.328	0.262
Diceraeus melacanthus	0.219–0.301	0.151–0.172	0.056–0.075	0.054–0.068
Dichelops (*Dichelops*) *leucostigmus*	0.228	0.056–0.084	0.053	0.035
Euschistus (*Euschistus*) *heros*	0.309–0.417	0.199–0.251	0.096–0.147	0.091–0.114
Glyphepomis adroguensis	0.058–0.118	0.000–0.061	0.012–0.049	0.014–0.036
Glyphepomis setigera	0.000–0.134	0.019–0.048	0.000–0.036	0.000–0.052
Hypanthracos meridionalis	0.466–0.665	0.269–0.387	0.188–0.292	0.157–0.229
Hypatropis inermis	0.270–0.333	0.147–0.224	0.090–0.142	0.077–0.099
Hypatropis sternalis	0.096	0.071	0.121	0.070
Lattinellica decora	0.215	0.080	0.000–0.021	0.001–0.046
Liscocephala fumosa sp.n.	0.149	?	?	?
Mecocephala acuminata	0.889	0.976	0.812	0.768
Mecocephala bonariensis	0.692–0.789	0.644–0.794	0.678–0.776	0.731–0.859
Mecocephala magna	0.877–1.000	0.823–0.999	0.863–1.000	0.921–1.000
Mormidea cornicollis	0.424–0.616	0.241–0.299	0.095–0.122	0.092–0.108
Ogmocoris hypomelas	0.334–0.476	0.452	0.365–0.522	0.203–0.311
Ogmocoris paranaensis	0.616	0.659	0.536	0.327
Pedinonotus catarinensis	0.297–0.410	0.243–0.272	0.181–0.221	0.145–0.158
Paratibraca infuscata	0.202–0.242	0.119–0.170	0.101–0.133	0.073–0.085
Tibraca exigua	0.225–0.505	0.162–0.224	0.135–0.205	0.103–0.137
Tibraca limbativentris	0.398–0.477	0.266–0.362	0.232–0.290	0.156–0.194
Tibraca similima	0.365–0.429	0.265–0.311	0.196–0.248	0.145–0.175
Paramecocephala australis	0.407–0.493	0.444–0.533	0.381–0.458	0.284–0.325
Paramecocephala foveata	0.365–0.514	0.226–0.657	0.127–0.622	0.127–0.425
Paramecocephala fusca	0.312–0.391	0.339–0.425	0.290–0.357	0.217–0.267
Triunfus carvalhoi sp.n.	0.197	0.191	0.153	0.186
Triunfus incarnatus sp.n.	0.197	0.191	0.153	0.206

observed by SEM at the Centro de Microscopia Eletrônica of UFRGS.

2.2.4. Photos and illustrations

Specimens were photographed in multiple focal planes with the Digital Sight DS-Fi2 camera coupled to a stereomicroscope Nikon AZ100M and stacked with the software NIS Elements AR, available at the Department of Zoology, UFRGS, and edited with Adobe Photoshop CS5. Line vector drawings were made with Adobe Illustrator CS5 over drawings using a camera lucida coupled to a stereomicroscope or made over photographs taken under light microscopy, and the specimens used in illustrations are indicated with the notation <illustrated specimen> in the Analyzed material sections.

2.2.5. Georeferencing and map

Distribution were retrieved from collection labels and the literature (i.e. Frey-da-silva et al. 2002, Grazia & Campos 1996) and georeferenced using online global gazetteers. Distributions were plotted with SimpleMappr using the layers "country" and "relief" in the geographic projection and edited in Adobe Illustrator CS5.

2.3. Abbreviations

Morphology. aa, articular apparatus; **aaf**, anterior annular flange; **cj**, conjunctiva; **cs**, *capsula seminalis*; **cx2**, mesocoxae; **cx3**, metacoxae; **dc**, dorsal connective; **dr**, dorsal rim; **ddr**, distal ductus receptaculi; **dpph**, dorsal process of phallotheca; **dsd**, ductus seminis distalis; **edr**,

Table 2 continued.

Character:	00000000	0000000000	0000000000	0000000000	0000000000	0000000000
	11111112	2222222223	3333333334	4444444445	5555555556	6666666667
Taxon:	34567890	1234567890	1234567890	1234567890	1234567890	1234567890
Carpocoris purpureipennis	02111000	0000011000	0100101110	-000210000	0010011111	0101011101
Agroecus griseus	01200111	0000001010	0101010111	0101201121	0110110-00	0001010001
Agroecus scabricornis	01200101	0000001110	0101010011	0001201121	0110110-00	0011110001
Berecynthus hastator	10100111	0000011010	0101000011	0020100121	0100100-01	1001111000
Chimerocoris luridus sp.n.	00000111	0001000001	0000101101	1011201120	1112111111	1111101001
Diceraeus melacanthus	12100001	000?011000	0111011001	0011001121	0012110-01	1001010000
Dichelops (*Dichelops*) *leucostigmus*	12100011	0000011000	0101010001	0010201121	0111001111	1111010000
Euschistus (*Euschistus*) *heros*	00100101	0000001110	0101010011	0020101121	0012101100	1001011101
Glyphepomis adroguensis	00000101	0011111100	0100110011	0110100220	1100100011	0011000010
Glyphepomis setigera	00000101	0011111100	0100110001	0010100220	1100100011	0011000010
Hypanthracos meridionalis	00001101	0001010100	0100010011	0000001111	0102100000	0011100000
Hypatropis inermis	01200011	0001110100	0102101101	0010001120	0111001011	1000000001
Hypatropis sternalis	02200011	0001110100	0102101101	0011001120	0111001111	1100000001
Lattinellica decora	00100011	0000001110	0100011010	-020210221	0012111101	1000100010
Liscocephala fumosa sp.n.	00000101	011110010?	?010101111	0101201121	0111011111	0110101001
Mecocephala acuminata	10011111	0001101101	0100101111	0011001100	0110011111	1101100000
Mecocephala bonariensis	10011111	0001101101	0112101111	0010001100	0111011111	1100100000
Mecocephala magna	10011110	0011101101	0102100111	0011001101	0111011111	1100100000
Mormidea cornicollis	00200011	0000001110	0112011010	-010001111	0100110101	0010100010
Ogmocoris hypomelas	01000101	0010011101	0102111001	1000001121	0112011111	1101000001
Ogmocoris paranaensis	01000101	001??01101	0102110001	0000001121	0110001111	0111000001
Paramecocephala australis	00000101	0011101101	0110101101	0011201120	1112001111	1111001001
Paramecocephala foveata	00000101	001??01101	0110101101	2011201101	1121011110	0101101001
Paramecocephala fusca	00000101	0011101101	0112111101	1010201120	1112001111	1111001000
Pedinonotus catarinensis	02200111	0001100100	0002100111	0021201121	1112111011	1101100000
Paratibraca infuscata	00000101	0001111100	0100010001	0001001101	1111001111	1111101101
Tibraca exigua	00000101	0001100100	0100101101	0010201121	1111001111	1111101101
Tibraca limbativentris	00000101	0001101100	0100011101	0011201101	1111001111	1111101001
Tibraca similima	00000101	0001000100	0100110001	0011201121	1111001111	1111001001
Triunfus carvalhoi sp.n.	00000101	1001111101	1010101121	000110110	0111001111	1111000000
Triunfus incarnatus sp.n.	00000101	1001111101	1010101121	000110110	0111001111	1111000000

extension of dorsal rim; **eses**, external thoracic scent efferent system; **ev**, evaporatorium; **ilvr**, inferior layer of ventral rim; **la8**, laterotergites 8; **la9**, laterotergites 9; **lmp**, lateral margin of pygophore; **lr**, lateral rim; **lpppph**, lateroposterior projection of phallotheca; **lvr**, layers of ventral rim; **mlcj**, median lobe of conjunctiva; **ms**; mesopleuron; **mt**, metapleuron; **om**, outer margin of evaporatorium; **pa**, posterolateral angle; **paf**, posterior annular flange; **par**, parameres; **pc**, *processus capitati*; **pcj**, process of conjunctiva; **pdr**, proximal ductus receptaculi; **pdpph**, posterodorsal projection of phallotheca; **per**, peritreme; **ph**, phallotheca; **pi**, *pars intermedialis*; **prX**, process of segment X; **pslvr**, projection of superior layer of ventral rim; **pve**, process of vesica; **rs**, ring sclerites; **slvr**, superior layer of ventral rim; **tvi**, thickening of vaginal intima; **va**, vesicular area; **va8**, valvulae 8; **va9**, valvulae 9; **vf8**, valvifers 8; **vf9**, valvifers 9; **vbpph**, ventrobasal projection of phallotheca; **vlcj**, ventral lobe of conjunctiva; **vr**, ventral rim; **X**, abdominal segment X.

Morphometric parameters measured. A1, length of antennomere 1; **A2**, length of antennomere 2; **A3**, length of antennomere 3, **A4**, length of antennomere 4; **A5**, length of antennomere 5; **BL**, body length, from the apex of the head to the apex of the abdominal tergite 7; **BW**, body width, abdominal width at level of sternite 3; **CL**, length of clypeus, from the apex to level of the clypeal suture; **HL**, head length; **HLE**, length of head at compound eye level; **HW**, head width; **IOD**, interocular distance; **L1,** length of labiomere 1; **L2,** length of labiomere 2; **L3,** length of labiomere 3; **L4,** length of labiomere 4; **PL**, medial pronotum length; **PW**, pronotum width, width of pronotum after humeral angles; **SL**, medial scutellum length; **SW**, basal scutellum width. Represented in Figure 1.

Depositories. AMNH – The American Museum of Natural History, New York, USA; **DARC** – David Rider Collection, North Dakota State University, North Dakota, USA; **DZUP** – Museu de Entomologia Pe. Jesus Santiago Moure, Universidade Federal do Paraná, Curitiba, Brazil; **FIOC** – Fundação Instituto Oswaldo Cruz, Rio de Janeiro, Brazil; **MACN** – Museo Argentino de Ciencias Naturales "Bernardino Rivadavia", Buenos Aires, Argentina; **MCNZ** – Museu de Ciências Naturais da Fundação

Table 2 continued.

0000000000	0000000000	0000000001	1111111111	1111111111	1111111111	1111111111	1111
7777777778	8888888889	9999999990	0000000001	1111111112	2222222223	3333333334	4444
1234567890	1234567890	1234567890	1234567890	1234567890	1234567890	1234567890	1234
0011001002	1101-0---0	-----?10--	100?0-10-0	?100001120	0011002111	000?0100?0	1?0?
0010101020	100000---0	-----110--	10100-0120	1111011010	1011112000	1101010010	0200
0010100020	100000---0	-----110--	10100-0120	1111011111	1012112000	1101000010	0200
0011002001	100000---0	-----100--	1000101120	-110010011	0020011000	1101010011	0000
1110101120	0000111001	1111121110	11????????	??????????	??????????	??????????	????
0011001001	101000---0	-----100--	10100-0110	-10-011000	1020011010	0101010001	2000
0011101001	101000---0	-----10101	10100-0110	0112011011	0000011110	0002000001	0011
0010111010	100000---0	-----00101	1002101100	0011010100	1021111010	1112000211	1200
100-110121	0000110001	1100-00100	1103111121	0011110000	0000112010	1111200011	0100
1010102121	0000111001	1100-00100	1103011121	0011110000	0000112010	1111200110	1100
0010002000	10000101-1	00-0-100--	0-131100-1	1112111000	1000111000	1111101110	0100
000-100121	1000-100-1	00-0-21100	0-02111111	1012110000	0011112010	1111101111	1000
100-100100	10000110-1	00-1121100	0-03111111	1012110000	0011212010	1111202101	1010
0011000010	110110----	-----00101	10????????	??????0110	11?0111001	1????00010	1210
110-10????	??????????	??????????	??????????	??????0000	10?1210000	??????????	????
010-001102	0000110001	0111121100	1103111111	0012110020	0011012010	1111201111	1000
010-010100	0010110001	0100-21100	1102111111	1111110000	0010112010	1110110201	1000
010-012101	0000110001	0101121100	1113111111	0010110000	1022010010	1111202111	1000
0011110020	111000----	-----200--	10000-00-1	000-100100	1100111001	1102000000	1000
1110002111	0000010101	1111000101	1003111111	0010111010	1111012010	1112202101	1000
0110102111	0010110101	0101120100	10????????	??????????	??????????	??????????	????
1110000101	1101110111	0110-20100	1102111111	1110111000	1000010010	1112202111	1000
1110110120	0000110001	0110-20100	1113111111	0011111000	00?00?1010	??????????	????
0110012100	1110110101	00-1120100	1103111111	1110111000	1000012000	1112202110	1100
000-000121	0000010101	1110-20100	1102111111	1112111010	1001012000	1102000011	1001
0010111121	0100110011	01111000--	1102111121	0110110100	1000212010	1110010211	3000
100-001111	0000011001	1101110110	1102111121	0110110000	0000012010	1111202111	1000
1010100111	0010111001	1111110110	1102111121	0110110020	0001011010	1111100211	1000
000-100111	0000110001	1101110110	1102111121	0110110000	1013012010	1111100111	0000
110-10????	??????????	??????????	??????????	??????1120	0000110011	1111201111	1101
110-10????	??????????	??????????	??????????	??????1100	0001010011	1112201111	1000

Zoobotânica do Rio Grande do Sul, Porto Alegre, Brazil; **MCTP** – Museu de Ciências e Tecnologia da Pontifícia Universidade Católica do Rio Grande do Sul, Porto Alegre, Brazil; **MECB** – Museu de Entomologia "Ceslau M. Biezanko", Faculdade de Agronomia, Universidade Federal de Pelotas, Brazil; **MIZA** – Museo Del Instituto de Zoología Agrícola, Maracay, Venezuela; **URMU** – Museo Nacional de Historia Natural, Montevideo, Uruguay; **MNRJ** – Museu Nacional, Universidade Federal do Rio de Janeiro, Brazil; **MPEG** – Museu Paraense Emílio Goeldi, Belém, Pará, Brazil; **MPUJ** – Pontificia Universidad Javeriana, Bogota, Colombia; **MZUSP** – Museu de Zoologia da Universidade de São Paulo, São Paulo, Brazil; **UEMA** – Universidade Estadual do Maranhão, São Luiz, Brazil; **UFRG** – Departamento de Zoologia – Universidade Federal do Rio Grande do Sul, Porto Alegre, Brazil; **USNM** – National Museum of Natural History, Washington, D.C., USA; **UYIC** – Museo de Entomologia, Departamento de Arthropodos, Faculdad de Ciencias, Universidad de la Republica, Montevideo, Uruguay; **ZMHB** – Museum für Naturkunde, Humboldt-Universität, Berlin, Germany.

Table 3. Summary of results from the phylogenetic analysis.— ***Symbol***: "*" best k-values. — ***Abbreviations***: EW – equal weighting; IW – implied weighting.

Analysis (K-value)	Kref	Tree length	Trees	Total fit
k0*	2.711	645.643	1	66.463
k1*	3.182	645.643	1	61.910
k2*	3.743	645.643	1	57.308
k3*	4.423	645.643	1	52.638
k4*	5.262	645.643	1	47.880
k5*	6.325	645.643	1	43.013
k6	7.715	643.732	1	37.999
k7	9.610	640.583	1	32.803
k8	12.348	640.583	1	27.427
k9	16.651	640.583	1	21.841
k10	24.396	640.583	1	16.007
IW (k-average)	4.274	645.643	1	53.5884
EW	—	640.583	2	—

Table 4. Morphometric parameters measured.— ***Abbreviations***: HL – head length; HW – head width; HLE – length of head at eye level; IOD – interocular distance; CL – length of clypeus; A1 – length of antennomere 1; A2 – length of antennomere 2; A3 – length of antennomere 3; A4 – length of antennomere 4; A5 – length of antennomere 5; L1 – length of labiomere 1; L2 – length of labiomere 2; L3 – length of labiomere 3; L4 – length of labiomere 4; PL – pronotum length; PW – pronotum width; SL – scutellum length; SW – scutellum width; BW – body width; BL – body length.

	Measurements																		
						Antenna					Labium								
Species	HL	HW	HLE	IOD	CL	A1	A2	A3	A4	A5	L1	L2	L3	L4	PL	PW	SL	SW	BL	BW
Hypanthracos meridionalis	2.62 2	2.35 2	1.74 2	1.35 2	1.65 2	0.68 2	0.52 2	1.65 2	1.16 2	—	1.54 2	2.28 2	1.71 2	1.48 2	3.65 2	6.93 2	5.25 2	4.62 2	14.38 2	6.38 2
Chimerocoris luridus sp.n.	2.79 1	2.25 1	1.65 1	1.38 1	1.65 1	0.60 1	0.45 1	1.32 1	0.99 1	1.29 1	1.32 1	2.85 1	2.16 1	1.89 1	2.60 1	6.00 1	4.50 1	4.00 1	12.25 1	6.88 1
Ogmocoris hypomelas	3.19±0.15 (3.06–3.39) 4	2.86±0.13 (2.70–3.00) 4	1.92±0.14 (1.80–2.04) 4	1.64±0.13 (1.50–1.80) 4	1.94±0.08 (1.86–2.01) 4	0.82±0.09 (0.75–0.90) 4	0.48 2	2.00 2	1.44 2	—	1.37±0.15 (1.14–1.44) 4	2.96±0.14 (2.85–3.15) 4	2.82±0.24 (2.47–3.04) 4	2.03±0.09 (1.90–2.10) 4	3.20±0.33 (2.75-3.50) 4	7.99±0.58 (7.22–8.55) 4	5.23±0.53 (4.65–5.75) 4	5.00±0.55 (4.35–5.50) 4	15.34±1.43 (14.12–16.88) 4	8.28±1.04 (6.88–9.12) 4
Ogmocoris paranaensis	3.39 1	3.21 1	2.70 1	2.04 1	2.10 1	0.84 1	0.66 1	2.10 1	—	—	1.63 1	3.80 1	3.23 1	2.28 1	3.60 1	8.30 1	6.00 1	5.00 1	17.88 1	9.38 1
Liscocephala fumosa sp.n.	1.74 1	1.53 1	1.05 1	0.93 1	1.05 1	0.39 1	0.09 1	0.78 1	0.54 1	0.78 1	0.75 1	—	—	—	1.65 1	3.60 1	2.90 1	2.50 1	8.55 1	4.32 1
Triunfus carvalhoi sp.n.	1.98 2	1.71 2	1.33 2	1.12 2	1.38 2	0.45 2	—	1.20 2	0.75 1	1.11 1	0.84 2	1.65 2	1.26 2	1.44 2	2.00 2	3.90 2	3.40 2	2.50 2	9.79 2	5.10 2
Triunfus incarnatus sp.n.	2.10 1	1.74 1	1.44 1	1.11 1	1.35 1	0.51 1	—	1.29 1	0.75 1	1.20 1	0.84 1	1.65 1	1.26 1	1.56 1	2.10 1	4.08 1	3.50 1	2.60 1	9.96 1	4.40 1

2.4. Terminology

Terminology follows Tsai et al. (2011) for general morphology; Dupuis (1955, 1970), Genevcius & Schwertner (2017) and Zhou & Rédei (2020) for terminalia and genitalia; Kment & Vilímová (2010) and Barão et al. (2017) for the external scent efferent system.

We suggest the term "layers of ventral rim" to "infoldings of ventral rim" proposed by Tsai et al. (2011). Therefore, "superior layer of ventral rim" and "inferior layer of ventral rim" for members of *Mecocephala* group, represented in Figure 2.

In past descriptions of the species that make up the *Mecocephala* group, the interpretation of the dorsal and ventral views of the phallus has been misconceived by the authors of species. The mobile processes of phallotheca are dorsal and the processes of the vesica are ventral. Here, we also updated the terminology using as an example *H. meridionalis*, used for the processes and projections of the phallus, as follows: "processo 1 da phallotheca, processo 2 da phallotheca, processo 1 da conjunctiva, processo 3 da conjuntiva, processo 4 da conjuntiva" of Grazia & Campos (1996: 15) correspond respectively to: posterodorsal projection of phallotheca, ventrobasal projection of phallotheca, dorsal process of phallotheca, median lobe of conjunctiva, ventral lobe of conjunctiva.

3. Results

Of the 144 characters used in the analyses, 71 are described here. The list and matrix of characters are given in Appendix 1 and Table 2.

3.1. Phylogenetic analysis

The phylogenetic analyses employing EW (Fig. S2A) produced two most parsimonious trees, and IW resulted in one best tree, with broad agreement in relationships between them. The absolute frequencies (AF) and GC Jackknife support values for the resulting EW and IW tree are mapped above the nodes (Figs. 3A, S2A). The average group support of the IW tree was 45.7. The monophyly of the *Mecocephala* group (clade **I**) was recovered in all analyses (AF = 96, GC = 95), and is supported by the following exclusive synapomorphies (discrete characters optimisations only): apex of mandibular plates inferior in relation to clypeal apex, in lateral view (15:0) (Figs. 18D, 20E–F); antennomere 4 conical (24:1) (Fig. 18Fi, iv); evaporatorium occupying less than half of width of mesopleuron (58:0) (Fig. 18H, O), this condition may be an evolutionary novelty in the *Mecocephala* group, present in *H. meridionalis*, *Glyphepomis*, *Pedinonotus* and *H. inermis*; ventral rim of pygophore composed of two layers (86:1)

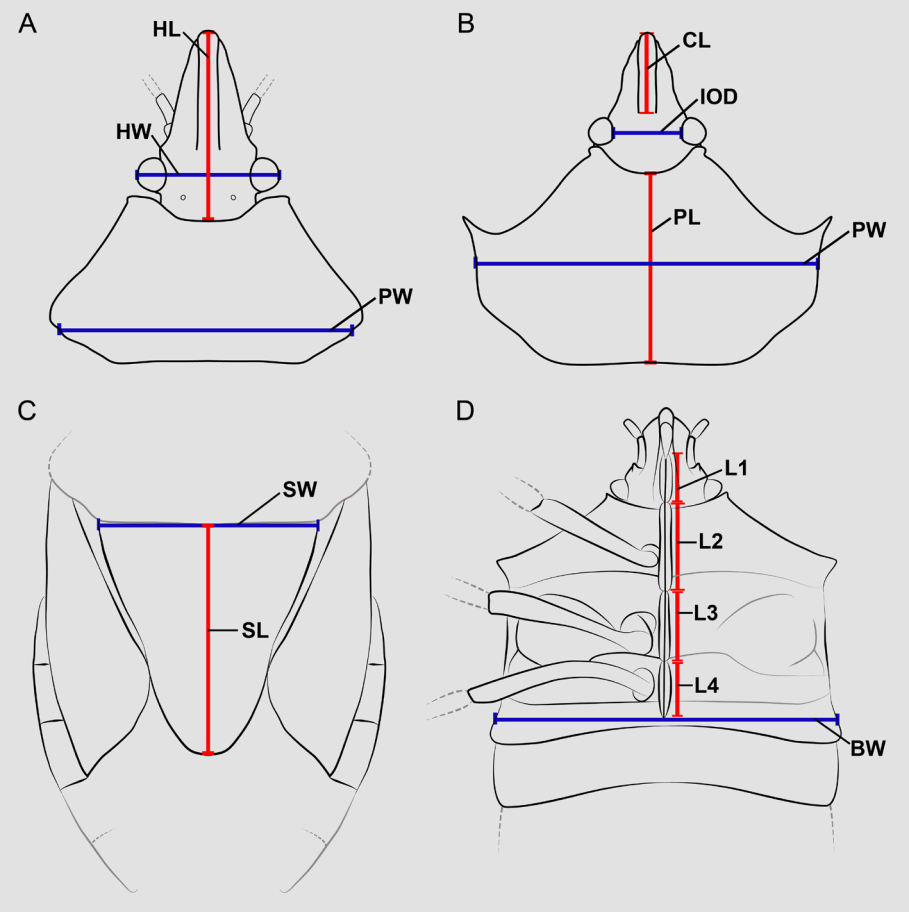

Fig. 1. Representation of measured morphometric parameters. — ***Abbreviations***: **A**: HL – head length; HW – head width; PW – pronotum width (width of pronotum after humeral angles). **B**: CL – length of clypeus; IOD – interocular distance; PL – pronotum length; PW – pronotum width. **C**: SL – scutellum length; SW – scutellum width. **D**: L1 – length of labiomere 1; L2 – length of labiomere 2; L3 – length of labiomere 3; L4 – length of labiomere 4; BW – body width (abdominal width at level of abdominal sternite 3).

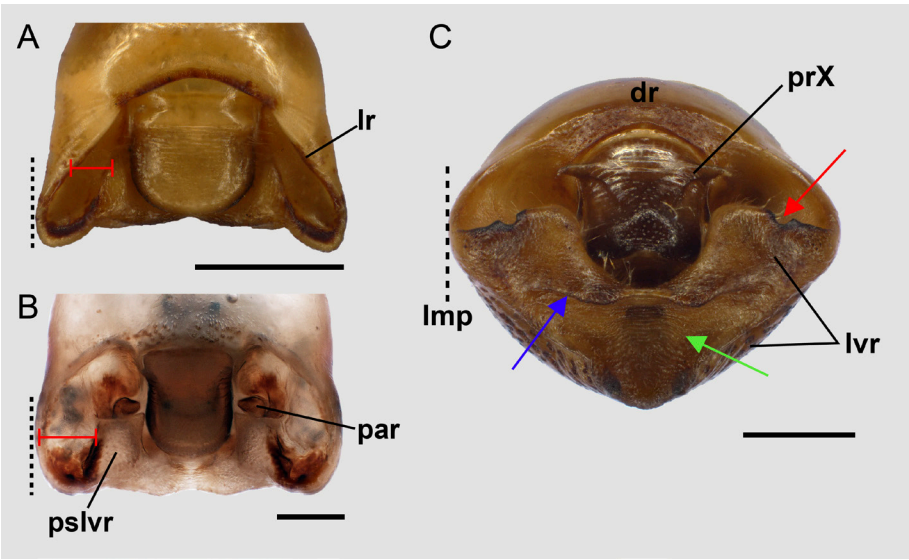

Fig. 2. Representation of male terminalia of genera of *Mecocephala* group. **A**–**B**: pygophore, dorsal view. **A**: showing the genital cup narrow and absence of parameres; **B**: showing the genital cup broad and reduced parameres; **C**: pygophore, posterior view, showing the layers of ventral rim, the carina between layers (blue arrow), the area between layers (green arrow), and lateral margins of projections of superior layer of ventral rim notched (red arrow). — (A): *Hypatropis inermis*; (B): *Tibraca similima*; (C): *Tibraca limbativentris*. The red line showing the distance between the lateral margin of pygophore and the lateral rim of pygophore. Scale bars = 1.0 mm.

(Figs. 2C, 5B, 7B, 10B, 12H, 19K, N, Q); distal ductus receptaculi convolute (138:1) (Figs. 5K, 11D, 16F, G), and also by homoplasies: labiomere 1 contained in the bucculae (29:0) (Figs. 14E, 18D–E); ductus seminis distalis long to extremely long in relation to the length of the conjunctiva (104:2, 3); proximal ductus receptaculi convolute (133:1); proximal ductus receptaculi longer than the vesicular area (135:1) (Fig. 16F–G). Most of the Jackknife frequencies for the relationships among genera of the *Mecocephala* group were relatively high. But because the investigation of intergeneric relationships within *Mecocephala* group is not the focus of this study, we do not discuss this result.

Hypanthracos was inferred to be the sister lineage of the remaining taxa of the *Mecocephala* group with high values of Jackknife AF and GC (Fig. 3A), with a combination of homoplasies. The exclusive synapomorphies of clade **II**, which *Hypanthracos* does not share

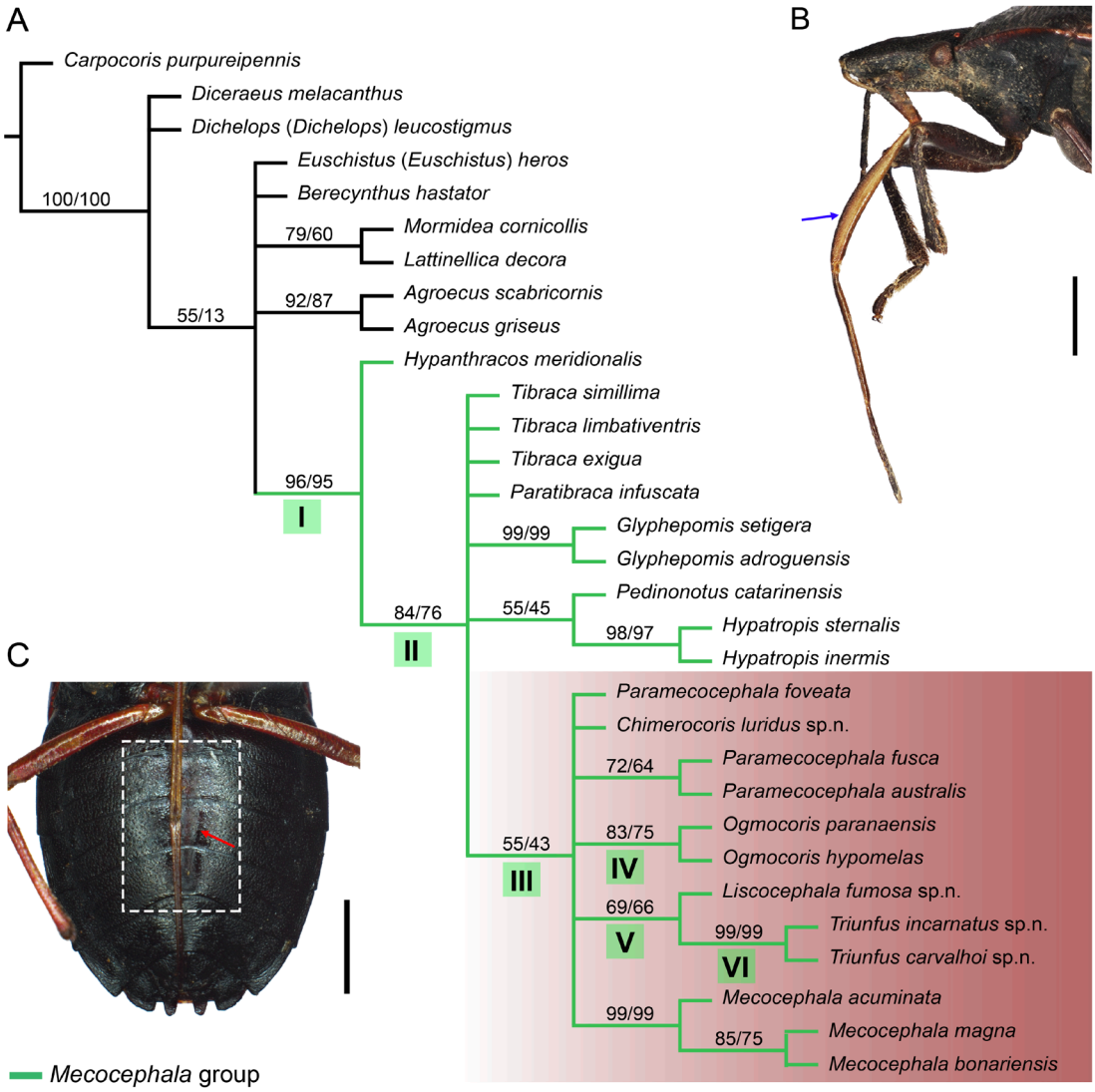

Fig. 3. Phylogenetic relations of genera of *Mecocephala* group. **A**: tree resulting from implied weighting scheme. Jackknife support values mapped above represent absolute frequencies and GC values, respectively. Number in capital letters indicated the target clades. **B**–**C**: exclusive synapomorphies of the clade III (labiomere 2 flattened laterally, blue arrow, and longitudinal groove on abdominal sternites, red arrow). — (B): *Parameccephala bergrothi* Frey-da-Silva & Grazia, 2002; (C): *Mecocephala magna*. Scale bars = 2.0 mm.

are (AF = 84, GC = 76): antennomere 4 slightly flattened dorsally (25:1) (Fig. 20G), evolutionary novelty of this clade, with reversion in species *T. similima*, *Chimerocoris luridus* sp.n. (Fig. 19D) and *O. hypomelas*; evaporatorium not concolourous to the metasternum (51:1) (Fig. 18I, M); genital cup opening dorsoposteriorly (78:1); lateral margins of dorsal rim bordering the lateral rim of pygophore (81:0) (Figs. 7A, 10A), with reversion in *H. sternalis*, *H. inermis* (Fig. 2A), *P. fusca* (Fig. 19M) and *P. australis*, and by homoplasies: outline of anterolateral margins of pronotum explanate (35:1) (Figs. 12D, 15D, 18B–C, 19D–E, 20I–J); evaporatorium present in the anterolateral angle of each mesopleuron (59:1) (Fig. 18I–O); genital cup occupying more than half the length of pygophore (79:2) (Figs. 12G, 19P); posterolateral angles of pygophore quadrate (80:1); segment X with processes (98:1) (Figs. 7A, D, 10I–K, 12H, 19P); posterior margins of laterotergites 8 obtusely projected (127:2); apices of laterotergites 9 surpassing tergite 8 (129:1) (Figs. 8C, 11A, 16B). In addition to these, another homoplasies from clade **II** (AF = 86, GC = 78, Fig. S2A) was recovered in the EW scheme: extension of dorsal rim of pygophore obsolete over segment X (85:1) and phallotheca with rounded projections on posterolateral margins (107:1) (Fig. 10L).

In addition, all the new taxa proposed in this study represented independent lineages (AF = 55, GC = 43, Fig. 3A, clade **III**) and we base our taxonomic decisions on these results. The synapomorphies that support clade **III** with the new genera are the following: labiomere 2 flattened laterally (30:1) (Figs. 3B, 6C, 12C, 20F); abdominal sternites with a longitudinal groove medially (72:1) (Figs. 3C; 13E). All representatives of this clade have a long labium (at least surpassing the middle of abdominal sternite 4).

The monotypic *Chimerocoris* gen.n. shares with the other genera of clade **III** the following combination of homoplasies: presence of anteocular process (19:1)

(Fig. 19D); antennomere 4 convex dorsally (25:0) (Figs. 18Fii–iii, 19D); bucculae truncate posteriorly (28:0) (Fig. 18D–E); anterior angles of pronotum without processes (32:0) (Figs. 19D, 20I–J); size of scutellar fovea equal to diameter of eyes (41:1); outer margin of each evaporatorium on metapleuron straight (54:2) (Fig. 18I–K, M); anterolateral margin of each evaporatorium on metapleuron tapered (55:1); pygophore sub-rectangular (77:1), and layers of ventral rim of pygophore separated by a carina (87:1) (Figs. 7B–E, 19Q).

The monophyly of the *Ogmocoris* (clade **IV**) was recovered (AF = 83, GC = 75, Fig. 3A) and is supported by the following combination of homoplasies: mandibular plates as long as clypeus (14:1) (Fig. 12D–E); anterolateral margins of pronotum concave (36:1) (Figs. 9A, 12A, D); humeral angles of pronotum developed (38:0) (Figs. 8A, 9A); apex of each radial vein punctate (43:0) (Fig. 21C); hemelytra surpassing apex of abdomen (44:0) (Figs. 9A, 12A); legs concolourous with abdominal venter (65:0) (Fig. 12B), and area between layers of ventral rim excavate (88:1) (Figs. 10B, 12H). In addition, *Ogmocoris* is the only genus assigned to the *Mecocephala* group that has the crown of the paramere well-developed (102:0) (Fig. 10D–H), which is a common character in genera outside of the *Mecocephala* group.

One of the characters shared by *Liscocephala* gen.n. and *Triunfus* gen.n., clade **V** (AF = 69, GC = 66, Fig. 3A), is the strong reduction of antennomere 2 in relation to antennomere 1 (characters 5 and 6) (Figs. 18Fiv–v, 20G–H). *Liscocephala* is supported by a series of apomorphies: antennomere 3 conical (22:1) (Figs. 13D, 20G), antennomere 3 slightly flattened dorsally (23:1) (Figs. 13D, 20G); the corial apices of hemelytra not reaching the apices of abdominal tergite 5 (42:1) (Fig. 20K); the evaporatorium absent along the outer margin of each mesopleuron (61:0); metathoracic spiracles narrow (64:0) (Fig. 18K); posterior margins of valvifers 8 sinuous [(121:1); Fig. 16A, C]; valvifers 9 depressed (125:2) (Figs. 13F, 16A, C), and laterotergites 9 not surpassing abdominal tergite 8 (129:0) (Fig. 16A, C).

The monophyly of the new genus *Triunfus* was recovered with high support values, clade **VI** (AF = 99, GC = 99, Fig. 3A) by the following synapomorphies: antennomere 2 obsolete, not apparent (21:1) (Figs. 14D, 15E, 20H) and posterior margin of pronotum emarginate in the middle (39:2) (Figs. 14A, 15A, D, 20J). In addition, both species share the following combination of homoplasies: antennomere 3 convex dorsally (23:0) (Figs. 14D, 15E, 20H); bucculae rectilinear (26:1) (Fig. 14E); ostioles of metathoracic glands circular (45:1); each ostiolar peritreme extending 2/3 of width to the outer margin of the evaporatorium (49:1) (Figs. 15F, 18L); legs concolourous with the ventral abdominal surface (65:0) (Fig. 14B); anterolateral angles of each connexiva concolour with discal colouration (67:0) (Figs. 14A, 20L); mesial margins of valvifers 8 not juxtaposed (118:1) (Fig. 16B, D), and valvulae 8 visible in ventral view (130:1) (Fig. 16D).

3.2. Taxonomy

According to the results of the phylogenetic analysis.

3.2.1. Supplementary description to genus *Hypanthracos*

***Hypanthracos meridionalis* Grazia & Campos, 1996**

Figs. 4A–C, 5A–K, 17, 18A, Fi, H

Hypanthracos meridionalis Grazia & Campos, 1996: 15–16, figs 1, 3, 5–8, 13–15, 19, 21; Ruschel et al. (2013: 552).

Diagnosis. Clypeal suture beginning before an imaginary line crossing anterior margin of compound eyes. Bucculae sub-rectilinear. Outline of anterolateral margins of pronotum flat. Humeral angles strongly developed into spinous processes. Basal angles of scutellum foveate, foveae smaller than the diameter of a compound eye. The outer margin of each metapleural evaporatorium is straight; gyrification of evaporatorium with low wrinkles. Sublateral margins of sternites concolourous with abdominal venter. Spiracles concolourous with sublateral margins of abdominal sternites. Genital cup narrow, open dorsally, occupying less than half the length of pygophore. Dorsal rim of pygophore with 1 + 1 dorsal processes; extension of dorsal rim well-developed over the segment X. Superior layer of ventral rim without processes; lateral margin of each projection of superior layer of ventral rim entire. Inferior layer of ventral rim without process. Segment X quadrangular, without process. Parameres absent. Phallotheca destitute of dorsal processes and rounded posterolateral projections. Conjunctiva with three pairs of lobes, apically sclerotized.

Redescription. ***Measurements***: Table 4. ***Colouration***: General colouration castaneous dorsally and dark castaneous to black ventrally. Dorsal and ventral surface of body with dense and dark-castaneous to black punctures. Head dark castaneous, brown punctate on basal half, concolourous apex. Antennomeres uniformly dark castaneous, black on distal half of antennomere 4 (Figs. 4A–B, 18Fi). Labium castaneous, apical labiomeres dark castaneous. Outline of anterolateral margins of pronotum black; dark castaneous punctate. Pro-, meso-, metasternum including evaporatorium dark castaneous to black. Legs castaneous, distal half of femora dark castaneous to black (Fig. 4B). ***Head*** (Figs. 4A, 18A): Head longer than wide, apex rounded; mandibular plates obtuse and convex apically; clypeal apex obtuse, clypeal suture beginning before an imaginary line crossing anterior margin of compound eyes; anteocular processes absent; antenniferous tubercles visible in dorsal view, each with an obtuse process laterally. Proportions of antennomeres: 1 > 2 < 3 > 4, 5 missing. Bucculae subrectilinear. ***Thorax***: Pronotum trapezoidal (Figs. 4A, 18A); anterior angles produced; outline of anterolateral margins concave, smooth,

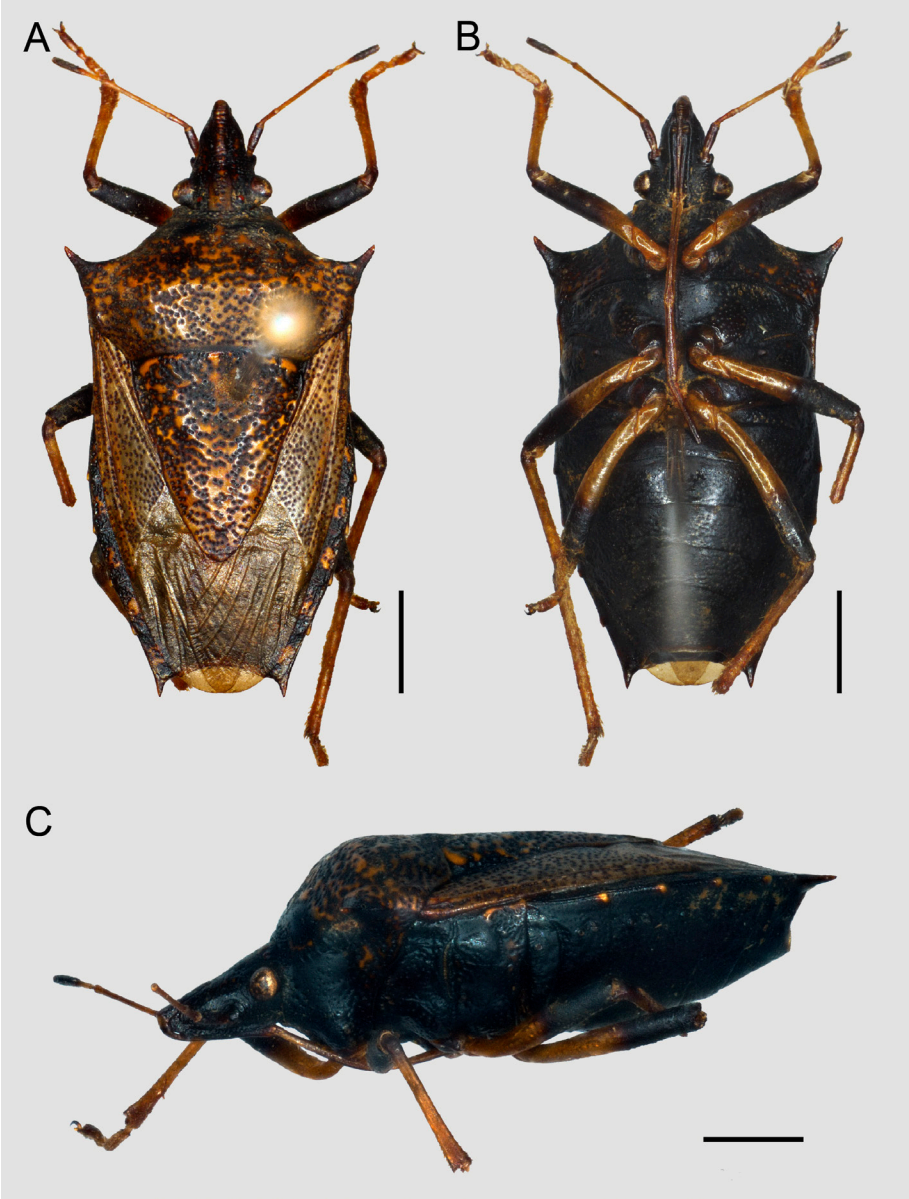

Fig. 4. *Hypanthracos meridionalis* Grazia & Campos, 1996: **A**: dorsal; **B**: ventral; **C**: lateral. Scale bars = 2.0 mm.

flat, not reflexed, impunctate; humeral angles strongly developed, into spinous processes, directed anteriorly; posterior margin rectilinear. Mesosternal carina elevated, smooth; metasternal furrow shallow. Each ostiole of ESES elliptical, opening posterolaterally; periostiolar depressions present; each peritrema spout-shaped, occupying about 2/3 of the distance to lateral margin of evaporatorium; medial furrow of the each ostiolar peritreme relatively long, occupying more than half of the length of peritreme; evaporatorium punctate, each occupying less than half of meso- and metapleuron; gyrification of evaporatorium with low wrinkles; anterolateral margin of each evaporatorium tapered; outer margin of each metapleural evaporatorium straight; evaporatorium on mesopleuron not reaching its anterior and posterior lateral angles, and the outer margins, as well as the anterior limits of mesocoxal sutures (Fig. 18H). Metathoracic spiracle wide. Length of femora and tibiae subequal; femora unarmed; tarsi 3-segmented. Scutellum longer than wide (Fig. 4A). Basal angles of scutellum foveate; foveae smaller than the diameter of a compound eye. Corium longer than scutellum, surpassing apices of abdominal tergite 5; apex of each radial vein punctate (inconspicuous callosity). Membrane with veins linear. Hemelytra surpassing apex of abdomen. ***Abdomen***: Connexivum exposed; posterolateral angles of each connexivum obtusely produced (Fig. 4A). ***Male terminalia***: Pygophore trapezoidal (Fig. 5A–F); posterolateral angles rounded. Genital cup nar-

→ **Fig. 5.** *Hypanthracos meridionalis* Grazia & Campos, 1996: **A**–**F**: male terminalia: **A**–**D**: dorsal; **B**–**E**: posterior: **C**–**F**: ventral; **G**–**I**: male genitalia: **G**: dorsal; **H**: lateral; **I**: ventral; **J**: female terminalia; **K**: female receptaculum seminis and ausenwand. Scale bars: A–F = 1.0 mm; G–I: 0.01 mm; J–K = 0.5 mm.

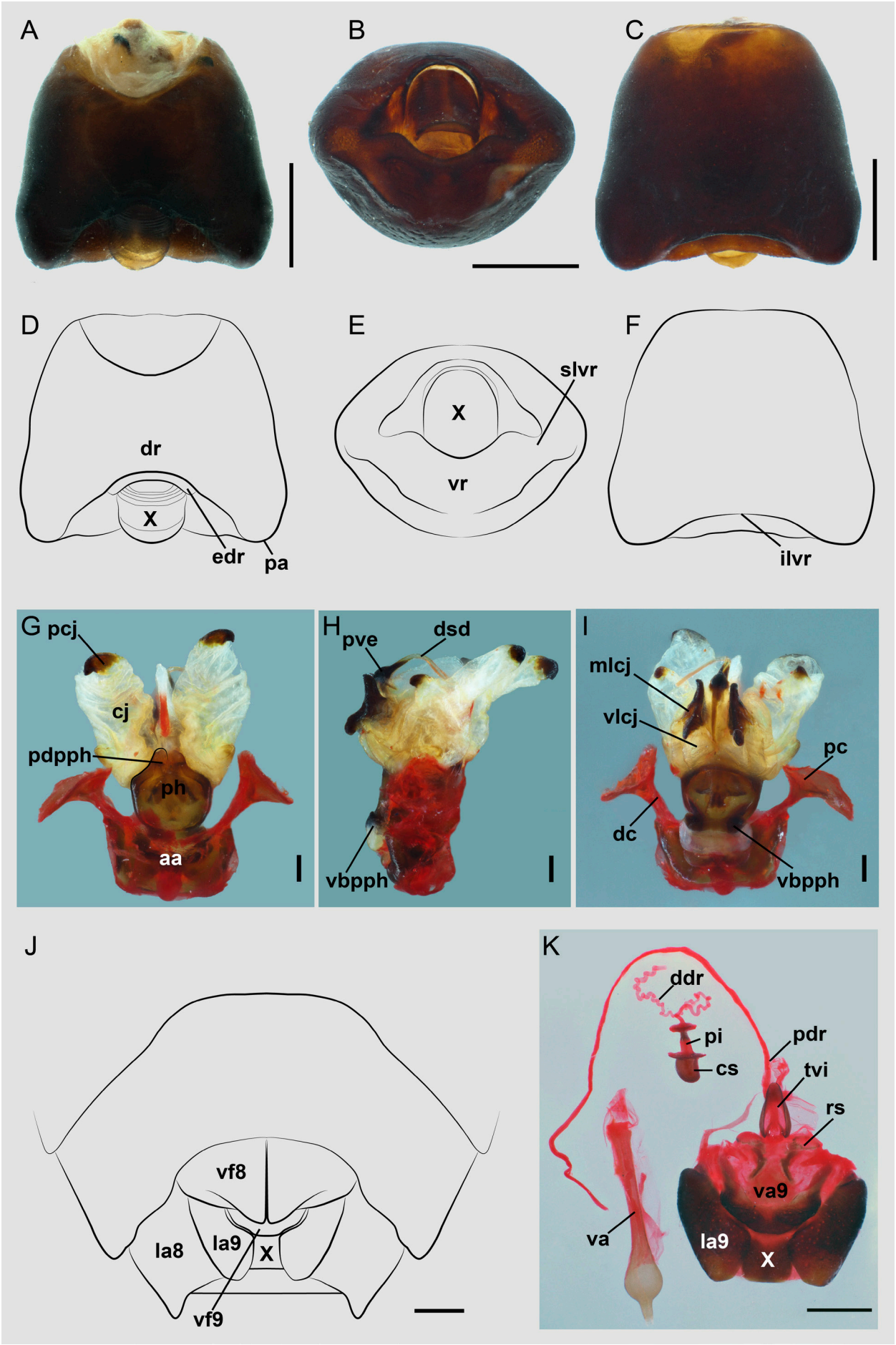
A
B
C
D
dr
X
edr
pa
E
slvr
X
vr
F
ilvr
G pcj
cj
pdpph
ph
aa
H pve
dsd
vbpph
I
mlcj
vlcj
pc
dc
vbpph
J
vf8
la8
la9
X
vf9
K
ddr
pi
cs
pdr
tvi
rs
va9
va
la9
X

row, open dorsally, occupying less than half the length of pygophore; dorsal rim medially entire with 1 + 1 dorsal processes; extension of dorsal rim well-developed over segment X; ventral rim forming two layers, inferior and superior layers of ventral rim, not separated by a carina; area between layers excavated. Superior layer of ventral rim projecting toward genital cup, developed laterally to segment X, without processes and lateral margin of each projection of superior layer of ventral rim entire (Fig. 5B, E). Inferior layer of ventral rim without processes (Fig. 5C). Segment X quadrangular, not carinate, without processes. Parameres absent. ***Male genitalia***: Phallus (Fig. 5G–I): Dorsal connectives of articulatory apparatus long, in relation to distal half of phallotheca. Processus capitati long, reaching phallotheca distal margin. Phallotheca piriform, longer than wide apically, without a pair of dorsal processes, and with two pairs of projections: 1 + 1 on posterodorsal margin and 1 + 1 ventrobasal. Conjunctiva with two pairs of processes and three pairs of lobes: lateral, median, and ventral lobes, apically sclerotized. Process of vesica long. Ductus seminis distalis extremely long, at least four times longer than the conjunctiva, convolute. ***Female terminalia*** (Fig. 5J): Valvifers 8 convex, subequal in length to laterotergites 9, partially covering valvifers 9; mesial margins juxtaposed, posterior margins sinuous; valvulae 8 not visible in ventral view. Laterotergites 8 with posterior margins acutely projected; spiracles absent. Valvifers 9 swollen, leveled, relative to the position of segment X, with anterior margins straight and posterior margins concave. Laterotergites 9 triangular, obtusely projected apically, not surpassing tergite 8. ***Female genitalia***: Valvulae 9 with 1 + 1 medially sclerotized areas. Ring sclerite elliptical. Ectodermal ductus (Fig. 5K): proximal ductus receptaculi convoluted, long in relation to length of vesicular area, at least two times longer; equal diameter. Median wall of vesicular area enlarged subproximally. Distal ductus receptaculi convoluted, long, at least two times longer than vesicular area, with diameter equal to median wall of vesicular area diameter. Annular flanges divergent. Capsula seminalis wider than posterior annular flange, globose, equal in relation to the length of *pars intermedialis*. *Pars intermedialis* enlarged.

Type material: Holotype ♀, 'URUGUAY, | Artigas, 17.xi.1955, F H C leg.' (MACN). – Paratypes: ♀, 'BRAZIL, Rio Grande do Sul, Osório, Capão Alto, 13.ii.1965, L Buckup leg.' | '2854' (MCNZ) <illustrated specimen>. ♂, 'URUGUAY, Artigas, Potrero Sucio-Arroyo Tres Cruces, 17.ii.1955, F H Y C leg.' (UFRG) <illustrated specimen>.

Comments. A detailed description of the external scent efferent system, an update of the terminology of male genitalia, photographs of paratypes and of terminalia and genitalia for both sexes, and a distribution map for *H. meridionalis* are provided.

In addition to this species, *H. ditarsus* is also known, not examined here for lack of material. *H. ditarsus* can be distinguished mainly by the morphology of the genitalia of both sexes and by tarsi 2-segmented. (Grazia & Campos 1996). *H. ditarsus* holotype is deposited in the MZUSP (Grazia & Campos 1996; Carrenho et al. 2020).

Distribution. Brazil: Rio Grande do Sul and Uruguay: Artigas (Fig. 17).

3.2.2. Description and diagnosis of *Chimerocoris*

Chimerocoris gen.n.

Type species. *Chimerocoris luridus* sp.n., here designated.

Diagnosis. Head longer than wider; labium long; surpassing the middle of abdominal sternite 6; labiomere 2 flattened laterally. Anterolateral margins of pronotum not reflexed. Basal angles of scutellum with foveae subequal to the diameter of a compound eye. Layers of ventral rim of pygophore separated by a carina; parameres reduced, with obsolete crown; segment X with a transverse carina and 1 + 1 thorn-like processes at base.

Description. Body ovate. ***Head***: Head longer than wide, apex rounded (Figs. 6A; 19D). Mandibular plates shorter than clypeus, obtuse at apices; lateral margins of mandibular plates sinuous. Clypeal apex obtuse, in a higher level than mandibular plates in lateral view; clypeal suture beginning after an imaginary line crossing anterior margin of compound eyes; antenniferous tubercles visible in dorsal view, each with an obtuse process laterally. Antennomere 1 not reaching apex of head; antennomere 2 visible; antennomere 3 cylindrical; antennomere 4 conical, convex dorsally (Fig. 18Fii). Bucculae sinuous, truncate posteriorly. Labium long, surpassing middle of sternite 6; first labiomere lying entirely between the bucculae; labiomere 2 flattened laterally and labiomeres 3 and 4 uniformly entire. ***Thorax***: Pronotum trapezoidal (Fig. 19D); anterolateral margins explanate, not reflexed, impunctate; posterior margin slightly convex. Mesosternal carina elevated, smooth; metasternal furrow shallow. Each of ostiole of ESES guttiform, opening posterolaterally; each peritreme spout-shaped; medial furrow of the each ostiolar peritreme long, occupying more than of length of peritreme; evaporatorium punctate, each occupying more than half of meso- and metapleuron; evaporatorium on mesopleuron reaching its anterior and posterior lateral angles, and surpassing the limits of mesocoxal sutures (Fig. 18I). Metathoracic spiracle wide. Length of femora and tibiae subequal; femora unarmed; tarsi 3-segmented. Scutellum longer than wide (Fig. 6A). Basal angles of the scutellum foveate; foveae subequal to diameter of a compound eye. Corium longer than scutellum, surpassing apices abdominal tergite 5 and apex of each radial vein conspicuously calloused. ***Abdomen***: Connexivum exposed (Fig. 6A). Sublateral margins of abdominal sternites not concolourous with abdominal venter (Figs. 6C, 19H). Medial longitudinal groove reaching sternite 6 (Fig. 6B). ***Male terminalia***: Genital cup of pygophore

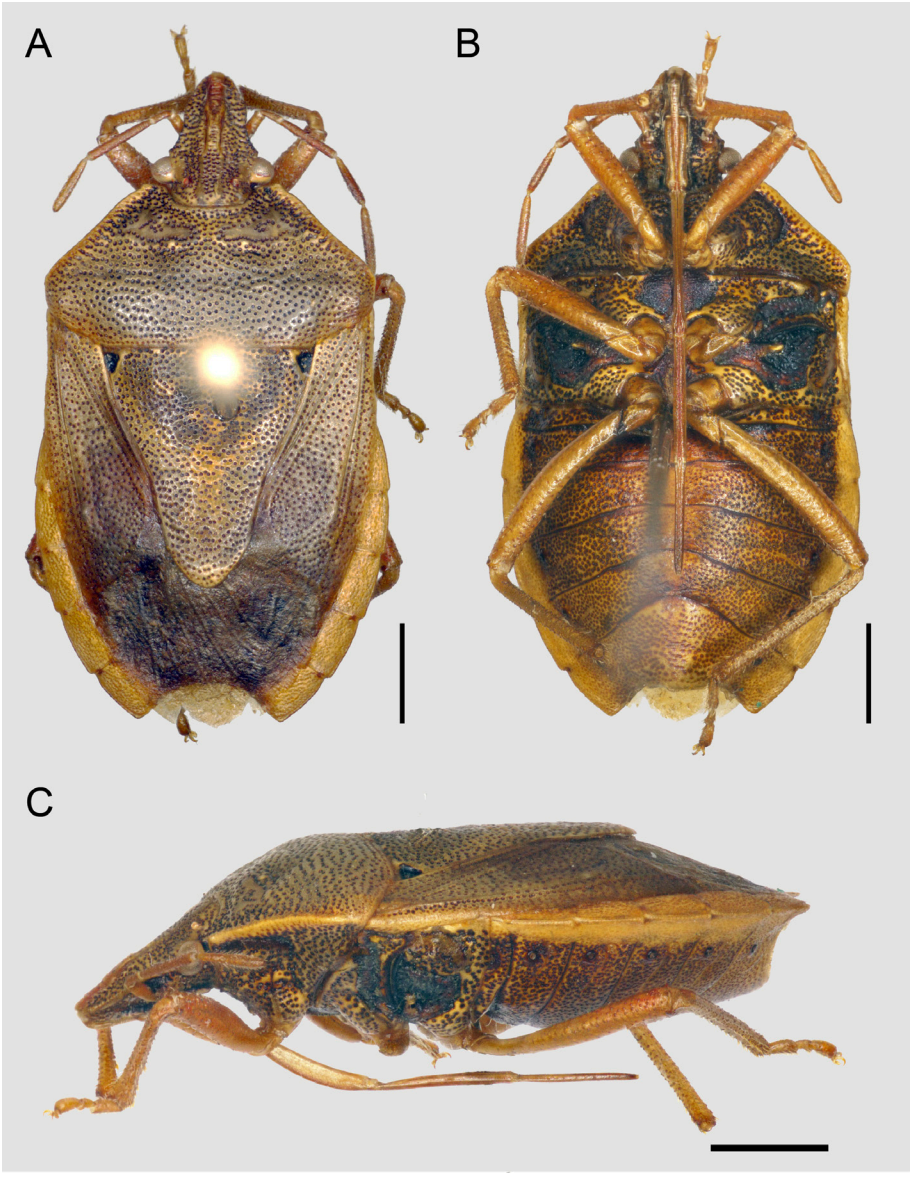

Fig. 6. *Chimerocoris luridus* sp.n. ♂: **A**: dorsal; **B**: ventral; **C**: lateral. Scale bars = 2.0 mm.

broad, open posterodorsally; ventral rim composed of two layers, the inferior and superior layers, separated by a carina (Figs. 6E, 19J–L). Superior layer of ventral rim, projecting toward genital cup, developed laterally to segment X, not covering parameres; lateral margin of each projection of superior layer notched. Segment X carinate and with 1 + 1 thorn-like processes at base. Parameres reduced, with obsolete crown.

Etymology. From Greek *Chimero-* mythological figure characterized by a hybrid appearance referring to the combination of characters of two genera (*Tibraca* and *Paramecocephala*); and *-coris*, stink bug; masculine.

Comments. *Chimerocoris* has the habitus and length of labium similar to *Paramecocephala*, and the morphology of pygophore similar to *Tibraca*. The comparison of these genera is presented in Figure 19.

Distribution. Brazil: Rio Grande do Sul (Fig. 17).

3.2.3. *Chimerocoris luridus* sp.n.

Figs. 6A–C, 7A–F, 17, 18 Fii, I, 19A, D, F, H, J–L

Diagnosis. Each antennomere 3 cylindrical, shorter than 5 and antennomeres 4 conical, convex dorsally. Bucculae truncate, reaching base of head. Labium long, surpassing the middle of abdominal sternite 6. Anterolateral margins of pronotum not reflexed. Basal angles of scutellum with foveae subequal to the diameter of a compound eye. Segment X ogival, with a transverse carina and 1 + 1 thorn-like processes at base.

Description. ***Measurements***: Table 4. ***Colouration***: General colour yellowish-brown dorsally and ventrally, densely punctate (Fig. 6A, B). Head with calloused, yellow longitudinal stripes on clypeus medially; antennomeres uniformly brownish (Fig. 6A); antenniferous tubercles and maxillary plates brown. Outline of anterolateral margins of pronotum yellowish. Femora, tibiae

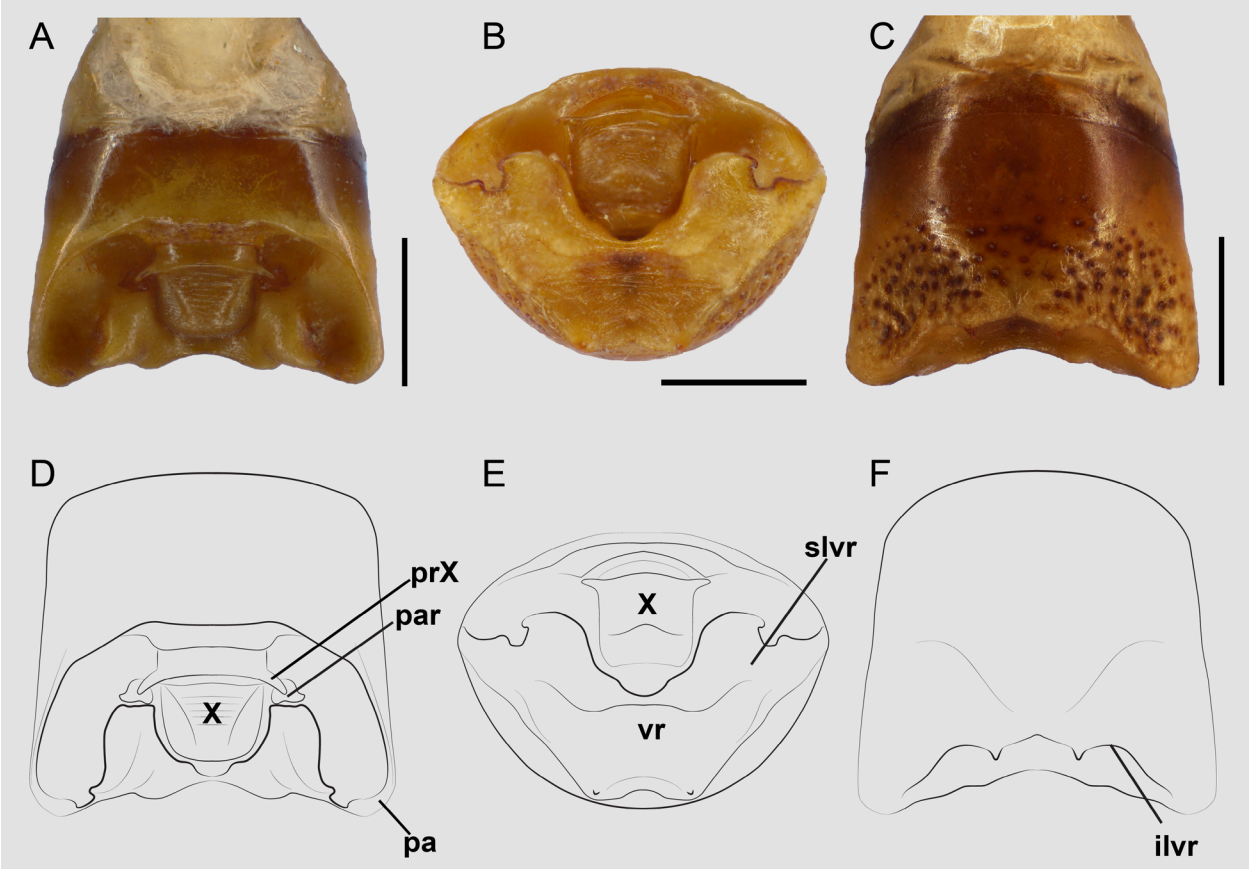

Fig. 7. *Chimerocoris luridus* sp.n. ♂: Male terminalia: **A**–**D**: dorsal; **B**–**E**: posterior; **C**–**F**: ventral. Scale bars = 1.0 mm.

and tarsi yellowish (Figs. 6A; 19D). Connexivum yellow, each connexivum with blotchy spot brown in the posterolateral angles (Fig. 6A). Sternites brown with darkened punctures; antero- and posterolateral angles of sternites dark brown (Fig. 6B). Sternites 3–7 yellow sublaterally, with concolourous trichobothria and punctures (Fig. 6C). Spiracles dark brown. ***Head***: Anteocular processes present. Proportions of antennomeres: 1 < 2 > 3 < 4 < 5. Posterior margins of bucculae reaching base of head. Labiomere 2 shorter than labiomeres 3 and 4 combined (Fig. 6C). ***Thorax***: Anterior angles of pronotum not produced; anterolateral margins of pronotum straight and smooth; humeral angles not produced (Fig. 19D). Periostiolar depressions of ESES present; each peritreme extending about ⅔ of the distance to lateral margin of evaporatorium; gyrification of evaporatorium with high wrinkles; anterolateral margin of each evaporatorium rounded; outer margin of each metapleural evaporatorium concave (Fig. 18I). Corium surpassing apices of abdominal tergite 5. Membrane with veins linear. Hemelytra not surpassing apex of abdomen (Fig. 6A). ***Abdomen***: Posterolateral angles of each connexivum not produced. ***Male terminalia***: Pygophore subrectangular (Figs. 7A–F; 19J–L); posterolateral angles rounded. Genital cup occupying more than half the length of pygophore; dorsal rim medially entire; extension of dorsal rim over segment X obsolete; area between layers of ventral rim depressed, striated; superior layer of ventral rim U-shaped medially, with two pairs of processes (Fig. 7C). Inferior layer of ventral rim with 1 + 1 processes (Fig. 7F). Segment X ogival. Crown of parameres trapezoidal (Fig. 7D).

Female. Unknown.

Etymology. *Luridus*, in Latin, yellow, referring to the colour of legs and connexiva; adjective.

Type material: Holotype ♂, 'BRAZIL, Rio Grande do Sul, [São Francisco de Paula], Pro-Mata | Projeto Sitel/ Corsan | 5.xii.1997 | C Weirauch leg.' (MCTP) <illustrated specimen>.

Distribution. Brazil: Rio Grande do Sul (Fig. 17).

3.2.4. Redescription and diagnosis of *Ogmocoris*

Ogmocoris Mayr, 1864

Ogmocoris Mayr, 1864: 908
Ogmocoris: Mayr 1866: 34; Stål 1872: 30; Lethierry & Severin 1893: 132; Kirkaldy 1909: 72; Silva 1945: 596; Costa Lima 1947: 312; Fernandes & Grazia 1998: 1058; Frey-da-Silva et al. 2002: 179–185; Silva et al. 2018: 432.
Ansa Walker, 1868: 548. (syn. by Stål 1872).

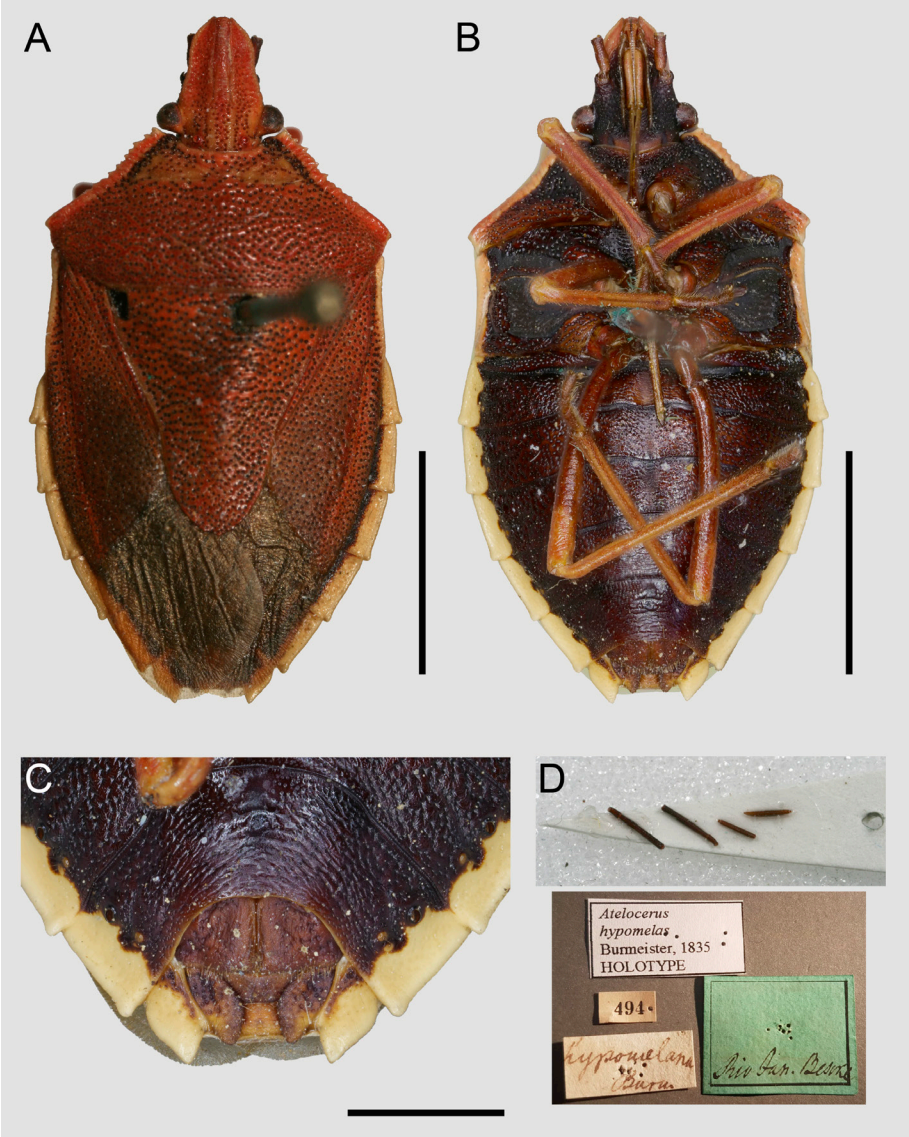

Fig. 8. *Ogmocoris hypomelas* (Burmeister, 1835) ♀, lectotype: **A**: dorsal; **B**: ventral; **C**: female terminalia; **D**: antenna and labels. Scale bars: A–B = 5.0 mm; C = 2.0 mm.

Type species. *Atelocerus hypomelas* Burmeister, 1835, by monotypy.

Diagnosis. Mandibular plates and clypeus subequal in length. Antennomere 2 shorter than first. Labium long, surpassing the middle of sternite 5. Ostioles elliptical. Conjunctiva with one pair of processes and two pairs of lobes: median and ventral lobes. Annular flanges convergent.

Redescription. Body elongate (Figs. 8A–B, 9A–B, 12A–B). ***Head***: Head longer than wide, apex rounded (Figs. 8A, 9A, 12A, D). Mandibular plates as long as clypeus, apices obtuse; lateral margins sinuous. Clypeal apex obtuse, in a higher level than mandibular plates in lateral view; clypeal suture beginning after an imaginary line crossing anterior margin of compound eyes. Antenniferous tubercles visible in dorsal view, each with an obtuse process laterally. Antennomere 1 not reaching apex of head; antennomere 2 shorter than 1, visible (Figs. 8D, 9A–B, 12D); antennomere 3 cylindrical, slightly flattened; antennomere 4 cylindrical, convex dorsally (Fig. 18Fiii). Bucculae tapering towards the base of head, not reaching its base. Labium long labium, surpassing middle of sternite 5 (Figs. 9C, 12C); labiomere 1 lying entirely between bucculae, labiomere 2 flattened laterally, shorter than labiomeres 3 and 4 combined and labiomeres 3 and 4 uniformly entire. ***Thorax***: Pronotum trapezoidal (Figs. 8A, 9A, 12A, D, 21A–B); anterolateral margins explanate, not reflexed and impunctate; posterior margin slightly convex. Mesosternal carina elevated, smooth; metasternal furrow shallow. Each ostiole of ESES elliptical, opening posterolaterally; periostiolar depressions present; each peritrema spout-shaped, occupying about 1/3 of the distance to lateral margin of evaporatorium; medial furrow of the each ostiolar peritreme long, occupying more than half of the length of peritreme; evaporatorium punctate, occupying more than half of meso- and metapleuron; anterolateral margin of each evaporatorium rounded; evaporatorium on mesopleuron reaching its anterior and posterior lateral angles, and surpassing the limits of mesocoxal sutures (Fig. 18J). Metathoracic

spiracle wide (Fig. 18J, red arrow). Legs concolourous with abdominal venter (Figs. 8B, 9B, 12B). Length of femora and tibiae subequal; femora unarmed; tarsi 3-segmented. Scutellum longer than wide (Figs. 8A, 9A, 12A) and basal angles foveate. Corium longer than scutellum, surpassing apices of abdominal tergite 5. Membrane with veins linear. Hemelytra surpassing apex of abdomen. ***Abdomen***: Connexivum exposed (Figs. 8A, 9A, 12A, 21C–D). Medial longitudinal groove on abdominal venter reaching sternite 6 (Figs. 8B, 9B, 12B). ***Male terminalia*** (Figs. 10A–N, 12G–I): Genital cup broad, open dorsoposteriorly. Ventral rim forming two layers, inferior and superior layers of ventral rim, not separated by a carina; area between layers excavated. Superior layer of ventral rim projected toward genital cup, developed laterally to segment X, not covering parameres. Segment X not carinate, with processes. Parameres well-developed. ***Female terminalia*** (Fig. 11A–C): Valvifers 8 convex. Valvulae 8 not visible. Laterotergites 8 lacking spiracles. Laterotergites 9 surpassing tergite 8 (Fig. 11A).

Distribution. Brazil: Amazonas, Rio de Janeiro and Paraná (Fig. 17).

3.2.5. Key to species of *Ogmocoris*

1 Outline of anterolateral margins of pronotum impunctate in dorsal view (Figs. 8A, 9A, 21A). Foveae on basal angles of scutellum relatively large, size equal to diameter of a compound eye (Figs. 8A, 9A, 21C). Sublateral margins of sternites lighter than of abdominal venter (Figs. 8B, 9B–C, 21F). Superior layer of ventral rim of pygophore with one pair of processes; lateral margin of each projection of superior layer of ventral rim notched (Fig. 10A–B). Segment X rectangular, with one process, medially (Fig. 10I–K). .. .. ***O. hypomelas*** (Burmeister)

1' Outline of anterolateral margins of pronotum punctate in dorsal view (Figs. 12A,D, 21B). Foveae on basal angles of scutellum relatively small, size less than diameter of a compound eye (Fig. 12A, 21D). Sublateral margins of sternites concolourous with disc of abdominal venter (Figs. 12B–C, 21G). Superior layer of ventral rim without process; lateral margin of each projection of superior layer of ventral rim entire (Fig. 12G–H). Segment X ogival, with 1 + 1 tumescent processes basally (Fig. 12H). .... ***O. paranaensis*** .....Frey-da-Silva, Grazia & Fernandes

3.2.6. *Ogmocoris hypomelas* (Burmeister, 1835)

Figs. 8A–D, 9A–C, 10A–N, 11A–D, 17, 18Fiii, J, 21A, C, F, H, J

Atelocerus hypomelas Burmeister, 1835: 362
Ogmocoris hypomelas: Mayr 1864: 908; Stål 1872: 30; Lethierry & Severin 1893: 132; Kirkaldy 1909: 72; Frey-da-Silva et al. 2002: 179–185; Silva et al. 2018: 432.
Ansa distincta Walker, 1868: 548–549. (syn. by Stål 1872)

Diagnosis. Bucculae rectilinear. Outline of anterolateral margins of pronotum impunctate in dorsal view. Fovea in each basal angle of the scutellum about the same size as the diameter of a compound eye. The outer margin of each metapleural evaporatorium straight; gyrification of evaporatorium with low wrinkles. Sublateral margins of abdominal sternites not concolourous with abdominal venter (pale yellow to orange). Spiracles concolourous with abdominal venter, dark-castaneous to ferruginous. Dorsal rim of pygophore with 1 + 1 dorsal processes; extension of dorsal rim well-developed over segment X. Superior layer of ventral rim with two pairs of processes; lateral margin of each projection notched. Inferior layer of ventral rim with one median process. Segment X rectangular, with one tumescent process, medially. Valvulae 9 with 1 + 1 lateral sclerotized areas placed along with ring sclerite and one medially.

Redescription. ***Measurements***: Table 4. ***Colouration***: General colour reddish-castaneous dorsally, with dense dark-brown to black punctures; ventral surface dark-castaneous to ferruginous with dense concolourous punctures. Head reddish-castaneous, punctures on basal half castaneous, those on distal half concolourous. Antennomeres uniformly dark-castaneous (Fig. 9A). Labium reddish-castaneous, apical labiomeres dark brown. Outline of anterolateral margins of pronotum and lateral margins of coria ferruginous; punctures dark-brown. Pro-, meso-, metasternum, and evaporatorium dark-castaneous to reddish-castaneous; lateral margins yellowish. Legs reddish-castaneous; femora and tibiae immaculate, yellowish-ferruginous. Connexivum ferruginous, lateral half yellow. Sternites dark brown to reddish-castaneous, with dark-brown punctures; sublateral band from sternite 3 to abdominal sternite 7 pale yellow to orange. Spiracles dark brown. Trichobothria yellowish. ***Head*** (Figs. 8A, 9A): Anteocular processes absent. Proportions of antennomeres: 1 > 2 < 3 > 4, 5 missing (Fig. 18Fiii). Bucculae rectilinear. ***Thorax***: Pronotum with anterior angles produced; anterolateral margins concave, crenulate; humeral angles slightly developed (Figs. 8A, 9A, 21A). Gyrification of evaporatorium with high wrinkles; outer margin of each metapleural evaporatorium straight (Fig. 18J). Fovea in each basal angle of the scutellum about the same size as the diameter of a compound eye (Fig. 21C, green arrow). Apex of each radial vein punctate (inconspicuous callosity, Fig. 21C, blue arrow). ***Abdomen***: Posterolateral angles of each connexivum produced (Fig. 21C, red arrow). Sublateral margins of abdominal sternites not concolourous with abdominal venter, pale yellow to orange (Figs. 8C, 9C, 11A–B, 21F, blue arrow). ***Male terminalia***: Pygophore trapezoidal (Fig. 10A–D); posterolateral angles somewhat explanate, apical margin sinuous. Genital cup occupying half the length of pygophore; dorsal rim medially entire with 1 + 1 dorsal processes (Fig. 10A–B); extension of dorsal rim well-developed over segment X. Superior layer of ventral rim with two pairs of processes (Fig. 10A); lateral margin of each projection notched (Fig. 10B). Inferior layer of ventral rim with one median pro-

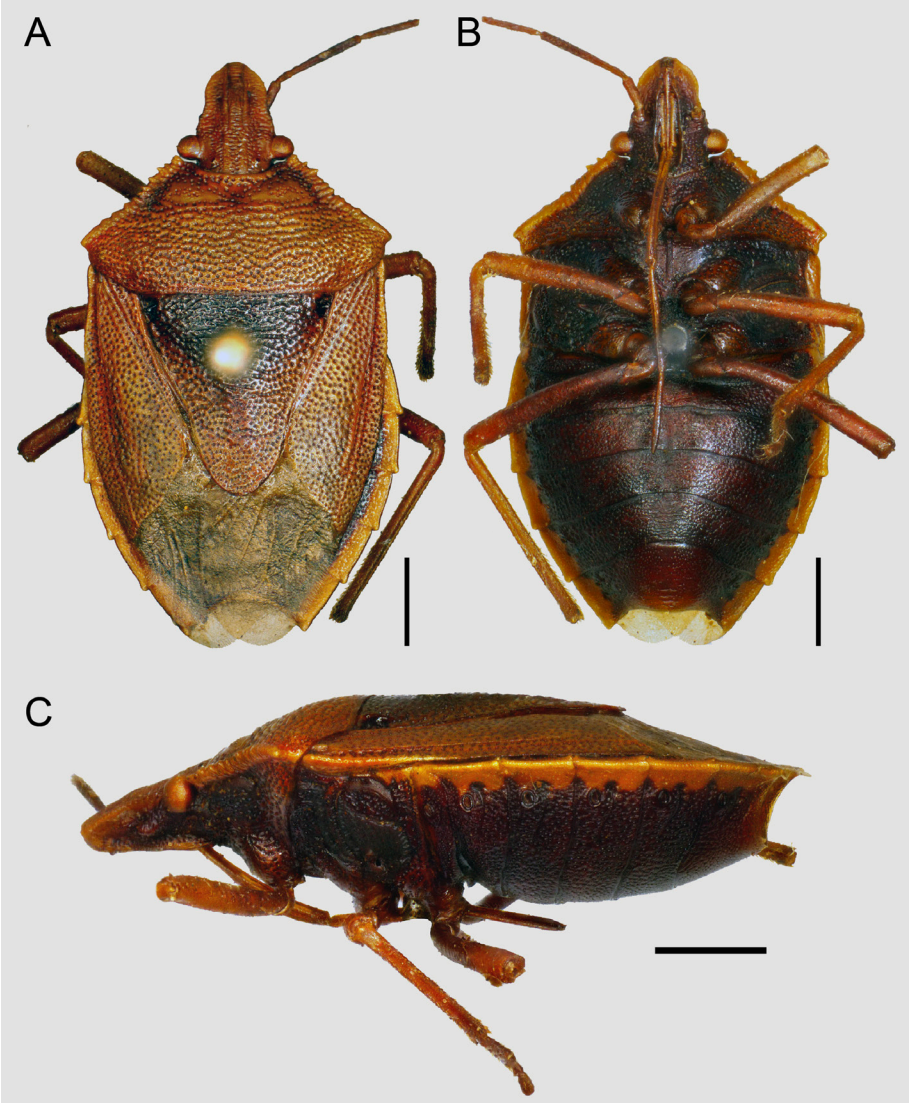

Fig. 9. *Ogmocoris hypomelas* (Burmeister, 1835) ♂: **A**: dorsal; **B**: ventral; **C**: lateral. Scale bars = 2.0 mm.

cess (Fig. 10C). Segment X rectangular, with one tumescent process medially (Fig. 10I–K). Crown of paramere well-developed, shell-shaped (Fig. 10D–H). ***Male genitalia***. Phallus (Fig. 10L–N): Dorsal connectives of articulatory apparatus long. Processus capitati long, reaching phallotheca distal margin. Phallotheca piriform, shorter than width apically, with a pair of dorsal processes, wider basally than medially, and three pairs of projections: 1 + 1 in posterodorsal margin, 1 + 1 ventrobasal, and 1 + 1 in posterolateral margin, rounded. Conjunctiva with one pair of processes and two pairs of lobes: median and ventral lobes, membranous. Process of vesica long. Ductus seminis distalis extremely long, at least five times longer than the conjunctiva, convolute. ***Female terminalia*** (Fig. 11A–B): Valvifers 8 convex, at least twice as long as laterotergites 9, partially covering valvifers 9; mesial margins juxtaposed, posterior margins sinuous; valvulae 8 not visible in ventral view. Laterotergites 8 with posterior margins obtusely projected; spiracles absent. Valvifers 9 flat, oblique, in an obtuse angle, relative to the position of segment X, with anterior margins concave and posterior margins straight. Laterotergites 9 triangular, obtusely projected apically, surpassing tergite 8. ***Female genitalia***: Valvulae 9 with 1 + 1 lateral sclerotized areas placed along with ring sclerite and one medially. Ring sclerite elliptical (Fig. 11C). Ectodermal ductus (Fig. 11C–D): proximal ductus receptaculi convoluted, extremely long in relation to the length of vesicular area, at least three times longer; greater diameter. Median wall of vesicular area enlarged subproximally. Distal ductus receptaculi convoluted, extremely long, at least three times longer than vesicular area, with diameter equal to median wall of vesicular area diameter. Annular flange convergent; posterior annular flange wider than length of *capsula seminalis*. *Pars intermedialis* rectilinear. *Capsula seminalis* globose and smaller than *pars intermedialis*.

Material examined. ***Type material***: Lectotype ♀, 'BRAZIL, Rio de Janeiro | *hypomelas* <sic> Burm. | Rio Jan[neiro] Beske' (ZMHB) <illustrated specimen>. — ***Other material***: BRAZIL, Rio de Janeiro: ♂, Estrada das paineiras, x.1943, H, Monteiro leg. (UFRJ); Amazonas: ♀, Itacoatiara, Dirings leg. (MCNZ-002851) <illustrated specimen>. No data: ♀, 'Ogmocoris hypomelas Burm.' | 'coll. E P V VanDuzee' | 'Cornell U[niversity], Lot. 96, Sub.; ♀, 'Rio. Nov.' | 'coll. P R Uhler' | 'Ogmocoris hypomelas (Burm.), H G Barber det. (USNMNH- 2068399) <illustrated specimen>.

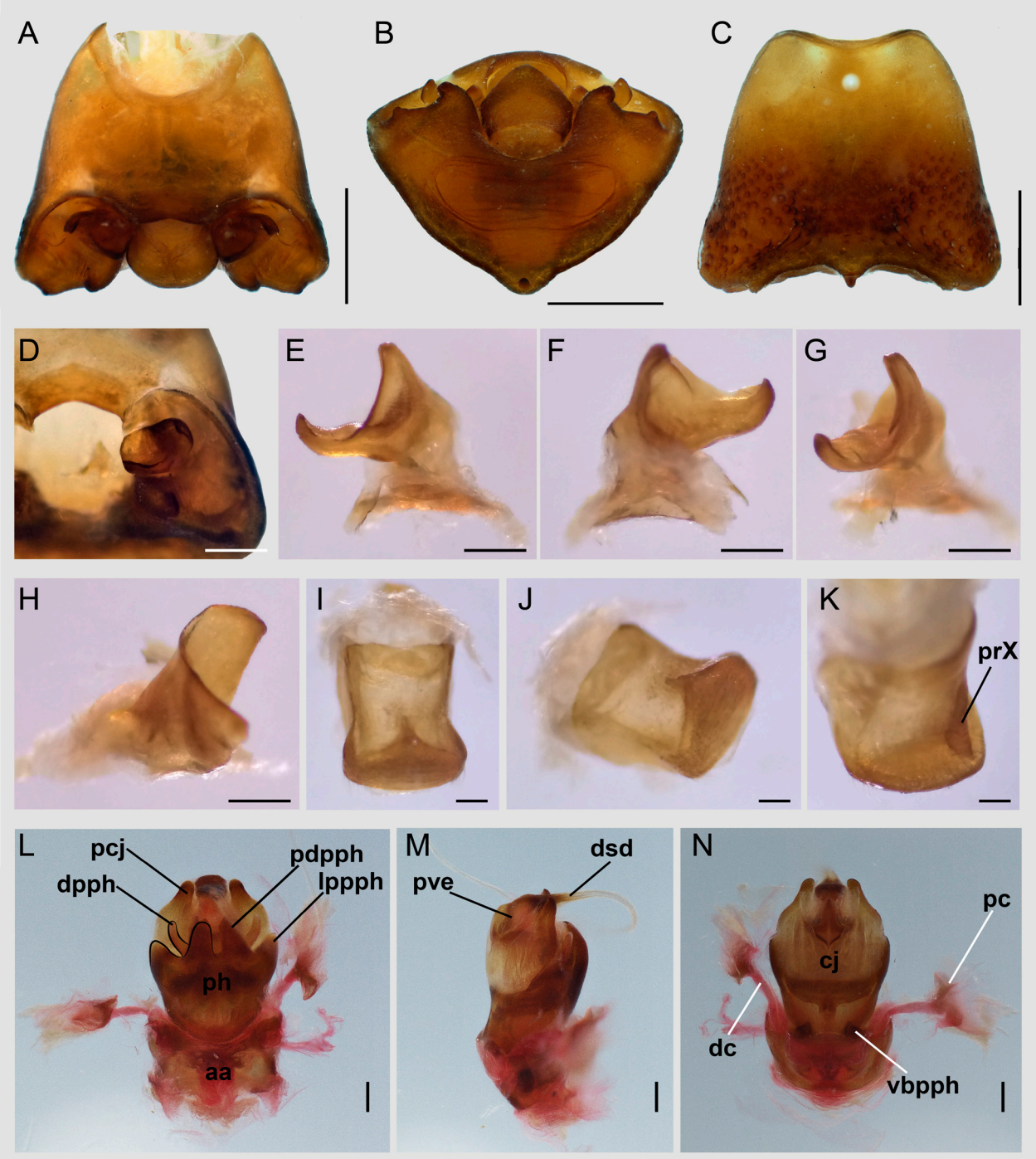

Fig. 10. *Ogmocoris hypomelas* (Burmeister, 1835): **A**–**C**: male terminalia: **A**: dorsal; **B**: posterior: **C**: ventral; **D**–**H**: paramere: **D**: left paramere, original position; **E**–**H**: right paramere, different views; **I**–**K**: segment X, different views; **L**–**N**: male genitalia; **L**: dorsal; **M**: lateral; **N**: ventral. Scale bars: A–C = 1.0 mm; D–H: 0.5 mm; I–N = 0.25 mm.

Distribution. Brazil: Amazonas and Rio de Janeiro (Fig. 17).

Comments. The female specimen deposited in the ZMHB examined by Frey-da-Silva et al. (2002) was mistakenly conceived as a holotype. From the original description by Burmeister, it is not possible to know the number of specimens examined by the author, so this specimen must be considered a syntype. Therefore, the designation of this specimen as a lectotype is made here.

We did not examine the type material of *Ansa distincta*, but we accept Stål's authority.

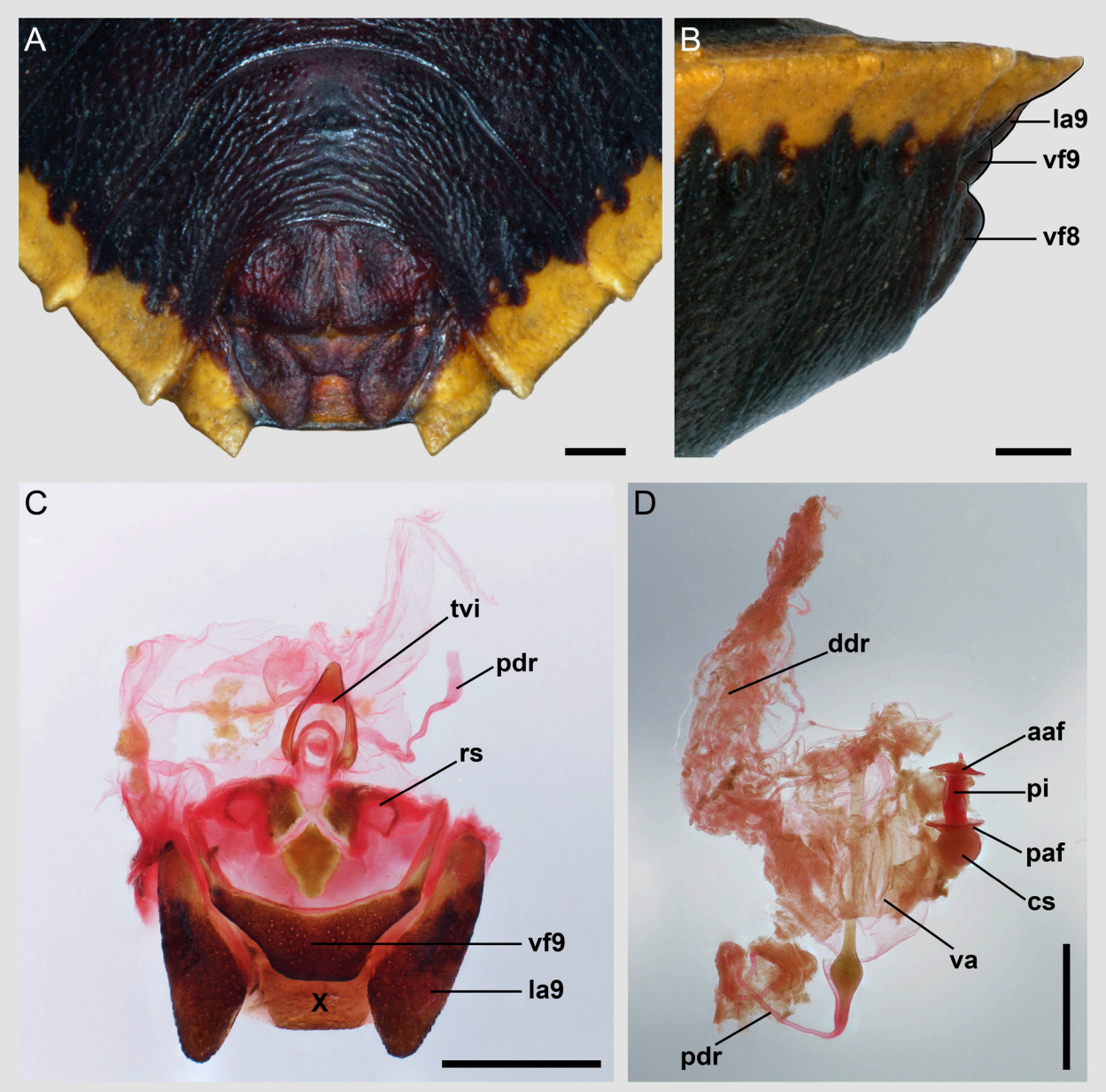

Fig. 11. *Ogmocoris hypomelas* (Burmeister, 1835): **A**–**B**: female terminalia: **A**: posteroventral view; **B**: lateral view; **C**–**D**: female receptaculum seminis and ausenwand. Scale bars = 0.5 mm.

3.2.7. *Ogmocoris paranaensis* Frey-da-Silva, Grazia & Fernandes, 2002

Figs. 12A–I, 17, 21B, D, G

Ogmocoris paranaensis Frey-da-Silva et al., 2002: 183–185.

Diagnosis. Bucculae sinuous. Outline of anterolateral margins of pronotum punctate. Foveae in basal angles of scutellum relatively small, each less than the diameter of a compound eye. The outer margin of each metapleural evaporatorium convex; gyrification of evaporatorium with low wrinkles. Sublateral margins of sternites concolourous with abdominal venter. Spiracles dark brown to black. Dorsal rim of pygophore without dorsal process; extension of dorsal rim over segment X obsolete. Superior layer of ventral rim with one pair of processes; lateral margin of each projection entire. Inferior layer of ventral rim with one pair of processes. Segment X ogival, with 1 + 1 tumescent processes basally.

Redescription. ***Measurements***: Table 4. ***Colouration***: General colour castaneous dorsally, with dense dark-brown to black punctures; ventral surface dark-brown to ferruginous, with dense concolourous punctures. Head reddish-castaneous, punctures on basal half brown, those on distal half concolourous. Antennomeres dark-brown. Labium yellowish-castaneous, apical labiomeres dark brown. Anterolateral margins of pronotum and lateral margins of coria castaneous; punctures dark brown. Pro-, meso-, and metasternum uniformly dark-brown to reddish-castaneous, densely punctate with dark-brown to black punctures. Legs reddish-castaneous. Connexivum

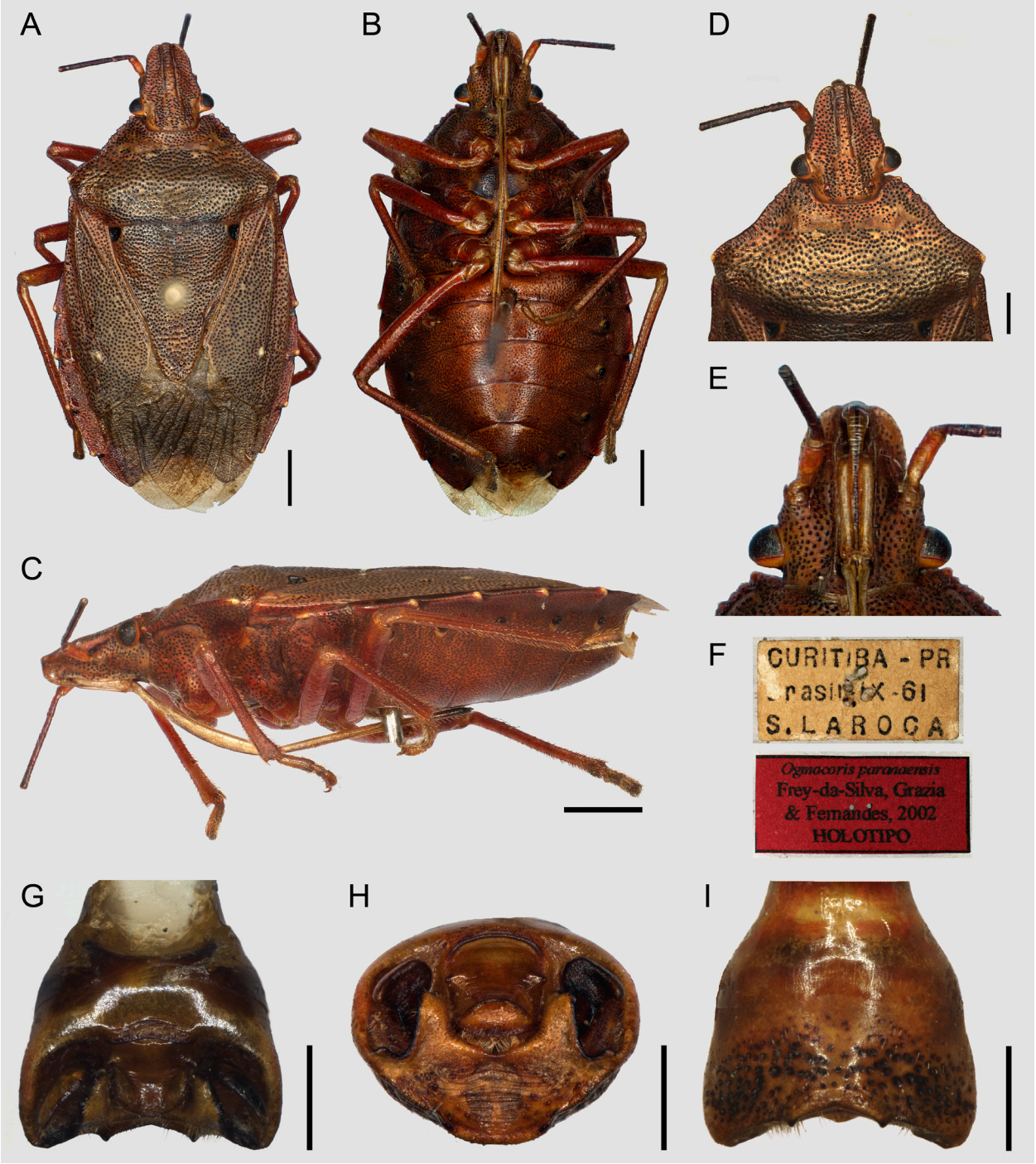

Fig. 12. *Ogmocoris paranaensis* Frey-da-Silva, Fernandes & Grazia, 2002 ♂, holotype: **A**: dorsal; **B**: ventral; **C**: lateral; **D**: head and pronotum; **E**: head, ventral view; **F**: labels; **G**–**I**: male terminalia: **G**: dorsal; **H**: posterior; **I**: ventral; Scale bars: A–C = 2.0 mm; D = 0.5 mm; G–H = 1.0 mm.

brown, anterolateral angles with black spot, posterolateral angles yellow. Sternites dark reddish-castaneous, with dark-brown punctures. Spiracles dark brown to black. Trichobothria reddish. ***Head*** (Fig. 12A, D): Anteocular processes absent. Proportions of antennomeres: 1 > 2 < 3 > 4 < 5. Bucculae sinuous (Fig. 12E). ***Thorax***: Pronotum with anterior angles produced; anterolateral margins concave, crenulate; humeral angles slightly developed (Figs. 12A, D, 21B). Gyrification of evaporatorium with low wrinkles; outer margin of each metapleural evaporatorium convex. Foveae in basal angles of scutellum relatively small, each less than the diameter of a compound eye (Fig. 21D). Apex of each radial vein conspicuously calloused (Fig. 21D, blue arrow) ***Abdomen***: Posterolateral angles of each connexivum produced (Fig. 21D, red arrow). Sublateral margins of abdominal sternites concolourous with abdominal venter, dark-brown to ferruginous (Figs. 12A, C, 21G, blue arrow). ***Male terminalia***: Dorsal rim of pygophore without dorsal process; extension of dorsal rim over segment X obsolete.

Superior layer of ventral rim with one pair of processes; lateral margin of each projection entire (Fig. 12H). Inferior layer of ventral rim with one pair of processes (Fig. 12I). Segment X ogival, with 1 + 1 tumescent processes basally (Fig. 12H). Crown of paramere well-developed, spatulate (Fig. 12H).

Female. Unknown.

Material examined. ***Type material***: Holotype ♂, 'BRAZIL, Paraná, Curitiba | [?].ix.1961 | S Laroca leg.' (DZUP) <illustrated specimen>.

Distribution. Brazil: Paraná (Fig. 17).

3.2.8. Description and diagnosis of *Liscocephala*

Liscocephala gen.n.

Type species. *Liscocephala fumosa* sp.n., here designated.

Diagnosis. Antennomere 2 much reduced, less than 1/4 of the length of antennomere 1, hardly visible and antennomere 3 conical, flattened dorsally, longer than antennomere 5. Posterior margin of pronotum rectilinear. Scutellum longer than wide, post-frenal width of scutellum more than the basal width of the scutellum. Foveae smaller than the diameter of a compound eye. Coria longer than scutellum, not surpassing apices of abdominal tergite 5. Metathoracic spiracle narrow. Valvifers 8 flat.

Description. Body oval, small (total length: 8.55 mm) (Fig. 13A–B). ***Head:*** Head longer than wide, apex rounded (Figs. 13A, 20C). Mandibular plates shorter than clypeus, apices obtuse; lateral margins sinuous. Clypeal apex obtuse, in a higher level than mandibular plates in lateral view; clypeal suture beginning after an imaginary line crossing anterior margin of compound eyes. Antenniferous tubercles visible in dorsal view, each with an obtuse process laterally. Antennomere 1 not reaching apex of head; antennomere 2 much reduced, less than 1/4 the length of the first antennomere, hardly visible; antennomere 3 conical, flattened dorsally; antennomere 4 conical, slightly flattened dorsally (Figs. 13D, 18Fiv, 20G). Bucculae sinuous, tapering toward the base of head. First labiomere robust, lying entirely between bucculae, labiomere 2 flattened laterally (Figs. 13D, 20E). ***Thorax***: Pronotum trapezoidal (Figs. 13A, 20I); anterolateral margins explanate, not reflexed, impunctate; posterior margin rectilinear. Mesosternal carina elevated, smooth (Fig. 13E); metasternal furrow shallow. Each ostiole of ESES guttiform, opening posterolaterally; each peritrema spout-shaped; medial furrow of the each ostiolar peritreme relatively long, extending more than half of the length of peritreme; evaporatorium punctate, occupying more than half of each meso- and metapleuron; evaporatorium on mesopleuron reaching its anterior and posterior angles, surpassing the limits of mesocoxal sutures (Fig. 18K). Metathoracic spiracle narrow (Fig. 18K, red arrow). Femora longer than tibiae; unarmed femora; tarsi 3-segmented (Fig. 13C). Scutellum longer than wide (Figs. 13A). Basal angles of scutellum foveate; fovea relatively smaller than the diameter of a compound eye (Fig. 20K, red arrow). Corium longer than scutellum, extending beyond apex of scutellum; apex of each radial vein punctate (inconspicuous callosity, Fig. 20K). ***Abdomen***: Connexivum exposed (Fig. 13A). Sublateral margins of abdominal sternites not concolourous with abdominal venter (lighter than abdominal venter, Fig. 13C). Medial longitudinal groove reaching abdominal sternite 6 (Fig. 13F, red arrow). ***Female terminalia*** (Figs. 13F, 16A, C): Valvifers 8 flat. Valvulae 8 not visible. Valvifers 9 leveled, relative to the position of X segment X in lateral view. Laterotergites 9 not surpassing tergite 8.

Etymology. *Lis-*, given in honour of Lis de Barros Borges, L. D. Barros's daughter; "*-cocephala*", relative to the *Mecocephala* group; feminine.

Distribution. Uruguay: Canelones (Fig. 17).

3.2.9. *Liscocephala fumosa* sp.n.

Figs. 13A–F, 16A, C, 17, 18Fiv, K, 20A, C, E, G, I, K

Diagnosis. Body oval. Head wider than longer. Antennomere 1 robust compared to the other antennomeres; antennomere 2 less than 1/4 of the first, hardly visible; antennomere 3 conical, flattened dorsally, longer than antennomere 5. Labiomere 1 robust. Anterior margin of pronotum strongly concave; posterior margin of pronotum rectilinear. Scutellum longer than wide. Foveae smaller than the diameter of a compound eye. Coria longer than scutellum, not surpassing apices of abdominal tergite 5. Valvifers 9 depressed. Laterotergites 9 not surpassing tergite 8.

Description. Body small (total length: 8.55 mm). ***Measurements***: Table 4. ***Colouration***: General coloration brownish gray dorsally, dark brown ventrally, densely punctate with large punctures. Head and clypeus with dark brown callosities. Ocelli red. Antennomeres uniformly brownish. Antenniferous tubercles and maxillary plates dark brown. A longitudinal line on pronotum, anterolateral margins of pronotum and lateral margins of coria pale yellow. Scutellum with impunctate brownish callosities, laterally foveate (Fig. 13A). Pro-, meso- and metasternum uniformly dark brown. Coxae, trochanters and basal ⅔ of femora pale yellow, apices of femora, tibiae and tarsi brown. Connexivum and tergite 8 pale yellow and brownish and anterolateral and posterolateral angles of connexivum. Sternites dark brown, sublateral band from prosternum to abdominal sternite 7 and laterotergites 8 pale yellow; anterolateral angles of sternites dark brown. Spiracles dark brown to black. Trichobothria

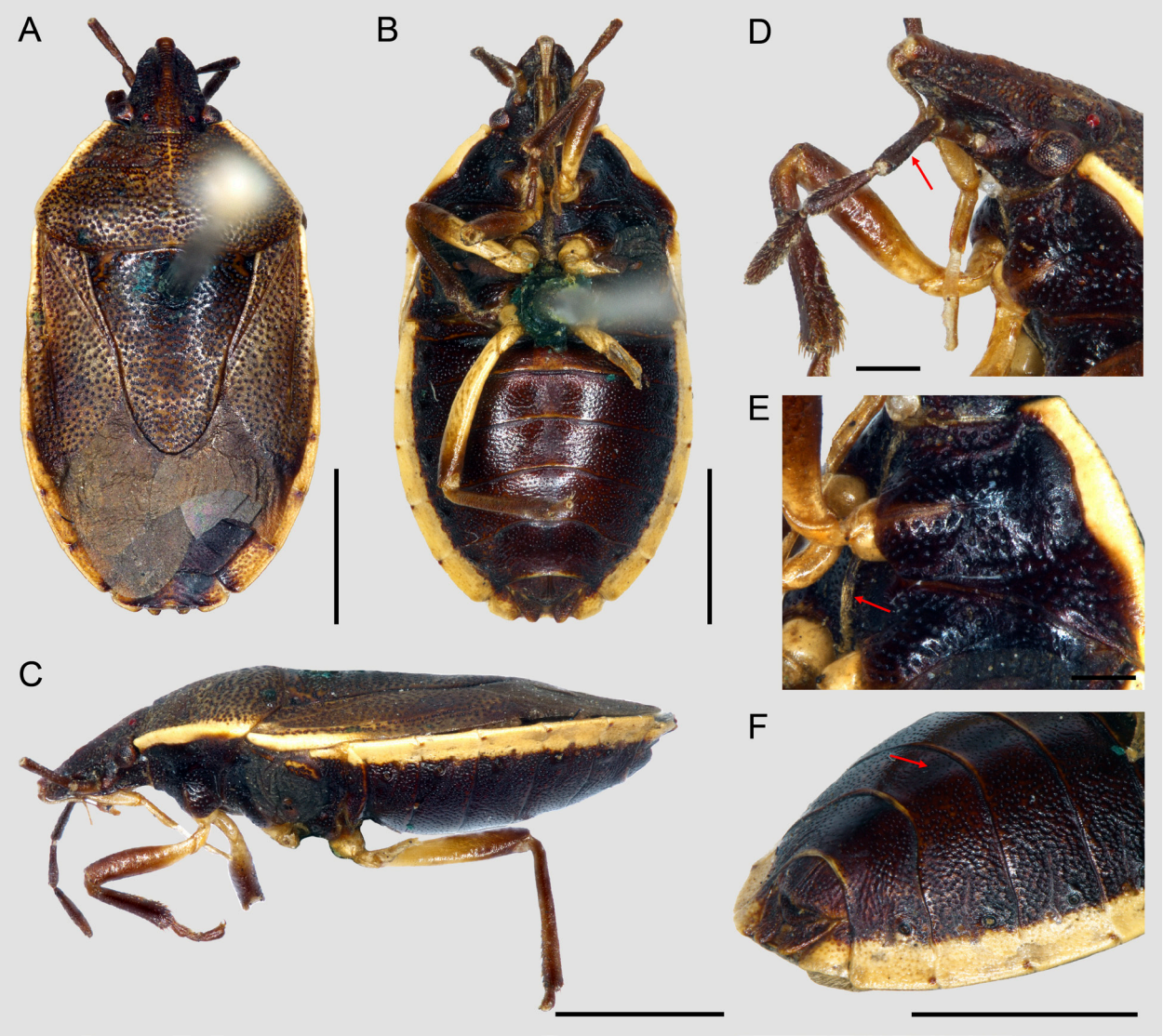

Fig. 13. *Liscocephala fumosa* sp.n. ♀: **A**: dorsal; **B**: ventral; **C**: lateral; **D**: head and pronotum, lateral view, antennomere 3 grooved (red arrow); **E**: pro- and mesosternum, ventral view, showing the carina mesosternal (red arrow); **F**: abdomen, lateral view, showing the abdominal groove (red arrow). Scale bars: A–C, F = 2.0 mm; D–E = 0.5 mm.

dark brown (Figs. 13C, F). ***Head*** (Figs. 13A, D, 20C, E, G): Anteocular processes absent. Proportions of antennomeres: 1 > 2 < 3 > 4 < 5 (Figs. 13D, 18Fiv, 20G). Bucculae reaching base of head. ***Thorax***: Pronotum with anterior angles not produced; anterolateral margins straight, smooth; humeral angles not produced (Figs. 13A, 20I) and posterior margin rectilinear. Periostiolar depressions of ESES present; each ostiolar peritreme occupying about 1/3 of evaporatorium; gyrification of evaporatorium with high wrinkles; outer margin of each metapleural evaporatorium concave; anterolateral margin of each evaporatorium rounded (Fig. 18K). Metathoracic spiracle narrow (Fig. 18K, red arrow). Foveae smaller than the diameter of a compound eye (Fig. 20K, red arrow). Corium not surpassing apices of abdominal tergite 5 (Figs. 13A, 20K, blue arrow). Membrane with linear veins, some bifurcate basally. Hemelytra not surpassing apex of abdomen. ***Abdomen*** (Figs. 13B–C, 20K): Posterolateral angles of each connexivum not produced. Sublateral margins of abdominal sternites pale yellow. ***Female terminalia*** (Figs. 13F, 16A, C): Valvifers 8 smaller than laterotergites 9, and partially covering valvifers 9, and posterior margins sinuous, mesial margins juxtaposed. Laterotergites 8 lacking spiracles; posterior margins straight. Valvifers 9 depressed, leveled, relative to the position of segment X; posterior margins rectilinear, lateral margins with 1 + 1 processes. Laterotergites 9 spatulate, obtusely rounded apically, not surpassing tergite 8.

Male. Unknown.

Etymology. The specific epithet refers to the brownish gray colour of the dorsal surface.

Type material: Holotype ♀, 'URUGUAY, Canelones, [Atlantida] | 28.ii.1932' | 'MNHN-1344'(URMU) <illustrated specimen>.

Distribution. Uruguay: Canelones (Fig. 17).

Comments. Labium lacking part of labiomere 2 and remaining labiomeres in single specimen. However, we believe that the labium is long, at least exceeding the middle of the abdominal sternite 4, due to the presence of a medial longitudinal groove reaching abdominal sternite 6 (Fig. 13D, F). This groove is observed only in species where the labium is considered long.

3.2.10. Description and diagnosis of *Triunfus*

***Triunfus* gen.n.**

Type species. *Triunfus carvalhoi* sp.n., here designated

Diagnosis. Antennomere 2 much reduced, not visible. Labium surpassing the middle of sternite 4; labiomere 1 robust, labiomeres 3 and 4 strongly flattened. Anterior margin of pronotum shallowly concave and posterior margin of pronotum emarginate medially. Post-frenal width of scutellum less than the basal width of the scutellum. Foveae smaller than the diameter of a compound eye. Ostioles circular. Valvifers 8 convex; mesial margins not juxtaposed, valvulae 8 visible.

Description. Body elongate, small (total length: 9.79 mm) (Figs. 14A–B, 15A–B). ***Head***: Head longer than wide, apex rounded (Figs. 14A, 15A, D, 20D, H). Mandibular plates shorter than clypeus, apices obtuse; lateral margins sinuous. Clypeal apex obtuse, in a higher level than mandibular plates in lateral view; clypeal suture beginning after an imaginary line crossing anterior margin of compound eyes. Antenniferous tubercles visible in dorsal view, each with an obtuse process laterally. Antennomere 1 not reaching apex of head; antennomere 2 much reduced, not visible; antennomere 3 cylindrical; antennomere 4 conical, slightly flattened dorsally (Figs. 14D, 15E, 18Fv, 20H). Bucculae rectilinear, tapering toward base of head, not reaching its base (Fig. 14E). Labium long, surpassing middle of sternite 4 (Figs. 14 B–C, 15C); labiomere 1 robust, lying entirely between bucculae (Figs. 14E, 15C), labiomere 2 flattened laterally, shorter than labiomeres 3 and 4 combined, and labiomeres 3 and 4 strongly flattened (Figs. 14C, 15C). ***Thorax***: Pronotum trapezoidal (Figs. 14A, 15A, D, 20J); anterolateral margins explanate, reflexed, impunctate; posterior margin emarginate medially (Fig. 15D). Mesosternal carina elevated, smooth; metasternal furrow shallow. Each ostiole of ESES circular, opening posterolaterally; periostiolar depressions present; each peritreme spout-shaped, extending about ⅔ of the distance to lateral margin of evaporatorium; medial furrow of the each ostiolar peritreme relatively long, occupying more than half of the length of peritreme; evaporatorium punctate, occupying more than half of meso- and metapleuron; evaporatorium on mesopleuron reaching its anterior and posterior angles and the outer margins, surpassing the limits of mesocoxal sutures (Figs. 15F, 18L). Metathoracic spiracle wide. Length of femora and tibiae subequal; femora unarmed; tarsi 3-segmented (Figs. 14C, 15C). Scutellum broader than long (Figs. 14A, 15A). Basal angles of scutellum foveate; foveae smaller than the diameter of a compound eye (Fig. 20L, red arrow). Corium longer than scutellum, extending beyond apex of scutellum, surpassing apices of abdominal tergite 5 (Fig. 20L, blue arrow); apex of each radial vein punctate (inconspicuous callosity, Fig. 20L). ***Abdomen***: Connexivum exposed (Figs. 14A, 20L). Sublateral margins of abdominal sternites not concolourous with the abdominal venter (lighter than abdominal venter, Fig. 14C). Medial longitudinal groove reaching sternite 6. Spiracles concolourous with abdomen. Trichobothria concolourous with abdominal venter (Fig. 14F). ***Female terminalia*** (Figs. 14F, 16B, D): Valvifers 8 convex; mesial margins not juxtaposed. Valvulae 8 visible. Laterotergites 8 lacking spiracles. Valvifers 9 leveled, relative to the position of segment X in lateral view. Laterotergites 9 surpassing tergite 8. ***Female genitalia***: Valvulae 9 with 1 + 1 lateral sclerotized areas placed along with ring sclerite. Ring sclerite elliptical. Ectodermal ductus (Fig. 16E–G): thickening of vaginal intima with anterior portion rounded, posterior portion conical. Proximal ductus receptaculi convoluted, extremely long in relation to length of vesicular area, at least three times longer. Median wall of vesicular area enlarged subproximally. Distal ductus receptaculi long, at least one and a half times longer than vesicular area, with diameter equal to median wall diameter. Posterior annular flange wider than *capsula seminalis*.

Etymology. *Triunfus*, corresponding to the type-locality Triunfo, Rio Grande do Sul, Brazil; masculine.

Distribution. Brazil: Rio Grande do Sul (Fig. 17).

3.2.11. Key to species of *Triunfus*

1 Valvifers 8 shorter in length than laterotergites 9; valvifers 9 swollen, posterior margins convex (Fig. 16E). Proximal ductus receptaculi equal in diameter to median wall of vesicular area; *capsula seminalis* subequal in length to *pars intermedialis* (Fig. 16F) .. .. ***Triunfus carvalhoi* sp.n.**

1' Valvifers 8 equal in length to laterotergites 9; valvifers 9 flat, posterior margins straight (Fig. 16G). Proximal ductus receptaculi greater in diameter than median wall of vesicular area; *capsula seminalis* shorter in length to *pars intermedialis* (Fig. 16G) .... ***Triunfus incarnatus* sp.n.**

3.2.12. *Triunfus carvalhoi* sp.n.

Figs. 14A–F, 16B, D–F, 17, 18Fv, L, 20B, D, H, J, L

Diagnosis. Valvifers 8 shorter than laterotergites 9. Valvifers 9 swollen, posterior margins convex. Lateral sclerotized areas of valvulae 9 well-defined, sclerotized. Diameter of proximal ductus receptaculi equal to diameter of

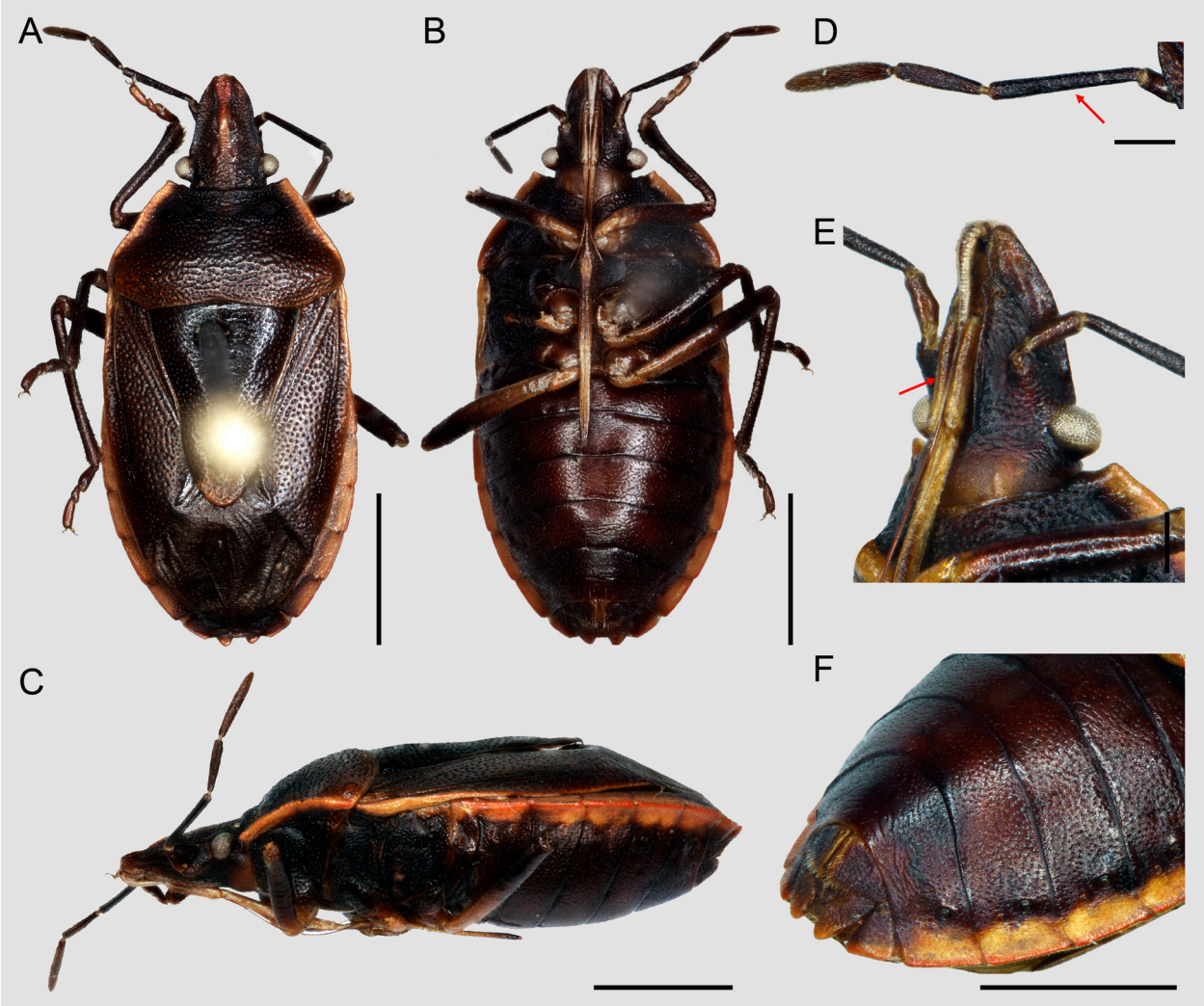

Fig. 14. *Triunfus carvalhoi* sp.n. ♀: **A**: dorsal; **B**: ventral; **C**: lateral; **D**: antenna, dorsal view, antennomere 3 convex (red arrow); **E**: head, ventral view, showing of labiomere 1 (red arrow); **F**: abdomen. Scale bars: A–C, F = 2.0 mm; D–E = 0.5 mm.

median wall of vesicular area. *Capsula seminalis* equal in length to *pars intermedialis*, with a process.

Description. ***Measurements***: Table 4. ***Colouration***: General colour dark brown dorsally and ventrally; densely punctate. Head and clypeus with ferruginous callosities; antennomeres uniformly brownish; brown blotches on antenniferous tubercles and maxillary plates. Sublateral margins of pronotum and lateral margins of coria ferruginous. Pro-, meso-, metasternum and evaporatorium dark brown. Coxae, trochanters, and apical half of each femur ferruginous, tibiae and tarsi brown. Connexivum ferruginous. Abdominal sternites brown, sublateral band from prosternum to abdominal sternite 7 ferruginous. Spiracles dark brown. Trichobothria brown. ***Head*** (Figs. 14A, D–E, 20D, F, H): Anteocular processes absent. Proportions of antennomeres: 1 > 2 < 3 > 4 < 5 (Figs. 14D, 18Fv, 20H). ***Thorax***: Pronotum with anterior angles not produced; anterolateral margins straight, smooth; humeral angles not produced (Figs. 14A, 20J). Gyrification of evaporatorium with high wrinkles; anterolateral margin of each evaporatorium rounded; outer margin of each metapleural evaporatorium concave (Fig. 18L). Membrane with veins linear, some bifurcated basally. Hemelytra not surpassing apex of abdomen. ***Abdomen***: Posterolateral angles of each connexivum not produced (Figs. 14A, 20L). ***Female terminalia*** (Figs. 14F, 16B, D): Valvifers 8 shorter than laterotergites 9, partially covering valvifers 9. Laterotergites 8 triangular, straight apically. Valvifers 9 swollen, leveled, relative to the position of segment X; posterior margins convex, lateral margins with 1 + 1 processes. Laterotergites 9 triangular, obtusely rounded apically (Fig. 16B). ***Female genitalia***: Ectodermal ductus (Fig. 16E–F): Diameter of proximal ductus receptaculi equal to diameter of median wall of vesicular area. Annular flanges divergent. *Pars intermedialis* rectilinear. *Capsula seminalis* globose, equal in length to *pars intermedialis*, with a process.

Male. Unknown.

Etymology. This species is named in honour to Dr. Gervásio Silva Carvalho, specialist dedicated to phylogeny and biogeography of Neotropical Auchenorrhyncha.

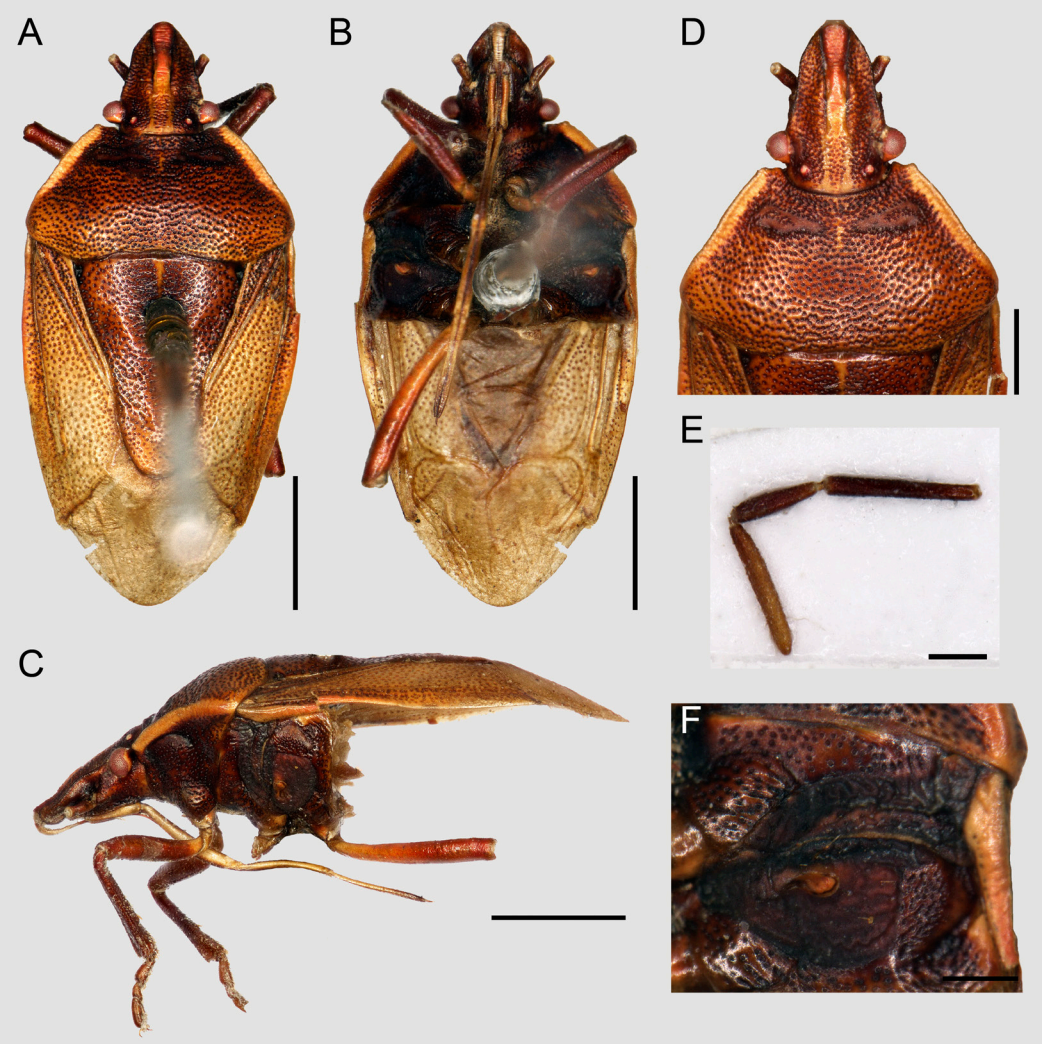

Fig. 15. *Triunfus incarnatus* sp.n. ♀: **A**: dorsal; **B**: ventral; **C**: lateral; **D**: head and pronotum; **E**: antenna; **F**: external scent efferent system. Scale bars: A–C = 2.0 mm; D = 1.0 mm; E–F = 0.5 mm.

Type material: Holotype ♀, 'BRAZIL, Rio Grande do Sul, Triunfo | Projeto Sitel/Corsan | 7–11.i.2002 | Equipe do Projeto leg.' | '17302-1 MCTP' (MCTP). – Paratype: ♀, 'BRAZIL, Rio Grande do Sul, Capão do Leão' (UFRG) <illustrated specimen>.

Distribution. Brazil: Rio Grande do Sul (Fig. 17).

3.2.13. *Triunfus incarnatus* sp.n.

Figs. 15A–F, 16G, 17

Diagnosis. Valvifers 8 equal in length to laterotergites 9. Valvifers 9 flat with posterior margins straight. Lateral sclerotized areas of valvulae 9 scarcely defined or sclerotized. Diameter of proximal ductus receptaculi greater than diameter of median wall of vesicular area. *Capsula seminalis* without processes, shorter than *pars intermedialis*.

Description. ***Measurements***: Table 4. ***Colouration.*** General colour orange-castaneous dorsally, dark brown ventrally; densely punctate. Head and clypeus with oranges callosities; ocelli orange; antennomeres brownish, except antennomere 5 orange-castaneous; yellow blotches on antenniferous tubercles and maxillary plates; labium orange-brown. Outline of anterolateral margins of pronotum and a medial longitudinal line on scutellum orange-castaneous. Pro-, meso-, metasternum and evaporatorium dark brown; ostiolar peritremes orange. Legs dark brown, except coxae, trochanters, and apical third of each femora orange. Connexivum yellowish-orange. Abdominal sternites dark castaneous, sublateral band from prosternum to abdominal sternite 7 yellowish-orange. Spiracles dark castaneous. Trichobothria castaneous. ***Head*** (Fig. 15A, D): Anteocular processes absent. Proportions of antennomeres: 1 > 2 < 3 > 4 < 5 (Fig. 15E). ***Thorax***: Pronotum with anterior angles not produced; anterolateral margins straight, smooth; humeral angles not produced (Fig. 15A, D). Gyrification of evaporatorium with high wrinkles; anterolateral margin of each evaporatorium rounded; outer margin of each metapleural evaporatorium concave (Fig. 15F). Membrane with veins linear, some bifurcate basally. Hemelytra not surpassing apex of abdomen. ***Female terminalia***: Valvifers 8 subequal in length to laterotergites 9,

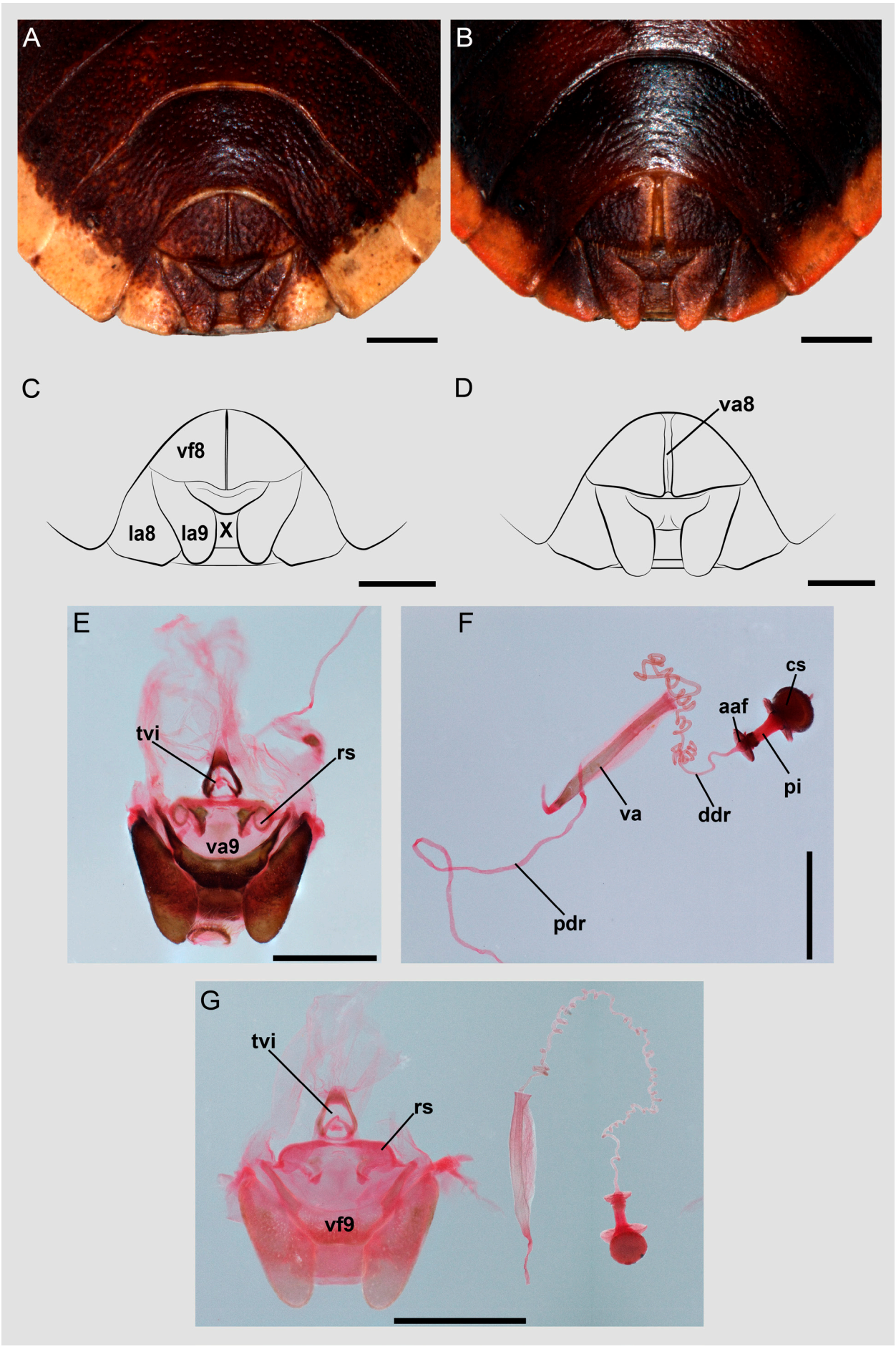
A
B
C
vf8
la8
la9
X
D
va8
E
tvi
rs
va9
F
cs
aaf
pi
va
ddr
pdr
G
tvi
rs
vf9

Fig. 17. Map of geographical distribution. — ***Colors***: yellow – *Chimerocoris luridus* sp.n.; purple – *Hypanthracos meridionalis*; red – *Liscocephala fumosa* sp.n.; green – *Ogmocoris* Mayr, 1864; blue – *Triunfus* gen. n.

partially covering valvifers 9. Laterotergites 8 triangular, posterior margins straight. Valvifers 9 flat, leveled, relative to the position of segment X; posterior margins straight, lateral margins entire. Laterotergites 9 triangular, posterior margins obtusely rounded. ***Female genitalia***: Valvulae 9 with 1 + 1 lateral areas scarcely defined or sclerotized, placed along with ring sclerite. Ectodermal ductus (Fig. 16G): diameter of the proximal ductus receptaculi greater than diameter of median wall of vesicular area. Annular flanges divergent. *Pars intermedialis* rectilinear. *Capsula seminalis* globose, without processes, shorter than *pars intermedialis*.

Male. Unknown.

Etymology. *Incarnatus*, in Latin, orange, referring to the orange body colour; adjective.

Type material: Holotype ♀, 'BRAZIL, Rio Grande do Sul, [probably São Lourenço do Sul] | [?].iv.1995 Loescher L. leg.' (MECB) <Illustrated specimen, abdomen and terminalia prepared>.

Distribution. Brazil: Rio Grande do Sul (Fig. 17).

3.3. Remarks

Hypanthracos shares with *Mecocephala* the basal limits of clypeal sutures arising anterior to an imaginary line connecting the anterior margins of the compound eyes (Fig. 18A–B). In this study, in addition to the synapomorphies for the *Mecocephala* group, *H. meridionalis* shares the antennomere 2 shorter than 1 (Fig. 18F), the ostiolar peritreme extending to 2/3 of the outer margin of the metapleural evaporatorium (from the origin of the

← **Fig. 16.** *Liscocephala* gen.n. and *Triunfus* gen.n. ♀: *L. fumosa*: **A**, **C**: female terminalia. *T. carvalhoi*: **B**, **D**: female terminalia; **E**, **F**: female receptaculum seminis and ausenwand. *T. incarnatus*: **G**: female receptaculum seminis and ausenwand. Scale bars = 0.5 mm.

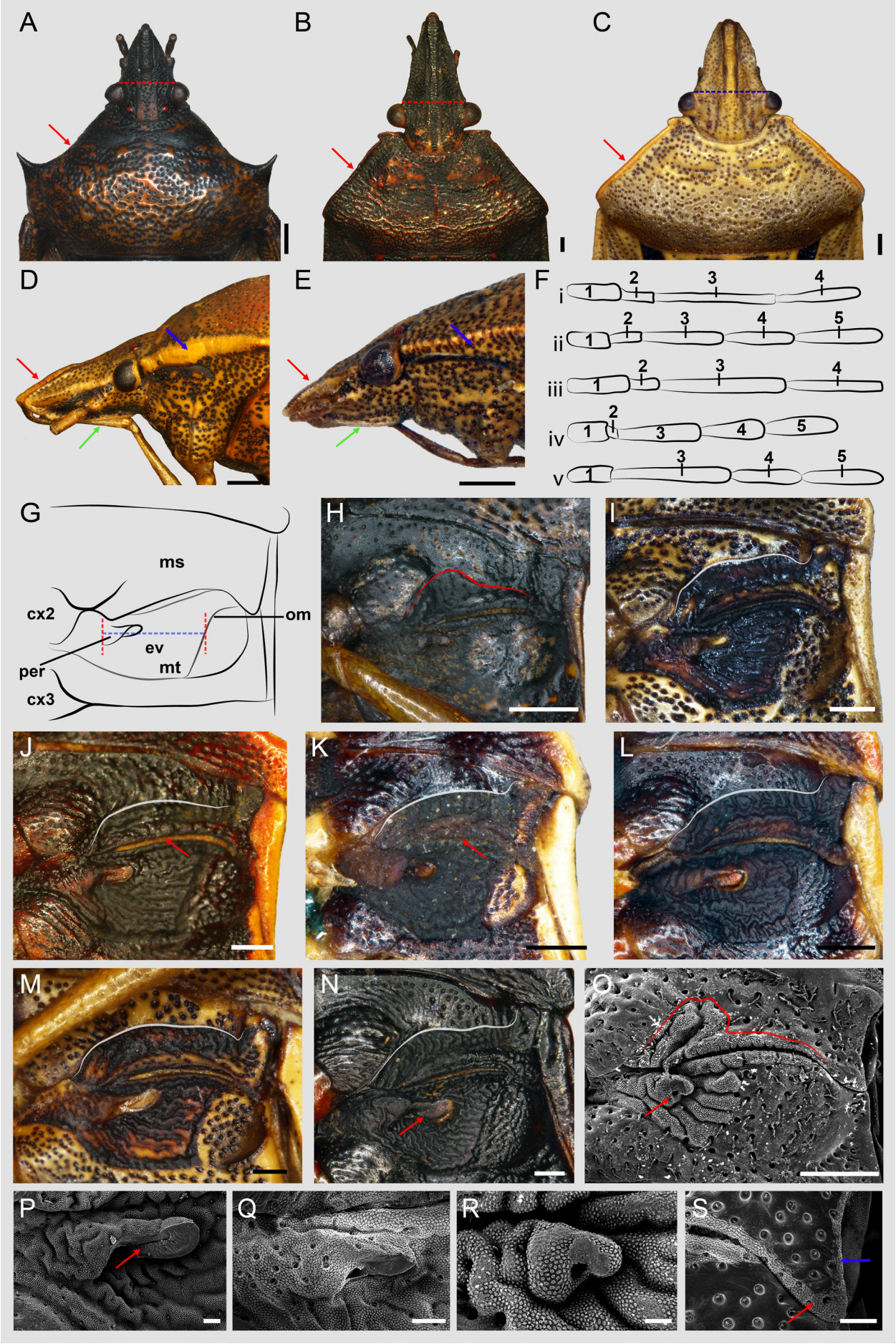
A
B
C
D
E
F
i
ii
iii
iv
v
1
2
3
4
5
G
ms
cx2
om
ev
mt
per
cx3
H
I
J
K
L
M
N
O
P
Q
R
S

peritreme to the outer margin of the evaporatorium; Fig. 18G–O) with *Triunfus*; the outer margin of the metapleural evaporatorium straight with *Pedinonotus catarinensis*, *Chimerocoris*, and *O. hypomelas*; the absence of the evaporatorium in the posterolateral angles of the mesopleuron with *P. foveata*; the pygophore trapezoidal with *Glyphepomis setigera*, *Paramecocephala fusca* and *Mecocephala magna*; the genital cup occupying less than half the length of the pygophore with *Hypatropis sternalis*; the absence of parameres with *Hypatropis* (Fig. 2A); the phallotheca medially longer than wide with *P. foveata* and *M. magna*; the conjunctiva with two pairs of processes, in dorsal view, with *P. catarinensis*, *Hypatropis*, *P. fusca*, *Paramecocephala australis* and *M. magna*; the valvifers 8 convex with *P. catarinensis*, *O. hypomelas* and *Paramecocephala*, and the distal ductus receptaculi long in relation to the length of the vesicular area with *Hypatropis inermis*, *Triunfus* and *Mecocephala acuminata*.

According to our study, *Chimerocoris* appears to be related to *Paramecocephala* and *Tibraca*. This relationship is observed by morphological similarity between *C. luridus* and *P. fusca*, and with *Tibraca exigua* (Fig. 19A–R). *Chimerocoris* resembles *Tibraca* and *Paramecocephala* by having the head longer than wide, the lateral margins of the mandibular plates sinuous, the reduced parameres, and the segment X of males with processes basally. *Chimerocoris* shares with *Tibraca* the sublateral margins of the abdominal sternites not concolourous with the abdominal venter (lighter than the abdominal venter, Fig. 19F–H), and the following characters of the male terminalia: posterolateral angles of the pygophore rounded, and the shape of the dorsal rim (Fig. 19J, P); inferior layer of ventral rim carinated, with 1 + 1 processes (Figs. 2C, 19K, Q); segment X with 1 + 1 thorn-like processes basally (Figs. 2C, 19J, P), and paramere trapezoidal. With *Paramecocephala*, it shares the anterolateral margins of the pronotum rectilinear (Fig. 19A–B, D), the length of labium which surpasses the middle of abdominal sternite 4, and the abdomen grooved along midline (Fig. 19H–I).

Liscocephala and *Triunfus* share a similar facies, a similar body length (Fig. 20A–L), antennomere 1 robust compared to the others antennomeres and antennomere 2 strongly reduced (Fig. 20G–H), the labiomere 1 short and robust (Figs. 14E, 20E–F), the anterior angles of the pronotum lacking processes (Fig. 20C–D), the posterolateral angles of sternites not produced (Fig. 20K–L), and the posterior margins of laterotergites 8 straight. *Liscocephala* can be distinguished from *Triunfus* by the antennomere 2 reduced but scarcely visible, antennomere 3 conical and flattened dorsally (Fig. 20G–H), the anterior margin of pronotum strongly concave (Fig. 20C–D, red dashed line), the posterior margin of the pronotum rectilinear (Fig. 20I–J, red dashed rectangle), the coria not surpassing the apices of abdominal tergite 5 (Fig. 20K–L, red arrow), ostiole guttiform, the metathoracic spiracle narrow, the valvifers 8 flat with mesial margins juxtaposed, and the valvulae 8 not visible in ventral view (Fig. 16A–B). *Triunfus* and *Liscocephala* species were described based on female specimens, while no male is known so far.

Triunfus resembles *Ogmocoris* by the head shape (distal portion of head rounded, as wide as interocular distance), and the morphology of the female terminalia (valvifers 8 separated from each other, and valvifers 9 tumescent). With *Mecocephala* the elongated head profile in lateral view and the strong flattening of labiomeres 3 and 4.

The terminalia of both sexes of *Ogmocoris* are peculiar, despite having the general pattern of the *Mecocephala* group. It is the only genus of the group with the crown of parameres well-developed (Fig. 10D–H). In addition, the inferior layer of the ventral rim of the pygophore has one or a pair of processes (Figs. 10C, 12I). In *O. hypomelas*, the male has the segment X rectangular, projected apically, with a tumescent process medially (Fig. 10I–K), the ductus seminis distalis is extremely long (Fig. 21H), the phallotheca has a pair of dorsal processes (Fig. 21J, red arrow), and three pairs of projections (Fig. 10L). The posterodorsal projections of phallotheca are well-developed and robust (Figs. 10L–M, 21J, green arrow). The conjunctiva has one pair of processes which is a character shared only with *P. foveata* (Fig. 21J–K, blue arrow). The female has the valvifers 9 obliquely placed in relation to segment X in lateral view, valvulae 9 have well-defined secondary thickenings, 1 + 1 along ring sclerite, and another medially, and the proximal and distal ductus receptaculi are extremely long and convoluted.

4. Discussion

The *Mecocephala* group was hypothesized as being a monophyletic grouping for the first time by Fernandes (1993), who empirically brought together four genera of similar habitus (*Mecocephala*, *Tibraca*, *Glyphepomis* and *Hypatropis*). Since the work of Fernandes (1993), this group has been subsequently studied by other authors which has resulted in the description and/or review of

← **Fig. 18.** Representation and comparison of head and thoracic characters. **A–C**: head, dorsal view; **D–E**: head and prothorax, lateral view (antennomeres not showing due to edition of photo); **F**: schematic drawing showing the antennomeres; **G–S**: external scent efferent system; **G–N**: meso- and metapleura, ventral view; **G**: schematic drawing showing the parts of eses; **O–S**: SEM images of characters of eses of mestasternal glands. — (A, Fi, H): *Hypanthracos meridionalis*; (B, N): *Mecocephala magna*; (C): *Paramecocephala foveata*; (D, M): *Tibraca limbativentris*; (E, S): *Hypatropis inermis*; (Fii, I): *Chimerocoris luridus*; (Fiii, J): *Ogmocoris hypomelas*; (Fiv, K): *Liscocephala fumosa*; (Fv, L): *Triunfus carvalhoi*; (O): *Glyphepomis adroguensis*; (P): *Paramecocephala fusca*; (Q): *Pedinonotus catarinensis*; (R): *Glyphepomis setigera*; Scale bars: A–E, H–N = 0.5 mm; O–S = 100 µm.

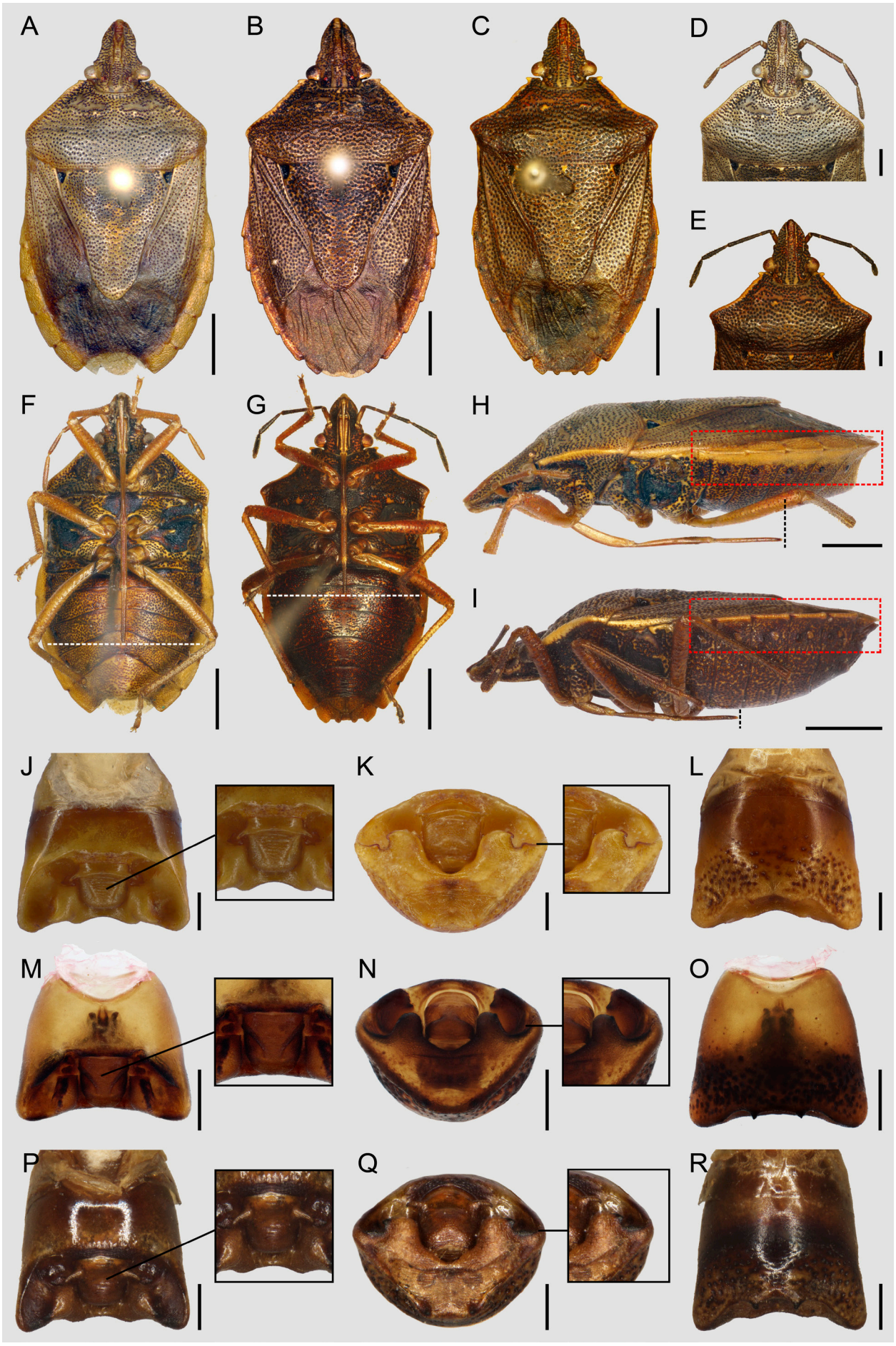
A
B
C
D
E
F
G
H
I
J
K
L
M
N
O
P
Q
R

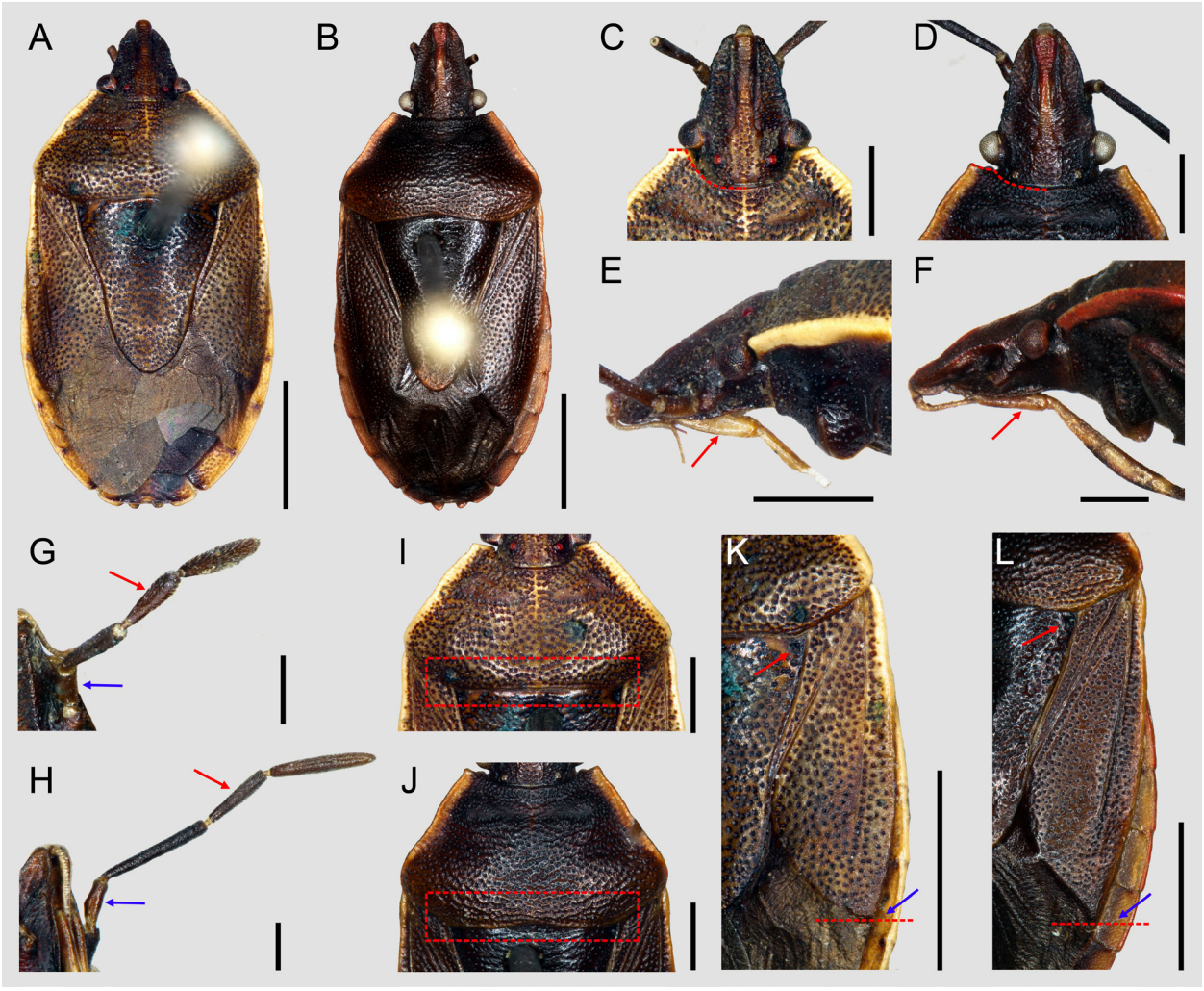

Fig. 20. Comparative figure of *Liscocephala* and *Triunfus*. **A–B**: habitus dorsal (antennomeres and legs not showing due to edition of photo); **C–D**: head and pronotum, dorsal view; **E–F**: head and prothorax, lateral view; **G–H**: right antenna; **I–J**: pronotum, dorsal view; **K–L**: hemelytra. — (A, C, E, G, I, K): *Liscocephala fumosa*; (B, D, F, H, J, L): *Triunfus carvalhoi*. Scale bars: A–C, K–L = 2.0 mm; C–F, I–J = 1.0 mm; G–H = 0.5 mm.

eight more genera (*Paratibraca*, *Parahypatropis*, *Amauromelpia*, *Luridocimex*, *Stysiana*, *Pedinonotus*, *Paramecocephala* and *Ogmocoris*), all of which have been historically grouped mainly by the characters of the head and by the morphology of the genitalia.

In a preliminary phylogenetic analysis by Frey-da-Silva (2005, unpublished data), the group was again found to be monophyletic, mainly by the shape of the lateral margins of the mandibular plates anteriorly to the compound eyes; the proportions of antennomeres 2 in relation to antennomere 1; the presence of a sub callous area on the mesial side of the trichobothria; the shape of mesial margins of valvifers 8; the ventral rim of the pygophore forming layers; the superior layer of the ventral rim of the pygophore forming 1 + 1 conical projections lateral to segment X; the number of projections on phallotheca; the shape of vesica; the number of processes of conjunctiva; the aspect and length of ductus seminis distalis.

More recently, Barão et al. (2017), in his study of the diversity of the external thoracic scent efferent system of the Carpocorini, discovered that all members of the *Mecocephala* group have a similar morphology of the external scent efferent system. That is, they have a well-developed evaporatorium on the meso- and metapleuron, a spout-shaped ostiolar peritreme (except *Glyphepomis*), and the presence of punctures on the evaporatorium.

In the present analysis, all diagnostic characters for the *Mecocephala* group proposed by Schwertner et al. (2002) were included, i.e., in the male genitalia, the

Fig. 19. Comparative figure of *Chimerocoris*, *Paramecocephala* and *Tibraca*. **A–C**: habitus dorsal (antennomeres and legs not showing due to edition of photo); **D–E**: head and pronotum; **F–G**: habitus ventral; **H–I**: habitus lateral; **J–R**: male terminalia: **J**, **M**, **P**: dorsal view; **K**, **N**, **Q**: posterior view; **L**, **O**, **R**: ventral view. — (A, D, F, H, J–L): *Chimerocoris luridus*; (B, I, M–O): *Paramecocephala fusca*; (C, E, G, P–R): *Tibraca exigua*. Scale bars: A–C, F–I = 2.0 mm; D–E = 0.5 mm; J–R = 1.0 mm.

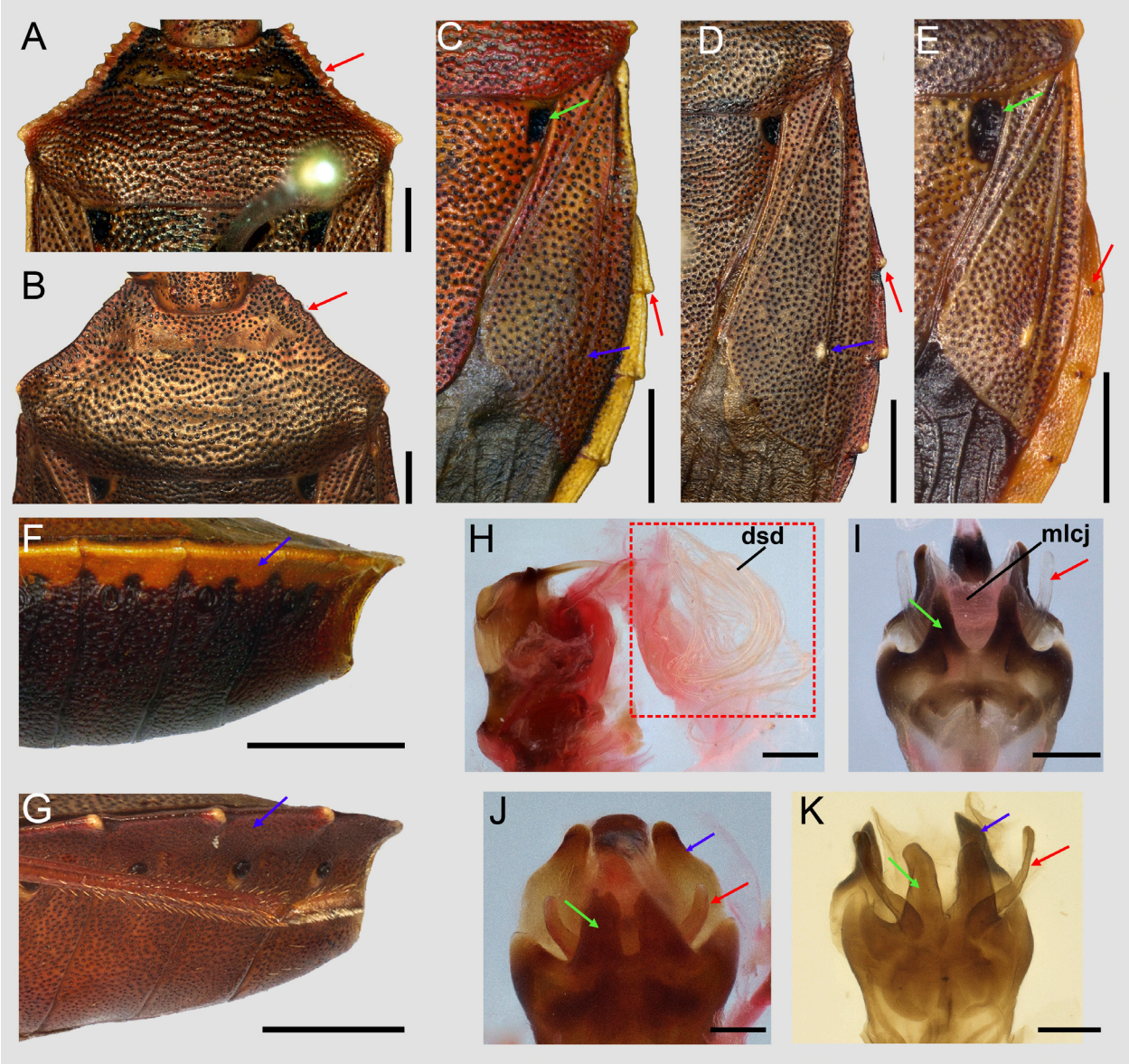

Fig. 21. Comparative figure of *Ogmocoris* species, and some male genitalia characters. **A–B**: pronotum, dorsal view; **C–E**: hemelytra; **F–G**: abdomen, lateral view; **H–K**: male genitalia. — (A, C, F, H–J): *Ogmocoris hypomelas*; (B, D, G): *Ogmocoris paranaensis*; (E, K): *Paramecocephala foveata*; (I), *Tibraca limbativentris*. Scale bars: A–B = 1.0 mm; C–G = 2.0 mm; H–K = 0.5 mm.

pattern of the pygophore structure, and in the female genitalia, the ductus receptaculi developed and strongly convolute, are here corroborated. Some exceptions include the reduced or missing parameres, the phallotheca with processes, and the conjunctiva with two pairs of processes. In *Ogmocoris,* the parameres are well-developed; this condition may be an evolutionary novelty in the *Mecocephala* group, with a reversal in this genus. In addition, the conjunctiva with a pair of processes is shared only with *P. foveata*. There are, however, no exclusive characteristics for any of the included genera. Each genus is distinguished by an exclusive combination of characters; that is, some characters are shared among the genera.

The monophyly of the *Mecocephala* group was recovered in all analyses under equal weights and implied weights. According to our results, we suggest that *H. meridionalis* should be included in the *Mecocephala* group. Grazia & Campos (1996) highlighted four putative diagnostic characteristics of *Hypanthracos*: the form and proportions of the antennomeres, the shape of the dorsal rim of the pygophore, the absence of parameres, and the form and size of the conjunctival processes. Rider et al. (2018) suggested the inclusion of *Hypanthracos* in the *Mecocephala* group mainly because they shared characters of the head and genitalia.

From our results, based on continuous characters, it is possible to tentatively recognize groupings by the shape and size of some structures, i.e. A. the total length of the labium: 1) short to medium labium in length – not surpassing the middle of abdominal sternite 3 – (*Glyphepomis*, *Hypatropis*, *Hypanthracos*, *Paratibraca*, *Pedinonotus* and *Tibraca*) or, 2) long to extremely long labium – surpassing the middle of abdominal sternite 4 to surpassing

the apex of the body – (*Chimerocoris*, *Liscocephala*, *Mecocephala*, *Ogmocoris*, *Paramecocephala* and *Triunfus*). B. Head length vs. head width: 1) wider than long (*Glyphepomis* and *Hypatropis*) or, 2) longer than wide (*Chimerocoris*, *Hypanthracos*, *Liscocephala*, *Mecocephala*, *Ogmocoris*, *Paramecocephala*, *Paratibraca*, *Pedinonotus*, *Tibraca* and *Triunfus*).

Chimerocoris, *Liscocephala*, and *Triunfus* have the head longer than wide, the labium long, reaching at least to the middle of abdominal sternite 4, and a shallow groove along abdominal midline. These characters are shared with *Mecocephala*, *Paramecocephala*, and *Ogmocoris*. The relation between the length of the head and the labial length is not yet known for the *Mecocephala* group; however, it is possible to recognize species that have a longer head and a longer labium, which surpasses the middle of abdominal sternite 6.

Another character treated in the literature as diagnostic for the *Mecocephala* group is the reduction of antennomere 2, compared with antennomere 1. This relationship between the two measurements was also observed in our results (characters 5 and 6). The only exception is the genus *Glyphepomis* in which antennomere 2 is longer than antennomere 1. Fernandes (1993) and Frey-da-Silva et al. (2005) proposed two states for this character: antennomere 2 subequal in length to antennomere 1, or that antennomere 2 is shorter than antennomere 1. Here, we record for the first time the very strong reduction of antennomere 2, occurring in *Liscocephala* (about of 1/4 of the length of antennomere 1) and *Triunfus* (total reduction).

5. Conclusion

The *Mecocephala* group was found to be monophyletic in all analyses, and *H. meridionalis* is a member of this group. The measurement ratios treated in the literature as diagnostic characters for the genera of the group were presented as a phylogenetic component. All new taxa proposed were recovered as independent lineages and therefore their descriptions were validated from a phylogenetic perspective. Now the *Mecocephala* group consists of seventeen genera.

6. Acknowledgements

The authors are grateful to the curators of the collections for the loan of specimens, and for the access to type specimens, and to Jürgen Deckert who provided images to *Ogmocoris hypomelas*. We are gratefull to David Rider, Petr Kment and Santhamma Salini, whose comments helped improve this manuscript. This study was financed in part by the Coordenação de Aperfeiçoamento de Pessoal de Nível Superior – Brasil (CAPES) – Finance Code 001 – as a Doctoral Scholarship granted to LDB. JG is supported by Conselho Nacional de Desenvolvimento Científico e Tecnológico – Brasil (CNPq) with a fellowship grant (PQ #305009/2015-0).

7. References

Barão K.R., Ferrari A., Adami C.V.K., Grazia J. 2017. Diversity of the external thoracic scent efferent system of Carpocorini (Heteroptera: Pentatomidae) with character selection for phylogenetic inference. – Zoologischer Anzeiger, **268**:102–111. doi:10.1016 / j.jcz.2016.08.003

Barão K.R., Ferrari A., Grazia J. 2020. Phylogenetic analysis of the *Euschistus* group (Hemiptera: Pentatomidae) suggests polyphyly of *Dichelops* Spinola, 1837 with the erection of *Diceraeus* Dallas, 1851, stat. rev. – Austral Entomology. https://doi.org/10.1111/aen.12489.

Barber H.G. 1941. A new species of *Tibraca* injurious to rice in Ecuador (Hemiptera–Heteroptera–Pentatomidae). – Proceedings of the Entomological Society of Washington, **43**: 110.

Barcellos A., Grazia J. 2008. Revision of the genus *Poriptus* Stål (Hemiptera: Heteroptera: Pentatomidae: Pentatominae). – Zootaxa, **1821**: 25–36. https://doi.org/10.11646/zootaxa.1821.1.3

Barros L.B., Brugnera R., Barão K.R., Grazia J. (in press.) The genus *Parahypatropis* Grazia & Fernandes, with description of two new species and description of a new similar monotypic genus (Hemiptera: Pentatomidae). – Journal of Natural History

Benvegnú G.Q. 1968. *Paramecocephala*, um novo gênero de Pentatomini do Brasil (Hemiptera: Pentatomidae: Pentatominae). – Revista Brasileira de Biologia, **28**(1): 87–96.

Campos L.A., Grazia, J. 1995. *Paratibraca*, um novo gênero de Pentatomini (Heteroptera: Pentatomidae). – Iheringia, Série Zoologia, **79**: 163–171.

Campos L.A., Grazia, J. 1998. Revisão de *Glyphepomis* Berg, 1891 (Heteroptera: Pentatomidae). – Revista Brasileira de Entomologia, **41**: 203–212.

Carrenho R., Rodrigues, H.D.D., Lima, A.C., Schwertner, C.F. 2020. Type specimens of true bugs (Hemiptera: Heteroptera) housed in the Museu de Zoologia da Universidade de São Paulo, Brazil. – Papéis Avulsos de Zoologia, **60**(e20206017): 1–16. http://doi.org/10.11606/1807-0205/2020.60.17

Dupuis C. 1955. Les genitália des Hémiptères Hétéroptères (génitalia externe de deux sexes; voies ectodermiques femelles) – Revue de la morphologie – Lexique de la nomenclature – Index bibliographique analytique – Memoires du Muséum National d'Histoire Naturelle (France). – Nouvelle Serie. Serie A. Zoologie, **6**: 183–278.

Dupuis C. 1970. Heteroptera. in: Tuxen S.L (ed), Taxonomist's Glossary of Genitalia of Insects. – Copenhagen – Munksgaard. 190–208 pp.

Farias P.M., Klein J.T., Sant'Ana J., Redaelli L., Grazia J. 2015. First records of *Glyphepomis adroguensis* (Hemiptera: Pentatomidae) and its parasitoid, *Telenomus podisi* (Hymenoptera: Platygastridae), on irrigated rice fields in Rio Grande do Sul, Brazil. – Revista Brasileira de Entomologia, **56**(3): 383–384. doi:10.1590/S0085-56262012005000044

Fernandes J.A.M. 1993. Análise filogenética e revisão do gênero *Hypatropis* Bergroth, 1891 (Heteroptera: Pentatomidae). Thesis, Universidade de São Paulo, São Paulo, Brazil.

Fernandes J.A.M., Grazia J. 1996. Revisão do gênero *Hypatropis* Bergroth, 1891 (Heteroptera: Pentatomidae: Pentatominae). – Revista Brasileira de Entomologia, **40**: 341–352.

Fernandes J.A.M., Grazia J. 1998. Revision of the genus *Tibraca* Stål (Heteroptera: Pentatomidae: Pentatominae). – Revista Brasileira de Zoologia, **15**(4): 1049–1060. doi:10.1590/S0101-81751998000400022

Fernandes J.A.M., Grazia J. 2002. *Pedinonotus*, a new southern Neotropical genus (Heteroptera: Pentatomidae: Pentatomini). – Zootaxa, **101**: 1–7. doi:10.11646/zootaxa.101.1.1

Frey-da-Silva A., Grazia J., Fernandes J.A.M. 2002. Revisão do gênero *Paramecocephala* Benvegnú, 1968 (Heteroptera: Pentatomidae). – Revista Brasileira de Entomologia, **46**(2): 209–225. doi:10.1590/S0085-56262002000200013

Frey-da-Silva A., Grazia J., Fernandes J.A.M. 2002. Revision of the genus *Ogmocoris* Mayr, 1864 (Heteroptera: Pentatomidae: Pentatomini). – Beaufortia, **52**: 179–185.

Frey-da-Silva A. 2005. Análise cladística e biogeografia do grupo Mecocephala (Heteroptera: Pentatomidae: Pentatomini). Thesis, Universidade Federal do Rio Grande do Sul, Porto Alegre, Brazil.

Genevcius B.C., Schwertner C. 2017. Strong functional integration among multiple parts of the complex male and female genitalia of stink bugs. – Biological Journal of the Linnean Society, **20**: 1–13. doi:10.1093/biolinnean/blx095

Goloboff P.A., Farris J.S., Nixon K.C. 2008. TNT, a free program for phylogenetic analysis. – Cladistics, **24**: 774–786. doi: 10.1111/j.1096-0031.2008.00217.x

Goloboff P.A., Catalano S. 2016. TNT, version 1.5, with a full implementation of phylogenetic morphometrics. – Cladistics, **32**(3): 1–18. doi:10.1111/cla.12160

Grazia J. 1978. Revisão do gênero *Dichelops* Spinola, 1837 (Heteroptera: Pentatomidae: Pentatomini). – Iheringia, Série Zoologia, **35**: 45–59.

Grazia J., Hildebrand, R. 1982. Revisão do gênero *Berecynthus* Stål, 1862 (Heteroptera: Pentatomidae: Pentatomini). – Revista Brasileira de Entomologia, **26**: 173–182.

Grazia J., Campos, L.A. 1996. *Hypanthracos*, um novo gênero de Pentatomini (Heteroptera: Pentatomidae). – Iheringia, Série Zoologia, **80**: 13–19.

Grazia J. 1997. Cladistic analysis of the *Evoplitus* genus group of Pentatomini (Heteroptera, Pentatomini). – Journal of Comparative Biology, 2: 115– 129.

Klein J.T., Barcellos A., Grazia J., Redaelli L.R. 2012. Contributions to the knowledge of *Dichelops* (*Dichelops*) with the description of new species (Hemiptera: Heteroptera: Pentatomidae: Pentatominae: Carpocorini).– Zootaxa, **3157**: 61–68. doi:10.11646/zootaxa.3157.1.6

Kment P., Vilímová J. 2010. Thoracic scent efferent system of Pentatomoidea (Hemiptera: Heteroptera) – a review of terminology. – Zootaxa, **2706**: 1–77. doi:10.11646/zootaxa.2706.1.1

Krinski D., Foerster L.A., Grazia J. 2015. *Hypatropis inermis* (Hemiptera: Pentatomidae) first record on rice crops. – Revista Brasileira de Entomologia, **59**: 12–13. doi:10.1016/j.rbe.2014.11.001

Maddison W.P., Maddison D.R. 2018. Mesquite: a modular system for evolutionary analysis. Version 3.51. – URL <http://www.mesquiteproject.org> [accessed 01 May 2019].

Mirande J.M. 2009. Weighted parsimony phylogeny of the family Characidae (Teleostei: Characiformes). – Cladistics, **25**: 574–613. doi:0.1111/j.1096-0031.2009.00262.x

Mulsant E., Rey C. 1866. Historie Naturelle de Punaises de France (Parti I.) Paris, 112pp.

Pantoja A., Triana M., Bastidas H., García C., Duque M.C. 2005. Development of – *Tibraca obscurata* and *Tibraca limbativentris* (Hemiptera: Pentatomidae) in rice in southwestern Colombia. – Journal of Agriculture of the University of Puerto Rico, **89**(3–4): 221–228.

Rider D.A., Rolston L.H. 1987. Review of the genus *Agroecus* Dallas, with the description of a new species (Hemiptera: Pentatomidae). – Journal of the New York Entomological Society, **95**(3): 428–439.

Rider D.A., Eger Jr J.E. 2008. Two new genera of Pentatomini for species previously placed in *Mormidea* Amyot & Serville (Hemiptera: Heteroptera: Pentatomidae: Pentatominae). – Proceedings of the Entomological Society of Washington, **110**: 1050–1058.

Rider D.A., Schwertner C.F., Vilímová J., Réidei D., Kment P., Thomas D.B. 2018. Higher systematics of the Pentatomoidea. Pp. 76–79 in: McPherson J.E. (ed), Invasive stink bugs and related species (Pentatomoidea) – biology, higher systematics, semiochemistry, and management – Boca Raton (USA), CRC Press, 819 pp.

Rolston L.H. 1974. Revision of the genus *Euschistus* in Middle America (Hemiptera: Pentatomidae: Pentatomini). – Entomologica Americana, **48**: 1–102.

Rolston L.H. 1978. A new subgenus of *Euschistus* (Hemiptera: Pentatomidae: Pentatomini). – Journal of the New York Entomological Society, **86**: 102–120.

Ruschel T.P., Guidoti M., Barcellos A. 2013. The Hemiptera type-material housed in the "Museu de Ciências Naturais, Fundação Zoobotânica do Rio Grande do Sul" of Porto Alegre, Brazil. – Zootaxa, **3716**(4): 539–564. http://dx.doi.org/10.11646/zootaxa.3716.4.3

Schwertner C.F., Grazia J., Fernandes J.A.M. 2002. Revisão do gênero *Mecocephala* Dallas, 1851 (Heteroptera: Pentatomidae). – Revista Brasileira de Entomologia, **46**: 169–184.

Sereno P.C 2007. Logical basis for morphological characters in phylogenetics. – Cladistics, **23**: 565–587. doi:10.1111/j.1096-0031.2007.00161.x

Silva V.J., Santos C.R.M., Fernandes J.A.M. 2018. Stink bugs (Hemiptera – Pentatomidae) from Brazilian Amazon: checklist and new records. – Zootaxa, **4425**(3): 401–455. doi:10.11646/zootaxa.4425.3.1

Stål C. 1860. Bidrag till Rio de Janeiro – traktens Hemipter – fauna. – Kongliga Svenska Vetenskaps-Akademiens Handlingar, **2**(7): 1–84.

Tsai J.F., Rédei D., Yeh G.F., Yang M.M. 2011. Jewel bugs of Taiwan (Heteroptera– Scutelleridae). – National Chung Hsing University – Taiwan. 309 pp.

Weiler L., Ferrari A., Grazia J. 2016. Phylogeny and biogeography of the South American subgenus *Euschistus* (*Lycipta*) Stål (Heteroptera: Pentatomidae: Carpocorini). – Insect Systematics & Evolution, **47**: 313–346. doi:10.1163/1876312X-47032145

Zhou Y., Rédei D. 2020. From lanceolate to plate-like: Gross morphology, terminology and evolutionary trends of the trichophoran ovipositor. – Arthropod Structure & Development, **54**(100914): 1–29. https://doi.org/10.1016/j.asd.2020.100914

Appendix 1: List of characters

Continuous characters.

1 Total length
2 Head length (Barão et al. 2020: 0)
3 Head width
4 Anteocular distance
5 Length of antennomere 1
6 Length of antennomere 2
7 Length of antennomere 3
8 Length of antennomere 5
9 Length of labiomere 1
10 Length of labiomere 2
11 Length of labiomere 3
12 Length of labiomere 4

Discrete characters.

Head

13 Mandibular plates, distal margin, shape: (0) obtuse

(e.g. Fig. 20C–D; (1) pointed (e.g. Fig. 18B). (modified from (Barão et al. 2020: 11)

14 Mandibular plates, length related to apex of clypeus: (0) shorter; (1) equal; (2) longer. (modified from Grazia 1997: 0; Weiler et al. 2016: 0)

15 Mandibular plates, apices position in relation to clypeal apex, in lateral view: (0) inferior (e.g. Figs. 9C, 18D, indicated with a red arrow); (1) leveled; (2) superior (e.g. Fig. 18E, indicated with a red arrow). (modified from Weiler et al. 2016: 3)

16 Mandibular plates, lateral margins before the eyes, shape: (0) sinuous (e.g. Fig. 18C); (1) rectilinear (e.g. Fig. 18B).

17 Clypeus, proximal limit of clypeal suture related to an imaginary line across anterior margins of compound eyes: (0) posterior (e.g. Fig. 18C, indicated with a blue dashed line); (1) anterior. (e.g. Fig. 18A–B, indicated with a red dashed line) (modified from Weiler 2016: 1)

18 Clypeus, height related to mandibular plates, longitudinally: (0) leveled; (1) higher (e.g. Fig. 18D). (Barão et al. 2020: 19)

19 Anteocular processes: (0) absent; (1) present. (Barão et al. 2020: 27)

20 Antenniferous tubercles, dorsal view of head: (0) not visible; (1) visible. (modified from Grazia et al. 2008:0)

21 Antenna, antennomere 2, dorsal view of head: (0) apparent; (1) not apparent (e.g. Fig. 14A).

22 Antenna, antennomere 3, form: (0) cylindrical (e.g. Fig. 20H); (1) conical (e.g. Figs. 13D, 20G).

23 Antenna, antennomere 3, dorsal region: (0) convex (e.g. Fig. 20H, indicated with a red arrow); (1) slightly flattened (e.g. Figs. 13D, 20G, indicated with a red arrow).

24 Antenna, antennomere 4, form: (0) cylindrical (e.g. Figs. 6A, 9A, 18Fii–iii); (1) conical (e.g. Figs. 4A, 13D, 18Fi, iv).

25 Antenna, antennomere 4, dorsal region: (0) convex (e.g. Fig. 20H, indicated with a red arrow; (1) slightly flattened (e.g. Figs. 13D, 20G, indicated with a red arrow).

26 Bucculae, ventral margin, form: (0) sinuous; (1) rectilinear.

27 Bucculae, posterior margin related to the base of head: (0) reaching; (1) not reaching.

28 Bucculae, posterior margin, form: (0) truncate; (1) tapering toward base of head. (modified from Weiler et al. 2016: 7)

29 Labium, length of labiomere 1 related to bucculae: (0) contained (e.g. Fig. 18D–E, indicated with a green arrow); (1) surpassing. (Barão et al. 2020: 22)

30 Labium, labiomere 2, form: (0) cylindrical (e.g. Fig. 18E); (1) flattened laterally (e.g. Figs. 3B, 11C).

31 Labium, labiomeres 3–4, form: (0) entirely cylindrical; (1) flattened (e.g. Fig. 15C).

Thorax

32 Pronotum, anterior angles, process: (0) absent; (1) present. (Barão et al. 2020: 29)

33 Pronotum, anterolateral margins, outline colour related to background colour of pronotum: (0) concolourous (e.g. Figs. 18A–B, 19D, 21B); (1) not concolourous (e.g. Figs. 18C–D, 19E, 20E–F, I–J, 21A).

34 Pronotum, anterolateral margins, ornamentation: (0) smooth (e.g. Fig. 18C); (1) serrate; (2) crenulate (e.g. Fig. 21A). (modified from Weiler et al. 2016: 10)

35 Pronotum, anterolateral margins, dorsal surface, outline: (0) flat (e.g. Fig. 18A); (1) explanate (e.g. Fig. 18C). (Barão et al. 2020: 31)

36 Pronotum, anterolateral margins, form: (0) straight (e.g. Fig. 18B–C); (1) concave (e.g. Figs. 18A, 21A–B). (modified from (Barão et al. 2020)

37 Pronotum, anterolateral margins, outline, impunctate area: (0) absent (e.g. Fig. 18A, indicated with a red arrow); (1) present (e.g. Figs. 18C, indicated with a red arrow, 19E).

38 Pronotum, humeral angles, development in relation to anterolateral margins: (0) developed (e.g. Figs. 9A, 18A, 21A–B); (1) not developed (e.g. Figs. 19A–C, 20I–J). (Barão et al. 2020: 34)

39 Pronotum, posterior margin, form: (0) slightly convex (e.g. Fig. 21B); (1) rectilinear (e.g. Fig. 20I, indicated with a red dashed rectangle); (2) emarginate in the middle (e.g. Fig. 20J, indicated with a red dashed rectangle).

40 Scutellum, foveae: (0) absent; (1) present.

41 Scutellum, basal angles, foveae in relation to the diameter of a compound eye, size: (0) < eye (e.g. Fig. 20K–L, indicated with a red arrow); (1) = eye (e.g. Fig. 21C, indicated with a green arrow); (2) > eye (e.g. Fig. 21E, indicated with a green arrow).

42 Hemelytrum, corium, length related to the apex of abdominal tergite 5: (0) reaching (e.g. Fig. 20L, indicated with a blue arrow); (1) not reaching (e.g. Fig. 20K, indicated with a blue dashed line).

43 Hemelytrum, corium, radial vein apex, aspect: (0) punctate (e.g. Fig. 21C, indicated a blue arrow); (1) calloused (e.g. Fig. 21D–E, indicated a blue arrow); (2) smooth. (modified from Weiler et al. 2016: 16)

44 Hemelytrum, length related to abdominal apex: (0) surpassing; (1) not surpassing. (Barão et al. 2020: 46)

45 External scent efferent system, ostiole, shape in ventral view: (0) elliptical; (1) circular; (2) guttiform.

46 External scent efferent system, ostiole, opening orientation: (0) posterolaterally; (1) ventrally. (modified from Barão et al. 2017: 3)

47 External scent efferent system, periostiolar depression: (0) absent; (1) present. (Barão et al. 2017: 4)

48 External scent efferent system, ostiolar peritreme, shape: (0) ruga; (1) spout-shaped (e.g. Fig. 18H–N); (2) bean-shaped (e.g. Fig. 18O, R). (modified from Barão et al. 2017: 5)

49 External scent efferent system, ostiolar peritreme, extension to the outer margin: (0) half; (1) ⅔ (e.g. Fig. 18H–N); (2) 1/3.

50 External scent efferent system, ostiolar peritreme, median furrow, development related to peritremal

length: (0) < half (e.g. Fig. 18R); (1) > half (e.g. Fig. 18N, P, indicated with a red arrow). (Barão et al. 2017: 6)

51 External scent efferent system, evaporatorium, colour, in relation to the metapleuron colour: (0) concolourous (e.g. Fig. 18N); (1) not concolourous (e.g. Fig. 18M).

52 External scent efferent system, vestiture, evaporatorium, punctures: (0) absent; (1) present (e.g. Fig. 18O, Q, S). (Barão et al. 2017: 22)

53 External scent efferent system, metapleuron, evaporatorium, development related to metapleuron width: (0) < half; (1)> half; (2) half. (modified from Barão et al. 2017: 8)

54 External scent efferent system, metapleuron, evaporatorium, shape of outer margin: (0) convex (e.g. Fig. 18L); (1) concave (e.g. Fig. 18I, K); (2) straight (e.g. Fig. 18H, J). (Barão et al. 2017: 10)

55 External scent efferent system, metapleuron, evaporatorium, form of anterolateral margin: (0) rounded; (1) tapered. (Barão et al. 2017: 11)

56 External scent efferent system, metapleuron, evaporatorium, area close to outer margin raised: (0) absent; (1) present. (Barão et al. 2017: 12)

57 External scent efferent system, mesopleuron, evaporatorium, development degree related to anterior limit of mesocoxal suture: (0) not attaining; (1) surpassing. (Barão et al. 2017: 13)

58 External scent efferent system, mesopleuron, range of evaporatorium related to mesopleuron width: (0) < half (e.g. Fig. 18O, indicated with a red line); (1) > half (e.g. Fig. 18M, indicated with a white line). (Barão et al. 2017: 14)

59 External scent efferent system, mesopleuron, evaporatorium at anterolateral angle: (0) absent; (1) present. (Barão et al. 2017: 15)

60 External scent efferent system, mesopleuron, evaporatorium at posterolateral angle: (0) absent; (1) present (e.g. Fig. 18S, indicated with a red arrow). (Barão et al. 2017: 16)

61 External scent efferent system, mesopleuron evaporatorium along the outer margin: (0) absent; (1) present (e.g. Fig. 18S, indicated with a blue arrow). (Barão et al. 2017: 17)

62 External scent efferent system, mesopleuron, evaporatorium, in a diagonal from mesepimeron to mesepisternum: (0) absent; (1) present. (Barão et al. 2017: 18)

63 External scent efferent system, evaporatorium, gyrification, height of the wrinkles: (0) low (e.g. Fig. 18H); (1) high (e.g. Fig. 18L). (modified from Barão et al. 2017: 21)

64 Metathoracic spiracle, form: (0) narrow (e.g. Fig. 18K, indicated with a red arrow); (1) wide (e.g. Fig. 18J, indicated with a red arrow). (Barão et al. 2017: 25)

65 Legs, colouration pattern related to the main colouration of abdominal venter: (0) concolourous; (1) not concolourous.

66 Legs, vestiture, femora, ventral surface, setae: (0) absent; (1) present.

Abdomen

67 Connexivum, colouration pattern of anterolateral angles in relation to discal colouration: (0) concolourous (e.g. Fig. 21C); (1) not concolourous. (Barão et al. 2020: 81)

68 Connexivum, colouration pattern of posterolateral angles in relation to discal colouration: (0) concolourous (e.g. Fig. 21C); (1) not concolourous (e.g. Fig. 21D–E). (Barão et al. 2020: 82)

69 Connexivum, in dorsal view, related to mesosternal wing development: (0) exposed (e.g. Fig. 21E); (1) concealed. **(**modified from Barão et al. 2020)

70 Sternites, colouration pattern of anterolateral angles related to discal colouration: (0) concolour; (1) not concolour (e.g. Fig. 19I). (Barão et al. 2020: 74)

71 Sternites, colouration pattern of sublateral margin in relation to discal colouration: (0) concolourous (e.g. Figs. 4C, 19I, indicated with a red dashed rectangle, 21G); (1) not concolourous (e.g. Figs. 13C, 14C, 19H, indicated with a red dashed rectangle, 21F).

72 Sternites, longitudinal groove medially: (0) absent; (1) present (e.g. Figs. 3C, 13E, indicated with a red arrow).

73 Sternites, posterolateral angles protruding from sternite edge: (0) absent (e.g. Fig. 21E); (1) present (e.g. Fig. 21C–D, indicated with a red arrow). (Barão et al. 2020: 72)

74 Sternites, posterolateral angles, form of apex: (0) obtuse; (1) acute. (Barão et al. 2020: 37)

75 Spiracles, colour in relation to venter abdominal colour: (0) concolourous (e.g. Fig. 21F); (1) not concolourous (e.g. Fig. 21G). (Barão et al. 2020: 79)

76 Trichobothria, colour of base in relation to abdominal colour: (0) concolourous (e.g. Figs. 13E, 21F–G); (1) not concolourous.

Male terminalia

77 Pygophore, shape: (0) subquadrangular, as wide as long; (1) subrectangular, longer than wide; (2) trapezoidal.

78 Pygophore, genital cup, opening orientation: (0) dorsal; (1) posterodorsally.

79 Pygophore, genital cup, length in relation to the length of pygophore: (0) < half (e.g. Fig. 5A); (1) half; (2) > half.

80 Pygophore, posterolateral angle, shape: (0) rounded (e.g. Fig. 2B); (1) quadrate; (2) acute. (Barão et al. 2020: 110)

81 Pygophore, dorsal rim, lateral margin related to lateral rim of pygophore, development: (0) bordering (e.g. Figs. 2B, 7A); (1) not bordering (e.g. Figs. 2A, 5A).

82 Pygophore, dorsal rim, marginal process: (0) absent; (1) present. (Barão et al. 2020: 107)

83 Pygophore, dorsal rim, superior process: (0) absent; (1) present. (Barão et al. 2020: 108)

84 Pygophore, dorsal rim, middle region, outline: (0) entire; (1) notched.

85 Pygophore, dorsal rim, extension of dorsal rim, development: (0) well-developed; (1) obsolete.
86 Pygophore, ventral rim, number of layers: (0) single; (1) double (e.g. Figs. 2C, 5B, 7B, 10B, 12H).
87 Pygophore, ventral rim, carina separating the layers: (0) absent (e.g. Figs. 10B, 12H, 19N); (1) present (e.g. Figs. 2C, indicated with a blue arrow, 7E, 19Q).
88 Pygophore, ventral rim, area between layers, surface: (0) depressed; (1) excavate (e.g. Fig. 2C, indicated with a green arrow).
89 Pygophore, ventral rim, superior layer, projection in relation to paramere, degree of development: (0) not covering (e.g. Figs. 7A, 10D, 12A); (1) covering.
90 Pygophore, ventral rim, superior layer projected toward genital cup: (0) absent; (1) present (e.g. Fig. 2A). (Barão et al. 2020: 113)
91 Pygophore, ventral rim, superior layer in superior view, lateral margin of projection, outline: (0) entire (e.g. Figs. 2A, 12H, 19N); (1) notched (e.g. Figs. 2B–C, indicated with a red arrow, 10B, 19K, Q).
92 Pygophore, ventral rim, superior layer, superior process: (0) absent; (1) present.
93 Pygophore, ventral rim, superior layer, number of process: (0) one pair; (1) two pairs.
94 Pygophore, ventral rim, inferior layer, process: (0) absent; (1) present (e.g. Fig. 2C).
95 Pygophore, ventral rim, inferior layer, number of processes: (0) one (e.g. Fig. 10C); (1) two (e.g. Figs. 7C, 12I, 19O, R).
96 Pygophore, segment X, shape: (0) rectangular, longer than wide (e.g. Fig. 10I); (1) quadrangular, as wide as long; (2) ogival, arcuate apex (e.g. Fig. 2A).
97 Pygophore, segment X, transverse carina: (0) absent; (1) present.
98 Pygophore, segment X, process: (0) absent; (1) present (e.g. Figs. 10J, 19J, P). (Barão et al. 2020: 120)
99 Pygophore, segment X, process shape: (0) tumescence (e.g. Fig. 2B); (1) thorn-like (e.g. Figs. 2C, 19P). (modified from Barão et al. 2020)
100 Pygophore, segment X, process, placement of insertion: (0) basally; (1) medially. (Barão et al. 2020: 123)
101 Pygophore, paramere: (0) absent (e.g. Fig. 2A); (1) present (e.g. Fig. 2B).
102 Pygophore, paramere, development of crown: (0) well-developed (e.g. Fig. 10D–H); (1) reduced (e.g. Figs. 2B, 19J, M, P).

Male genitalia

103 Phallus, phallotheca, length medially related to width apically: (0) shorter; (1) longer. (Barão et al. 2020: 126)
104 Phallus, phallotheca, ductus seminis distalis, length in relation to conjunctiva: (0) shorter; (1) equally; (2) longer, up to three times longer; (3) extremely long, at least five times longer (e.g. Fig. 21H).
105 Phallus, phallotheca, posterodorsal margin, median projections: (0) absent; (1) present. (modified from Barão et al. 2020)
106 Phallus, phallotheca, posterodorsal margin, number of projections, medially: (0) one; (1) two. (Barão et al. 2020: 130)
107 Phallus, phallotheca, posterolateral margins, rounded projections: (0) absent; (1) present (e.g. Figs. 10L, 21I–K). (Barão et al. 2020: 131)
108 Phallus, phallotheca, process of phallotheca: (0) absent; (1) present. (Barão et al. 2020: 133)
109 Phallus, phallotheca, process of phallotheca, width basally related to width medially: (0) narrower; (1) wider; (2) uniformly wide. (Barão et al. 2020: 134)
110 Phallus, phallotheca, projections ventrobasally: (0) absent; (1) present (e.g. Figs. 5I, 10N).
111 Phallus, conjunctiva, number of processes: (0) one pair (e.g. Figs. 10L, 21J–K); (1) two pairs (e.g. Figs. 5H, 21I).
112 Phallus, conjunctiva, lateral lobes: (0) absent; (1) present. (Barão et al. 2020: 137)
113 Phallus, conjunctiva, median lobes: (0) absent; (1) present (e.g. Figs. 5H, 10L, 21I). (Barão et al. 2020: 138)
114 Phallus, conjunctiva, median lobes, aspect: (0) entirely membranous (e.g. Fig. 21I–J); (1) sclerotized apically (e.g. Fig. 5H); (0) entirely sclerotized. (Barão et al. 2020: 139)
115 Phallus, conjunctiva, ventral lobes: (0) absent; (1) present. (Barão et al. 2020: 141)
116 Phallus, process of vesica: (0) absent; (1) present. (Barão et al. 2020: 142)

Female terminalia

117 Genital plates, valvifers 8, discal surfaces: (0) flat (e.g. Fig. 16A); (1) convex (e.g. Figs. 5J, 11A, 16B); (modified from Weiler et al. 2016: 24)
118 Genital plates, valvifers 8, mesial margins related to each other: (0) juxtaposed (e.g. Figs. 5J, 16A); (1) not juxtaposed (e.g. Fig. 15B).
119 Genital plates, valvifers 8, length in relation to laterotergites 9: (0) subequal; (1) at least twice as long; (1) smaller.
120 Genital plates, valvifers 8, development degree over valvifers 9: (0) partially covering; (1) completely covering. (Barão et al. 2020: 87)
121 Genital plates, valvifers 8, posterior margins, shape: (0) straight; (1) sinuous.
122 Genital plates, valvifers 9, position in relation to segment X: (0) leveled; (1) oblique, in an obtuse angle. (Weiler et al. 2016: 29; Barão et al. 2020: 89)
123 Genital plates, valvifers 9, anterior margins, shape: (0) straight; (1) concave; (1) convex.
124 Genital plates, valvifers 9, posterior margins, shape: (0) convex; (1) straight; (2) concave; (3) emarginate.
125 Genital plates, valvifers 9, surface: (0) flat; (1) swollen; (2) depressed. (Barão et al. 2020: 90)
126 Genital plates, valvifers 9, sclerotized lateral arms: (0) absent; (1) present. (Barão et al. 2020: 91)

127 Genital plates, laterotergites 8, posterior margins, form: (0) straight; (1) acutely projected; (2) obtusely projected. (Barão et al. 2020: 92)
128 Genital plates, laterotergites 8, spiracles: (0) absent; (1) present. (Barão et al. 2020: 93)
129 Genital plates, laterotergites 9, apices in relation to abdominal tergite 8: (0) not surpassing; (1) surpassing. (Barão et al. 2020: 95)
130 Genital plates, valvulae 8, visible in ventral view: (0) absent; (1) present. (Barão et al. 2020: 96)
131 Genital plates, valvulae 9, sclerotized areas: (0) absent; (1) present. (Barão et al. 2020: 97)

Female genitalia

132 Ectodermal ductus, thickening of vaginal intima, length of arcuate posterior portion related to round anterior portion: (0) shorter; (1) longer. (Barão et al. 2020: 98)
133 Ectodermal ductus, proximal ductus receptaculi, aspect: (0) straight; (1) convolute.
134 Ectodermal ductus, proximal ductus receptaculi, diameter, in relation the diameter of the distal ductus receptaculi: (0) smaller; (1) subequal; (2) larger.
135 Ectodermal ductus, proximal ductus receptaculi, length in relation to vesicular area: (0) shorter; (1) longer, up to three times longer (e.g. Fig. 16F); (2) extremely long, at least four times as long (e.g. Fig. 11D).
136 Ectodermal ductus, vesicular area, median wall, shape subproximally: (0) enlarged (e.g. Fig. 5K); (1) cylindrical. (Barão et al. 2020: 100)
137 Ectodermal ductus, distal ductus receptaculi, length in relation to vesicular area: (0) shorter; (1) longer, up to three times longer (e.g. Fig. 5K); (2) extremely long, at least four times as long (e.g. Fig. 11D).
138 Ectodermal ductus, distal ductus receptaculi, form: (0) straight; (1) convolute (e.g. Fig. 16F–G); (2) twisted.
139 Ectodermal ductus, distal ductus receptaculi, annular flanges, related to each other: (0) convergent; (1) divergent.
140 Ectodermal ductus, posterior annular flange, width related to *capsula seminalis* width: (0) thinner; (1) wider. (Barão et al. 2020: 104)
141 Ectodermal ductus, *pars intermedialis*, form: (0) enlarged; (1) rectilinear; (2) twisted; (3) posteriorly fan-fold.
142 Ectodermal ductus, *capsula seminalis*, length related to *pars intermedialis*: (0) smaller; (1) subequal; (2) longer.
143 Ectodermal ductus, *capsula seminalis*, form: (0) globose; (1) elongate.
144 Ectodermal ductus, *capsula seminalis*, process: (0) absent; (1) present. (Barão et al. 2020: 106)

Electronic Supplement Files

at http://www.senckenberg.de/arthropod-systematics

ASP_78-2_Barros_Electronic_Supplements.zip

DOI: 10.26049/ASP78-2-2020-07/1

File 1: Barros_et_al_Systematics_Mecocephala_group_Electronic_Supplement 1.docx

Fig. S1. Barros_et_al_Figure_1_S1.tif

Fig. S2. Barros_et_al_Figure_2_S2.tif

Authors' contributions

L.D.B., K.R.B. and J.G have done that together.

Zoobank registrations

at http://zoobank.org

Present article: http://zoobank.org/urn:lsid:zoobank.org:pub:8B6966E5-F6A6-43D6-A28F-8456243C76C6

***Chimerocoris* Barros, Barão & Grazia – 2020:** http://zoobank.org/urn:lsid:zoobank.org:act:AD32CD7A-A676-42A5-B09E-25DB7E0D2B72

***Chimerocoris luridus* Barros, Barão & Grazia – 2020:** http://zoobank.org/urn:lsid:zoobank.org:act: EADD5737-2814-4308-B69A-DA6D02694E85

***Liscocephala* Barros, Barão & Grazia – 2020:** http://zoobank.org/urn:lsid:zoobank.org:act:4887FD01-9AEE-4DCC-8E18-DB99A98EE3AF

***Liscocephala fumosa* Barros, Barão & Grazia** – 2020: http://zoobank.org/urn:lsid:zoobank.org:act: 1DC424E9-F754-497A-859E-25DB4A5F8945

***Triunfus* Barros, Barão & Grazia – 2020:** http://zoobank.org/urn:lsid:zoobank.org:act: 584E63A1-2794-4453-AA75-86B6054218E2

***Triunfus carvalhoi* Barros, Barão & Grazia – 2020:** http://zoobank.org/urn:lsid:zoobank.org:act:31CE1E56-49EE-4069-BA9A-C7C3CEBAC2D3

***Triunfus incarnatus* Barros, Barão & Grazia – 2020:** http://zoobank.org/urn:lsid:zoobank.org:act:973DFC78-6204-49C5-8F6A-CF725F631275